STRATEGIES FOR PROCESS CONTROL AND TABLET DIVERSION IN A DIRECT COMPACTION PROCESS

By

FERNANDO NUNES DE BARROS

A thesis submitted to the

School of Graduate Studies

Rutgers, the State University of New Jersey

In partial fulfillment of the requirements

For the degree of

Master of Science

Graduate Program in Chemical and Biochemical Engineering

Completed under the direction of

Ravendra Singh

And approved by

_____

_____

_____

New Brunswick, New Jersey

OCTOBER, 2018

ABSTRACT OF THE THESIS

Strategies for Process Control and Tablet Diversion in a Direct Compaction Process

by FERNANDO NUNES DE BARROS

Thesis Director:

Ravendra Singh

The increasing array of challenges faced by the pharmaceutical industry during drug development has led to a push for more efficient manufacturing techniques. With the implementation of continuous manufacturing, the importance of process modeling and control has become evident, being subject of multiple studies. Dynamic models with fast execution speeds are needed for the development of control strategies. Additionally, as robust as a control system can be, it is still not possible to ensure that the entirety of a production run is within quality specifications. For this reason, strategies for material diversion in real time need to be implemented.

The first part of this work focuses on the modeling of the tablet compaction operation. The experimental residence time distribution (RTD) of the tablet compaction process is determined through tracer experiments, and the resulting data is used to generate and validate an RTD model based on two different approaches. A framework for the

development of control relevant dynamic models is then introduced. To exemplify the presented framework, a validated dynamic model for the tablet compaction operation is created. An *in silico* study using this model is conducted to evaluate different control algorithms and strategies for tablet compaction. One of the evaluated control strategies is selected and successfully implemented in a direct compaction pilot plant to demonstrate the applicability of the validated model for control strategy development.

In the second part of this thesis, a framework for the implementation of a material diversion system based on RTD is presented. A tablet diversion system is created according to the introduced framework, and the proposed diversion system is implemented in a commercial control platform, where its functionality is demonstrated using the developed RTD model and a simulated input.

Cite this work as follows: Barros, F. N., Singh, R. (2018). Strategies for Control and Material Diversion of a Direct Compaction. MS Thesis, Department of Chemical and Biochemical Engineering, Rutgers University, NJ, USA.

Acknowledgements

I would like to thank my advisor, Dr. Ravendra Singh, for the guidance and support provided toward the completion of my thesis. His mentorship assisted me through the challenges of graduate school and improved my understanding of the pharmaceutical industry. I would also like to express my gratitude toward the committee members, Dr. Rohit Ramachandra and Dr. Alberto Cuitiño, for dedicating time to review this thesis and contribute valuable inputs.

I would like to acknowledge Rutgers Research Council, U. S. Food and Drug Administration (FDA) and GlaxoSmithKline (GSK) for funding this project.

I would like to thank every member of the C-SOPS and Pharmaceutical System Engineering research group, especially Dr. Andrés Roman, who supported this thesis with his expertise on spectroscopy, and Dr. James Scicolone, who was always available to help with any technical questions regarding the continuous manufacturing line.

Ultimately, my graduate research would not have been possible without the daily support from my colleagues Aparajith Bhaskar and Matthew Billups with their invaluable and motivating discussions. Furthermore, my gratitude goes out to my close friends who I had the pleasure of meeting during my time spent at Rutgers University.

Finally, I would like to acknowledge my parents for their endless support throughout the span of my educational career. Their work ethics and resilience inspire me every day, and I hope to continue learning from them.

Table of Contents

List of Figures

List of Tables

Chapter 1 : Introduction

1.1. Literature Review

In the recent years, the pharmaceutical industry is facing a growing array of challenges in new drug product development. With the average cost for the development of a new drug surpassing $2.87 billion and a jump in the generic share of prescriptions filled from 49% to 91% between 2000 and 2015, the profitability of new drugs has been drastically diminished [1], [2]. The increasing cost and market share domination by generics, coupled with a reduced effective patent life of new products, higher-regulatory constraints, and relatively inefficient quality by testing (QbT) manufacturing paradigm, led to an evolving interest in more efficient and automated processing techniques [3], [4]. In face of this scenario, several pharmaceutical companies have started a transition from batch-based production to continuous processing [5]. Continuous manufacturing has presented itself as an attractive alternative with flexibility, and time and cost-saving features [6]. Additionally, continuous manufacturing has the advantage of achieving steady state quickly in a few minutes, facilitating the implementation of efficient control strategies and enabling true quality by design (QbD).

The concept of QbD, as presented in the ICH Q8 guidance on pharmaceutical development, requires manufacturers to demonstrate an understanding on how multiple process variables affect the quality of the final product [7], [8]. This entails the ability to correlate critical process parameters (CPP) to critical quality attributes (CQA) of each unit operations. Even if this relationship is well defined and understood, variations in properties

of raw materials can cause deviations in product quality. For this reason, another important aspect of QbD is the development of a control strategy that can mitigate the effects that process disturbances and variations in raw material properties have in the final product quality.

There have been multiple contributions in the scientific domain of process control for the pharmaceutical industry. Generalized strategies and frameworks for the implementation of process controls in pharmaceutical processes have been developed [9], [10]. The control of individual unit operations such as wet granulation [11]–[13], dry granulation [14], [15], feeding and mixing [16], and tablet compaction [17], [18] have been studied. The integrated control of continuous processing lines has also been the subject of various manuscripts. Singh et. al. has demonstrated the control of direct compaction and roller compaction manufacturing strategies through simulation studies [15], [19], [20]. Mesbah et. al. has introduced, in a simulation platform, a model predictive control strategy for a fully integrated continuous pharmaceutical manufacturing line, from API crystallization to tablet production [21]. Experimental implementations of plan-wide control have been achieved by Singh et. al., and Huang and Pla [22]–[24].

Most modern control strategies still rely on feedback loops, which take the system output into consideration in order to adjust actuators and achieve a desired output response. Among feedback control algorithms, model predictive control (MPC) is highlighted here. This algorithm is based on an optimization scheme and is inherently capable of dealing with multi input multi output (MIMO) systems with interactions and dead times. The inclusion of process variable constraints is also possible in MPC due to its optimization-based nature. These advantages led to its popularization and widespread usage in industry

[25]–[27]. Multiple variations of MPC have been developed, including schemes that consider model uncertainty and scenario based approaches [28]–[34]. However, despite the constant developments in this area in the chemical and petrochemical industries, little effort has been done towards the implementation of MPC in pharmaceutical process and more specifically, tablet compaction operations [17].

Although continuous manufacturing has gained attention from the pharmaceutical industry as a mean of modernizing production, the implementation of continuous particulate processing systems still faces a major challenge related to material and batch traceability as well as diversion of out of specification production. Muzzio and Engisch have proposed the use of residence time distributions (RTD) for means of material traceability [35]. Residence time distributions have thoroughly studied as a classical chemical engineering topic, but it was only recently that this concept has been introduced in the pharmaceutical industry.

A review on the applications of RTDs on solid unit operations has been presented by Gao et. al. [36]. Continuous mixers have been thoroughly characterized using RTDs in previous studies [37]–[40]. Work has also been conducted in the determination of the RTD of wet granulation processes [41], [42]. Recently, the mixing profile of granulators has been characterized and its RTD has been used for control and material diversion purposes [43], [44]. Studies have been conducted in the experimental determination and modeling of the RTD of a tablet press feed frame [45], [46]. The approach utilized by the authors during the modeling of the mixing profile of the feed frame involved the assumption that ideal mixing occurs within the vessel.

1.2. Objectives

This thesis has been carried out in two separate parts. The first part has the objective of introducing frameworks for development of validated control relevant models, creation of a validated model for the tablet compaction operation and demonstration of an advanced control strategy for tablet compaction. The second part of this work will focus on a framework for residence time distribution based diversion systems and its implementation. Following are the specific objectives of this work:

1. To determine, model, and validate the residence time distribution to the tablet compaction unit and chute assembly.
2. To present a systematic framework for creating control relevant validated models of pharmaceutical unit operations.
3. To develop a validated model of the tablet press by applying the modeling framework presented in Objective 2.
4. To determine the ideal control algorithm for the compaction process.
5. To evaluate three different control strategies for the tablet press.
6. To present a framework for implementation of residence time distribution based diversion system
7. To demonstrate implementation of a residence time distribution based diversion system.

1.3. Overview of Thesis

In this thesis, the reader will be walked through the development and, in some chapters, implementation of tools and strategies for control and material diversion in a continuous direct compaction process. This material should also serve as a base for similar efforts in different continuous pharmaceutical manufacturing routes (e.g. dry granulation and wet granulation).

Chapter 2 introduces key concepts required for the full understanding of this work. A description of the experimental setup available at Rutgers University as well as overviews on the tablet compaction process, feedback control, model predictive control (MPC), and residence time distributions is given in this chapter.

A systematic framework for development of validated models of pharmaceutical processes is presented in Chapter 3. Additionally, a model for tablet compaction is developed and validated based on experimental data. In Chapter 5, the applicability of this model is demonstrated through studies that evaluate different control algorithms and control strategies under set point tracking and disturbance rejection scenarios. A comparison between the simulated and experimental results for one of the control strategies is also presented.

The residence time distribution (RTD) of a tablet compaction unit is determined and modeled in Chapter 3. A novel strategy for accurately sampling tablets in real time is presented, and tracer experiments are conducted. Two different modeling approaches are evaluated, and their results are validated. The developed RTD model serves as a base to demonstrate the implementation of a tablet diversion system in Chapter 6. A framework

for the complete implementation of this diversion system is presented in this chapter as well.

Results and discussions from all the previous chapters are agglomerated in Chapter 7. Finally, Chapter 8 elaborates on conclusions of this work and future perspectives on the presented topics.

Chapter 2 : Background

2.1. Continuous Direct Compaction Process

2.1.1. Process and Pilot Plant Description

A continuous direct compaction pilot-plant situated at the ERC-SOPS, Rutgers University, has been used in this study (Figure 1). The pilot-plant spans an area of 10 x 10 feet and is built in three levels to take advantage of gravity as the driving force for material flow. The top level houses three loss-in-weight feeders (Coperion K-Tron KT20 and KT35), with the possibility of expansion, used for introducing excipients and APIs into the process in a controlled manner. The middle level is assigned to the de-lumping or milling of powders (Quadro Comill), the addition of lubricant to the process (Coperion K-Tron KT20), and blending (Glatt GCG-70). The ground floor is designated for compaction (Fette 1200). The upper and middle levels are connected through flexible connections, while the middle and lower levels are connected through a chute, where spectroscopical tools can be installed to monitor the process [3], [6].

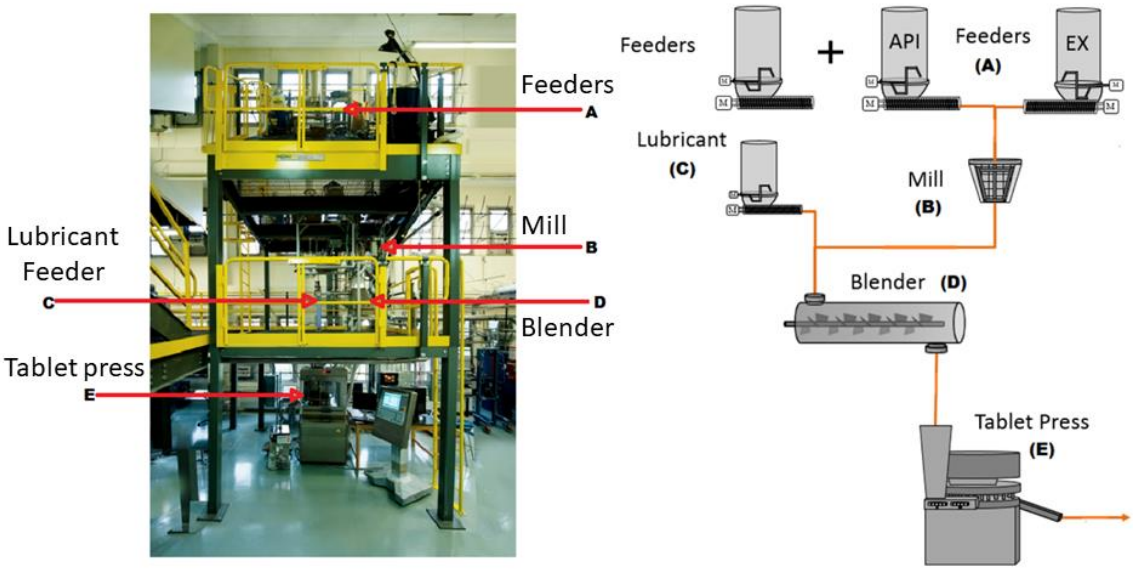

Figure 1. Continuous direct compaction process.

The modular design of the pilot-plant allows for quick reconfiguration based on experimental requirements, avoiding the need to run the entire plant for specific experiments. Multiple configurations have been used throughout this study, demonstrating the flexibility of the plant.

2.1.2. Tablet Compaction

Tablets are the most widely commercialized pharmaceutical dosage form and are manufactured by compacting the formulation using a rotary tablet press. It is estimated that more than 70% of the pharmaceutical products sold worldwide are tablets, with an approximated market value of over $300 billion dollars per year [47]. The tablet compaction process takes place in a series of four main steps: die filling, pre-compression, main compression, and ejection. Each of these steps is crucial for a consistent tablet quality, hence it is necessary to understand and control them.

Consistent and uniform filling of dies is often the rate-limiting factor in the entire tablet compaction process [48]. Powder properties and operating parameters play a major role in the quality of die filling, having effects on tablet weight and ultimately affecting the performance and mechanical properties of the final product [45]. Initially, the formulation enters the feed frame through a vertical chute. Once inside the feed frame, two rotating blades force the powder into the die. The excess powder in the die is then removed by a scraper and the die proceeds to the next compaction stages. The volume of powder fed into the die and the density of the bulk powder can be varied according to the tablet filling depth and feed frame speed respectively, allowing for accurate control of tablet weight. It is also important to acknowledge the presence of powder mixing within the feed frame, which can further dampen any upstream fluctuations in blend properties and reduce variations in tablet quality. This mixing can be characterized by tradition residence time distribution approaches.

Subsequent to die filling, the powder is subjected to two compression stages. The first stage, known as pre-compression, is required to achieve de-aeration of the powder and reduce the occurrence of tablet defects, such as capping. The second stage, main compression, is when the powder in the die is pressed to its final height, forming the tablet through sintering mechanisms. During compression, rotating drums push the punches into the die compacting the powder. The distance between the drums determines the height to which the powder is compressed (main and pre-compression heights) and this distance can be adjusted by changing the vertical position of the bottom drum. Pre and main compression forces are measured during these stages, being a function of the fill depth divided by the compression height (compression ratio).

In the final stage of the tableting operation, a rotating drum pushes the bottom punch upwards, forcing the tablet to leave the die. A sensor located under the drum measures the force required to eject the tablet. This ejection force is a function of composition, amount of lubricant present in the tablet, compression ratios and turret speed, being useful in the diagnostics of problems in the final product.

2.2. Feedback Control

The transition from batch to continuous processing has increased the opportunities for the application of process control in the pharmaceutical industry. Many control systems, including on-off control, proportional-integral-derivative (PID) control, and model predictive control (MPC), rely on the real time feedback of process variables to generate a control action. PID controllers present a vast advantage over on-off control, being more flexible and offering fine adjustments in the manipulated variables. A block diagram demonstrating a generalized implementation of a PID controller is presented in Figure 2.

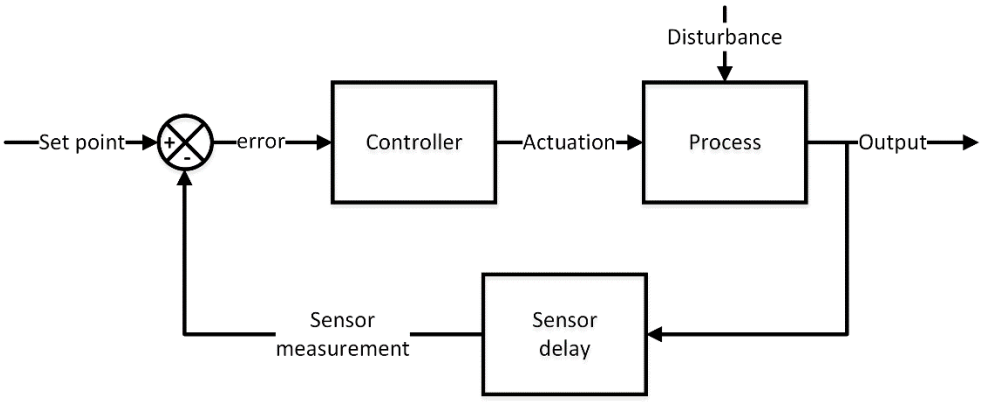

Figure 2. Generalized feedback control implementation.

During operation, the PID controller receives the error between the set point and the actual value of the controlled variable. The actuation is then calculated based on the

magnitude of the error (proportional action), on integral of the error over time (integral action) and on the rate of change of the error (derivative action). The response of the process to this actuation is then detected by the sensor and the error is recalculated, closing the control loop.

The PID controller can be represented in different ways. The expanded form of the PID controller, which is used in Simulink and Matlab implementations is presented in Equation 1. This is well suited for optimization based controller tuning because the gains can be used to independently adjust the influence of each control mode.

$$p(t) = \bar{p} + K_c e(t) + K_I \int_0^t e(\tau) d\tau + K_D \frac{de(t)}{dt} \quad (1)$$

where $p(t)$ is the controller output, $\bar{p}$ is the steady state value of the output, $e(t)$ is the error between set point and actual values, τ is the dummy variable of integration, and K_c, K_I and K_D are the proportion, integral and derivative tuning parameters, respectively.

A review on the applications of PID controllers on modern processes has been published by Visioli [49]. Applications of this control algorithm in the pharmaceutical field have also been studied by multiple authors. Bhaskar et *al*. has demonstrated the implementation of feedback controller on a tablet compaction unit [17]. The performance of a PID based control loop on a continuous direct compaction process has been also studied [50]. Although PID controllers are a widespread and time-tested solution, a few processes might require more advance control algorithms, leading to studies on hybrid and MPC based control strategies [20], [23], [51].

2.3. Model Predictive Control

Model predictive control is an important advanced control technique for difficult multivariable control problems [52]. The MPC concept, presented in [53] consists of the combination of a linear process model with current process measurements to predict the future output of the process for a given number of steps in the future (prediction horizon). This combination allows the controller to calculate the optimal control action to be taken over the control horizon (number of calculated future control movements) without violating any constraints imposed in the process. MPC offers several advantages over traditional control methods and few are listed here:

1. The linear process model captures the interactions between significant process variables.

2. Transport delays are taken into account by the linear process models.

3. Smoother control, with less noise propagation can be achieved through MPC.

4. Constraints on inputs and outputs are considered when performing a control action.

5. Can efficiently handle multi input multi output (MIMO) control problem

6. It is easier to tune.

7. The control calculations can be coordinated to optimize set points.

These reasons justify the widespread implementation of MPC in critical processes such as power plants and oil refineries. Recently, attention has been drawn for the implementation of MPC in pharmaceutical processes. As mentioned in the previous section, Singh *et al.* have developed a hybrid MPC-PID control strategy for direct

compaction tablet manufacturing process [20], [23], [51]. Singh et al. have also presented a systematic framework for implementation of the MPC into the pilot-plant [19], [20], [23], [51]. A hybrid MPC-PID control system has been also proposed for API separation and purification process [20], [23], [51]. Nunes de Barros et. al. demonstrated model predictive control strategies for the tablet compaction operation, and Bhaskar et. al. have implemented these strategies in a pilot plant [17], [54]. Mesbah et. al. studied the use of MPC to control both downstream and upstream pharmaceutical manufacturing processes [21]. These publications exemplify the multiple applications of MPC in continuous pharmaceutical manufacturing.

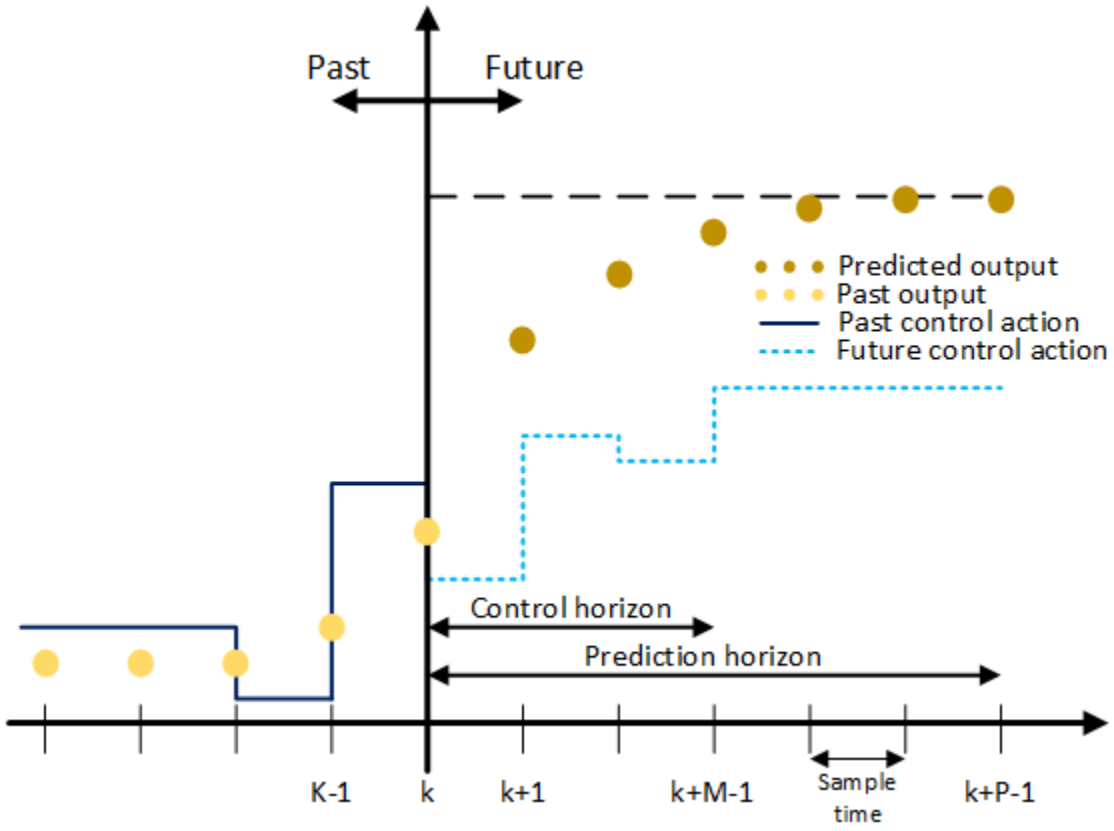

Figure 3. MPC operating principle (adapted from Singh et al., 2013) [20].

Adapted with permission from Singh, R., et al. (2013). System-wide hybrid MPC–PID control of a continuous pharmaceutical tablet manufacturing process via direct compaction. Eur J Pharm Biopharm. 85:1164–1182. Copyright Elsevier.

2.4. Residence Time Distribution

Residence time distribution (RTD) is a probability distribution function that describes how long a fluid or powder element spends inside a given operation. RTDs are used to characterize the mixing that occurs inside a compartment and can be determined experimentally through the injection of a tracer material into the process in the form of a pulse or a step [20]. The outlet tracer concentration is measured until the effects of the injection settle down. In powder processes, these concentration measurements can be

recorded online using PAT tools, or samples can be collected for offline measurements. If offline measurements are used, it is important to appropriately select the sampling intervals to ensure that the samples can be analyzed in a timely manner, while ensuring that enough information is collected to accurately represent the residence time distribution of the system. This trade-off can be achieved by having a shorter sampling interval initially, when high variations in concentration are expected, followed by wider interval when the effects of the tracer injection taper off.

A key aspect to be considered during the experimental determination of residence time distributions is the tracer selection. The addition of tracer should not influence the flow properties of the bulk powder while still being readily detectable through analytical techniques. Commonly, tracers are inert and completely distinguishable from the bulk formulation, but since multicomponent formulations are used in the pharmaceutical industry, it is possible to use one of the components of the mixture as a tracer as long as changes in concentration do not affect the flow properties of the bulk powder.

The residence time distribution profile is also heavily dependent on process parameters, meaning that it is necessary to experimentally determine a profile for each operating condition used during production. The RTD of the tablet press feed frame is expected to vary with feed frame speed, tablet production rate (turret speed) and tablet fill depth, where the later should have a lesser influence on the process.

For an ideal pulse tracer injection, the resulting concentration profile has the same shape as the residence time distribution. The RTD can be determined by normalizing the concentration profile according to Equation 2.

$$E(t) = \frac{C(t) - C_0}{\int_{t_0}^{\infty} (C(t) - C_0)dt} \quad (2)$$

Where $C(t)$ is the tracer concentration in the outlet, t_0 is the injection instant and C_0 is the initial tracer concentration before injection.

Pulse injection experiments are advantageous in situations where an expensive tracer is used, since it minimizes the amount of tracer consumed. In powder systems, the pulse technique also minimizes the effects of slight differences in flowability between the tracer and the bulk formulation. For pulse injection experiments to result in an accurate RTD, data should be collected for the entire concentration profile, including its tail. In situations where data is not available, the tail can be approximated by an exponential decay [35], [55]. Another major downside of this technique is that it relies on a close to instantaneous pulse injection, which is not always possible.

If a close to ideal pulse injection is not feasible, a step injection can be used as an alternative. The step injection is also adequate for tracers that can be detected in low concentrations. Care must be taken to ensure that the injection of tracer does not affect the bulk flow properties of the powder. This technique results in a curve in the shape of the cumulative distribution function ($F(t)$). The cumulative distribution function can be calculated by normalizing the process data according to Equation 3.

$$F(t) = \frac{C(t) - C_0}{C_f - C_0} \quad (3)$$

Where $C(t)$ is the tracer concentration profile, C_0 is the initial tracer concentration, and C_f is the final tracer concentration.

The resulting distribution from both techniques are related according to Equation 4.

$$E(t) = \frac{dF(t)}{dt} \tag{4}$$

2.5. Control Hardware and Software Integration

The central piece in the control hardware and software integration is the control platform, which serves as a hub for the connection between all the process equipment, sensors and software. Multiple communication protocols are commercially available, and their usage depends on the equipment being integrated.

Commonly, spectroscopic tools are operated through their own standalone computers, which contain instrument specific software. The software outputs the spectra collected at each sampling interval in files of various formats, which can then be accessed by other software in the control network via file pooling. Modern PAT tools can also communicate directly to the spectral tool through instrument specific drivers.

Process equipment and traditional sensors can establish communication through industrial protocols such as 4-20 mA HART, 0-20 VDC or 0-10 VDC, network protocols (Ethernet, TCP/IP), serial connections (RS-232, RS-485), PROFIBUS and OLE for Process Control (OPC). Where latter is becoming more common in modern processes due to its flexibility and increase in popularity of ethernet based industrial communications.

The diagram presented in Figure 4 demonstrates the control network established for the experiments conducted in Chapter 3. In this integration, the NIR instrument (Bruker Matrix-F FT-NIR) is connected to a laptop dedicated to data acquisition. The data acquired through this software is deposited in files located in a shared folder in the control network. From this folder, the spectral data is made available to all the members of the network. The PAT software (Process Pulse II) reads the spectral files and applies a calibration model to the data, generating concentration predictions for the different components of the powder blend. These concentration values read by an OPC client (Kepware) which also communicates through OPC Data Access (OPC DA) to the tablet press unit and the control platform (DeltaV). The controller then reads and interprets all process variables, generating actuation signal which are sent to the plant through OPC connections and 24 VDC digital signals. A control software (DeltaV Control Studio) allows the user to interact with the controller, with the possibility of introducing new control strategies into the system and perform open loop actuation on the process.

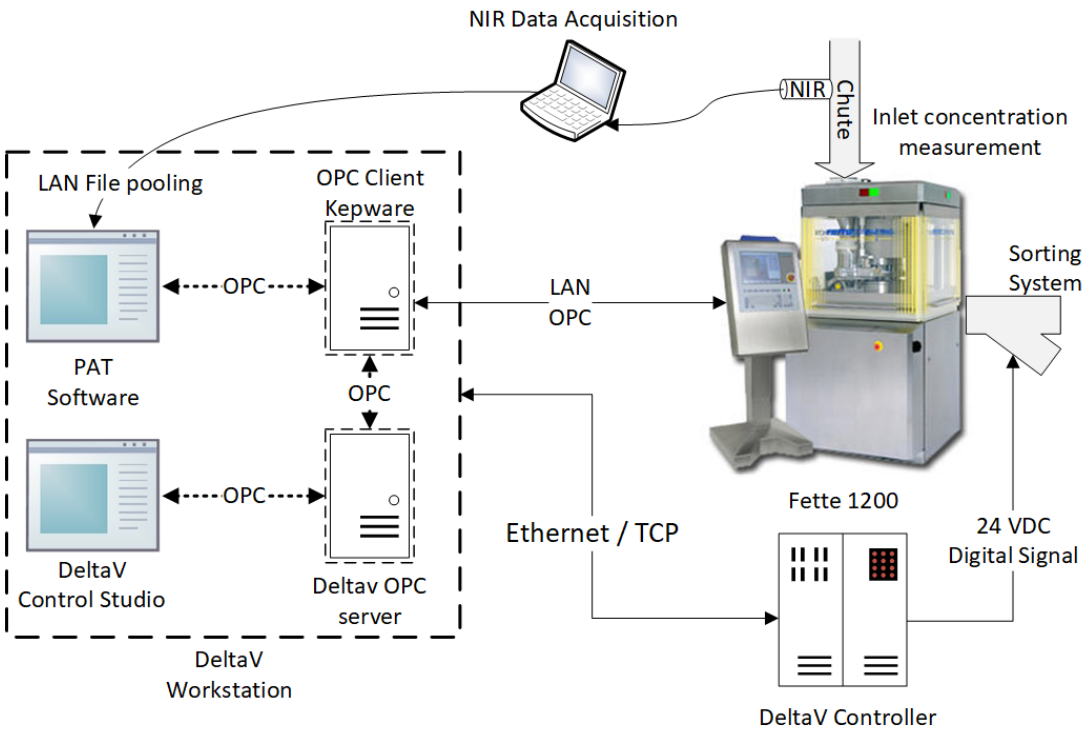

Figure 4. Control hardware and software integration. OPC: OLE for process control; PAT: Process analytical technology; LAN: Local area network.

Chapter 3 : Residence Time Distribution (RTD) Model of Tablet Press Feed Frame

Acknowledgements

This work is supported by the Glaxo Smith Kline (GSK) and National Science Foundation Engineering Research Center on Structured Organic Particulate Systems.

3.1. Materials and Methods

The blends used during the feed frame RTD experiments were composed of Lactose PH-310 (excipient, Foremost Farms), Acetaminophen (API, Mallinckrodt) and Magnesium Stearate (lubricant, Mallinckrodt). Two blends with 9 % and 12 % API loading were pre-mixed using a V-blender (Patterson-Kelley liquid-solids blender) at 25 revolutions per minute for 30 minutes with a layered loading order to ensure that complete mixing is achieved.

Tablet samples for the NIR calibration model development were prepared using a single station compaction simulator (Presster) with a target weight of 400 mg, and pre- and main compression forces of 3 kN and 12 kN respectively. The compaction experiments were conducted using a Fette 1200 tablet press with flat round punches (10mm in diameter) and 20 stations. The tablet press was set-up to closely match the compaction profile to which the NIR calibration tablets were subjected. The detailed tablet press parameters used in this experiment are presented in Table 1.

Table 1. Tablet press parameters

FD (mm)	MCH (mm)	PCH (mm)	PR (tablets/h)	FF speed (RPM)
7.5	3.2	3.91	20,000	40

FD: Fill depth; MCH: Main compression height; PCH: Pre-compression height; PR: Production rate; FF: Feed frame

A Bruker Matrix-F FT-NIR spectrometer was used for the online blend composition measurements. The tablet samples were collected, and their API composition was measured offline using through an MPA Multi-Purpose Analyzer (Bruker). Reflectance spectroscopy was applied for online measurements of blend composition, while transmittance spectroscopy was used for tablet measurements.

3.2. NIR Model Calibration

The NIR calibration model used to measure concentration of API in the blend was developed in an experimental setup which allowed powder to flow with a vertical speed similar to the one observed in the plant. The setup consisted of a loss in weight feeder which fed powder into a standalone feed frame through a vertical chute. The NIR sensor was placed on the chute replicating what is seen in the pilot plant. Accurate control of the rotational speed of the feed frame, and consequently flow rate, was achieved by rotating the feed frame using a direct current (DC) motor. Calibration spectra for the online PAT model were collected for five different blends with API composition ranging from 7 % to 15 % in weight.

The offline NIR calibration model for tablets was developed using blends with compositions ranging from 8 % to 14 % API. Ten tablets of each concentration level were

analyzed and divided into calibration and validation datasets according to Table 2. Additionally, ten spectra for an individual calibration tablet were collected to incorporate the characteristic noise of the instrument into the calibration model. Figure 5 shows a comparison between the reference and predicted API composition values for the validation tablets. It is observed that the model predicts the API composition with reasonable accuracy with calculated root mean square error of prediction (RMSEP) of 0.093, relative standard error of prediction (RSEP) of 0.0069% and bias of 0.00012.

Table 2. Composition of tablets for model calibration and validation.

Composition (%w/w)			Number of tablets (-)	
APAP	**Lactose**	**MgSt**	**Calibration**	**Validation**
8	91	1	6	4
10	89	1	7	3
12	87	1	7	3
14	85	1	6	4

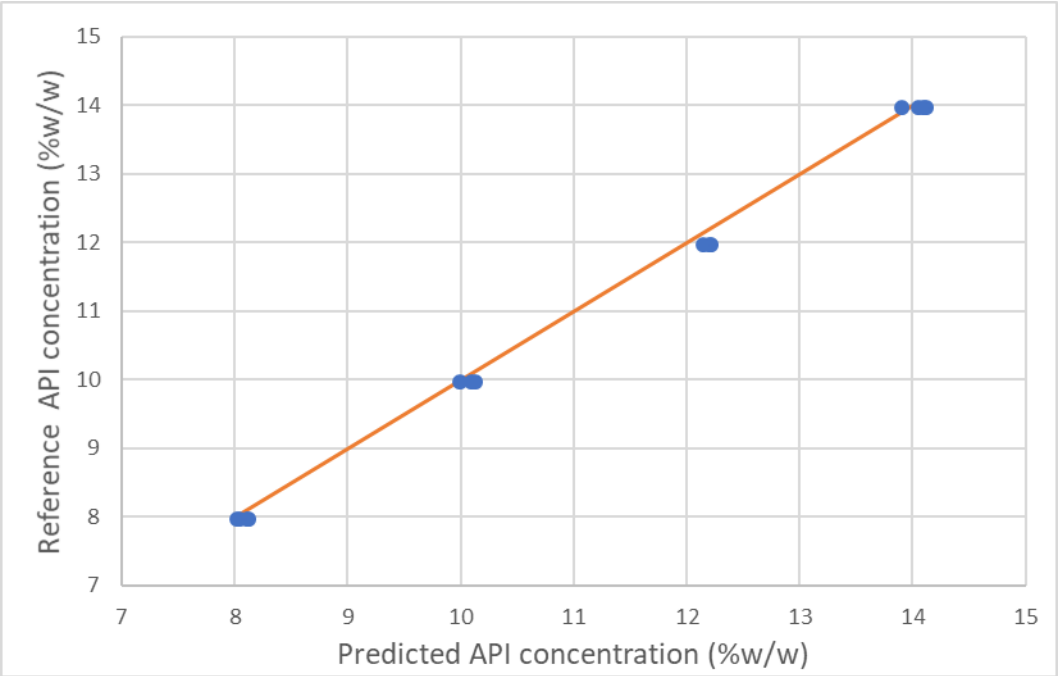

Figure 5. NIR tablet calibration model validation.

3.3. Experimental RTD Determination

3.3.1. Experimental Setup

Experiments were conducted to determine and validate the residence time distribution of a tablet compaction unit. The experimental setup consisted of two loss-in-weight feeders (Coperion K-Tron KT20 with coarse auger screws) connected to the tablet press directly through a vertical chute, where the NIR instrument was installed (Figure 6). The feeders were loaded with two different blends with nominal API concentration of 9% and 12%, in order to achieve sharp concentration changes.

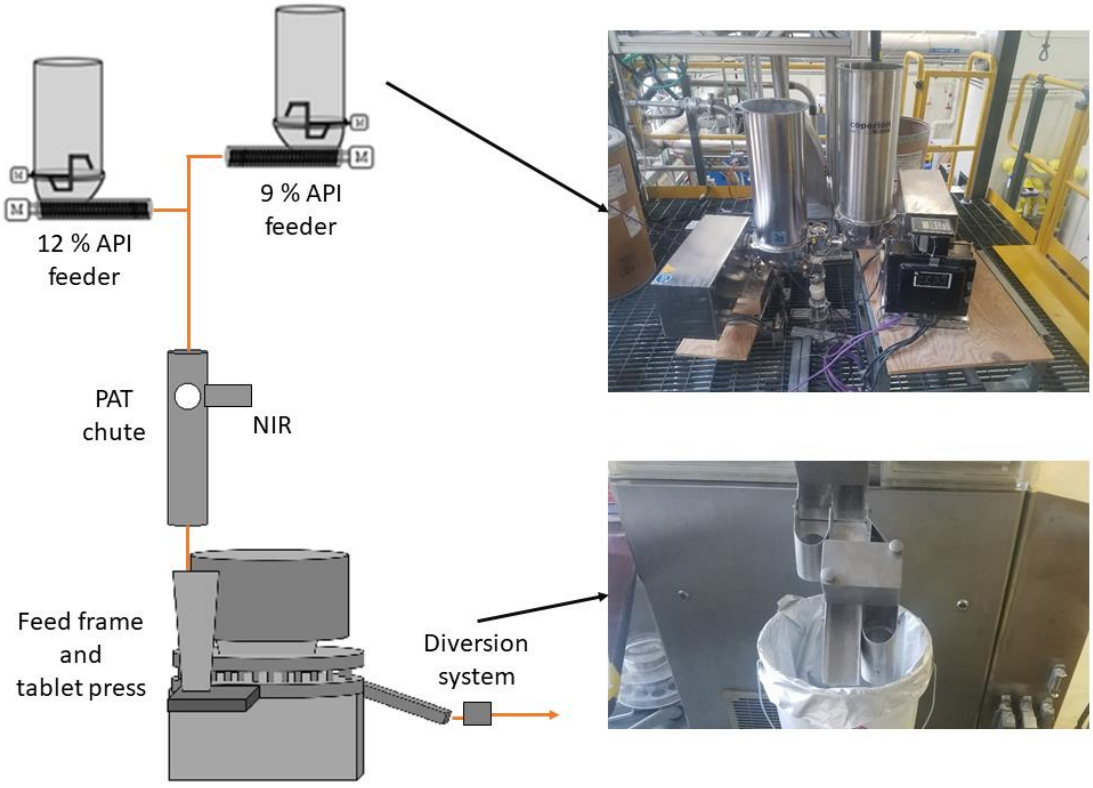

Figure 6. Experimental setup for RTD experiments.

In these experiments, API was selected as a tracer to minimize variations in flow properties. The first experiment involved a step change in API concentration from 12% to 9%. This step change data will later be used to fit the F(t) curve. In the second experiment, a 2-minute-long pulse from 9% to 12% API was injected into the system. This data will serve as the validation dataset. Tablets were sampled during the experiments to determine the concentration profile at the tablet press output.

3.3.2. Preliminary Experiments

Preliminary experiments were conducted to obtain an approximated RTD of the tablet compaction unit. A step, in density, was applied to the system by switching from a low density blend to a high density blend, where both blends had similar flow properties

as the material used in the RTD determination. The response of the system was analyzed using a PAT free approach which consisted in the detection of changes in powder density through fluctuations in the force required to eject the tablets from the dies. The preliminary results aided in the definition of the time at which sampling should be started and ended, as well as the sampling rate that should be used during the RTD determination experiments.

3.3.3. Tablet Sampling Strategy

As determined per the preliminary experiments, tablets were sampled every 20 seconds. The sampling for the step and pulse experiments started at 320 seconds and 430 seconds, respectively, after the disturbance was applied to the system and was ceased 700 seconds after the last change in the system input. A diversion gate allowed samples to be collected at accurate intervals. Each collection lasted 2 seconds, ensuring that at least three tablets were collected.

Each sample was collected in individual numbered bags. The use of the diversion gate coupled with the control platform continuous historian allowed the sampling bags to be traced to an exact time instant. Spectral data from the incoming powder blend was collected online while the tablet concentration was measured offline after the experiments.

3.4. Residence Time Distribution Models

3.4.1. Tank-in-Series Model

Multiple models are available for characterizing the mixing of systems. According to the study conducted by Mateo-Ortiz & Méndez, the feed frame of a tablet press should behave as a close to ideal constantly stirred tank reactor (CSTR) [46]. However, Engisch

& Muzzio have suggested that powder systems can be modeled using a series of CSTRs [35]. This model can be fitted in two different ways. In the first one, the mean residence time (MRT) and the number of tanks in the model are the fitted variables. In the second method, the MRT is calculated from experimental data and the only fitted variable is the number of tanks. For this study, a tank-in-series model followed by a plug flow reactor (PFR) has been used to characterize the RTD of the tablet press, where the TIS portion represents the feed frame and the PFR portion represents the pipes and turret of the tablet press. The mean residence time of the TIS and PFR models, as well as the number of tanks have been optimized to fit the experimental data.

The tank-in-series model approximates the RTD of a system as a series of equally sized CSTRs, resulting in a realistic mixing description. The number of tanks is an integer varying from 1 to infinity, and a larger number of tank results in a narrower RTD, tending to a plug flow reactor with no axial mixing (PFR) as the number of tanks tends to infinity. The generalized tank-in-series model followed by a PFR is presented in Equation 5.

$$E(t) = \begin{cases} 0, & t < \tau_{PFR} \\ \dfrac{t^{n-1}}{(n-1)!\left(\dfrac{\tau_{TIS}}{n}\right)^{n}} e^{\left(-\frac{nt}{\tau_{TIS}}\right)}, & t \geq \tau_{PFR} \end{cases} \quad (5)$$

where τ_{TIS} and τ_{PFR} are the mean residence times of the TIS and PFR models respectively, $E(t)$ is the residence time distribution of the system, and n is the number of tanks in the TIS model.

3.4.2. Dispersion Model

The axial dispersion model describes the RTD of the feed frame as an ideal plug flow within a tube superimposed by a diffusion term resulting in a system characterized by back mixing [36], [56]. This model has a similar fitting procedure as the tank in series model with the only difference being the fact that the main fitted parameter of the dispersion model is the Peclet number (Pe), which represents the ratio between convective and diffuse transport. The dispersion RTD function for open-open boundaries as developed by Taylor is presented in Equation 6 [57]. As the Peclet number tends to infinity, the behavior of the system approaches an ideal plug flow reactor, where no axial dispersion is present.

$$E(t) = \begin{cases} 0 & , \quad t < \tau_{PFR} \\ \dfrac{1}{2\sqrt{\dfrac{\pi\tau t}{Pe}}} e^{-\frac{Pe(\tau - t)^2}{4\tau t}} & , \quad t \geq \tau_{PFR} \end{cases} \tag{6}$$

where τ is the mean residence time, τ_{PFR} is the system dead time, and Pe is the Peclet number.

3.5. RTD Modeling Toolbox

A toolbox to has been created in Matlab to facilitate the fitting of residence time distribution models to a new set of experiments. The procedure is composed of three major scripts: raw data preprocessing, the model fitting function, and RTD model function. A

diagram with the overall functionality of the toolbox is presented in Figure 7. A detailed description of each step in the process will be provided in the following sections.

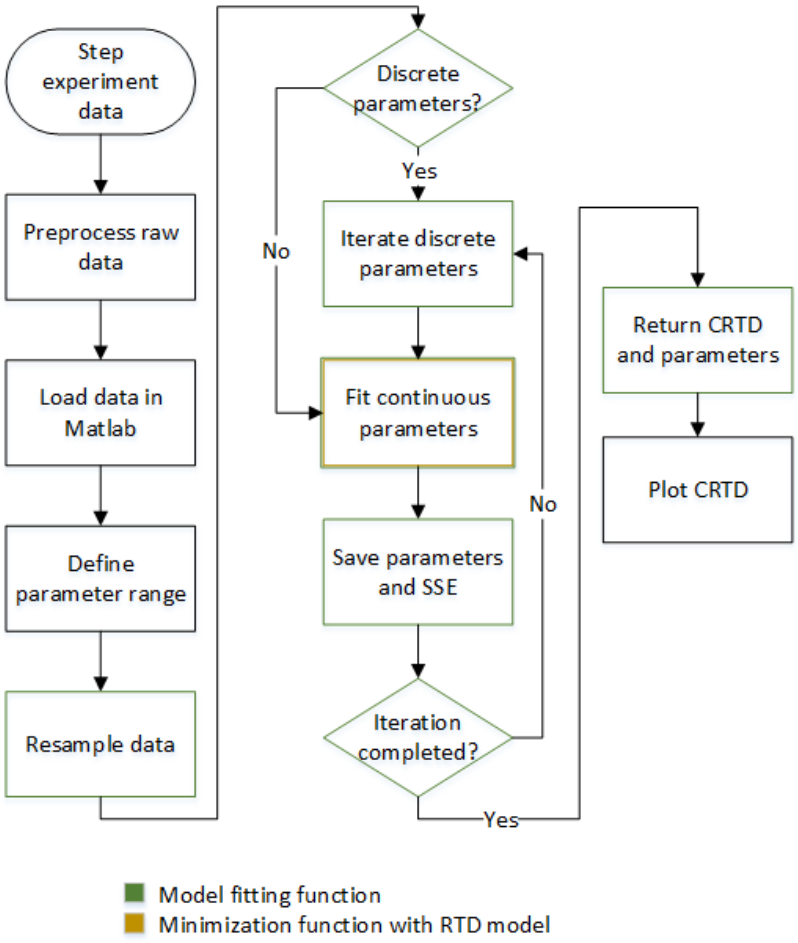

Figure 7. RTD toolbox overview

3.5.1. Raw Data Preprocessing

The raw process data is extracted from the control system in the form of a spreadsheet containing the value of each process variable and their respective timestamps. The first step in preprocessing is to convert the excel spreadsheet into a Matlab data table. The timestamps from the data table are then converted from absolute to relative time, elapsed in seconds from the beginning of the tracer experiment. Once the timestamps are

converted, individual timeseries are created for each data stream and these timeseries are stored in a timeseries collection object.

Data incoming from the offline NIR analysis of the tablets is originally organized in a spreadsheet and each datapoint is correspondent to a tablet sample. Timestamps are attributed to each datapoint based on their sampling instant according to the procedure described in Section 3.3.3.

3.5.2. Model Fitting Function

The preprocessed data is loaded in a Matlab script and inputted in the model fitting function along with the initial guesses for the parameters and their feasible ranges. Two distinct model fitting functions can be used depending on the nature of the model parameters. If all parameters are continuous, a built-in minimization algorithm is used to fit the model by minimizing the sum of the squared error between the experimental data and model prediction. If at least one of the parameters is discrete (e.g. number of tanks), the function iterates through all the possible discrete values within a user defined range while fitting the continuous parameters at each point. The performance of the fitted models is then compared and the best performing discrete point is selected. Performance metrics ,and the cumulative RTD response are also computed in the model fitting function and returned to the user.

The *fminsearchbnd* function built into Matlab was used to achieve the minimizations [58]. The sum of the squared error (SSE) between the experimental and model values was selected as the cost function of the minimization (Equation 7).

$$SSE = min \sum \left(E(t)_{exp} - E(t)_{model}\right)^2 \quad (7)$$

where SSE is the sum of the squared errors, $E(t)_{exp}$ is the experimental residence time distribution and $E(t)_{model}$ is the fitted residence time distribution.

3.5.3. RTD Model

Each RTD model involves two functions, one used for parameter fitting and another used for the computation of the CRTD curve. The minimization routine used to fit the continuous model parameters requires the specification of a function that returns the error between the predicted and experimental RTD. This function takes the model parameters as inputs and uses Equations 5 and 6 to calculate the simulated $E(t)$ curve, which is then integrated resulting in the predicted CRTD of the system. The CRTD is then compared with the experimental values to compute the sum of the squared errors of the model. Similarly, a second function is also created to generate and return the CRTD of the system when the model inputs are known.

Chapter 4 : Development of Validated Tablet Press Model

Acknowledgements

This chapter is based on the following manuscript previously published by the authors which is highly acknowledged [54]". The use of the manuscript as the core element of this chapter has been authorized by the co-authors. The author has contributed to in the elaboration of the manuscript, development of the model described in the publication, and execution of the experiments.

F. Nunes de Barros, A. Bhaskar, and R. Singh*, "A Validated Model for Design and Evaluation of Control Architectures for a Continuous Tablet Compaction Process," *Processes*, vol. 5, no. 4, p. 76, 2017.

This work is supported by the Rutgers Research Council through grant 202342 RC-17-Singh R, the US Food and Drug Administration (FDA) through grant 11695471, Glaxo Smith Kline (GSK) through grant AWD00002346 to Singh, and National Science Foundation Engineering Research Center on Structured Organic Particulate Systems.

*Corresponding author (Email: ravendra.singh@rutgers.edu)

4.1. Materials and Methods

The experiments conducted in this chapter were based on a blend with a composition of 89% lactose monohydrate 310 (excipient), 9% semi-fine acetaminophen

(API) and 1% magnesium stearate (lubricant). The materials were loaded in Glatt container blender in a layered loading order and the blender was run at 25 revolutions per minute (RPM) for 30 minutes. Multiple individual batches of 7 kilograms were prepared.

To obtain dynamic information about the process variables, open loop experiments consisting of a series of step changes were conducted in the tablet compaction unit operation. The parameters presented in

Table 3, and the ranges of these step changes were defined based on operational constraints and previous knowledge of the process. This data was used in the development and validation of the simulation tool.

Table 3. Key tablet press parameters [54].

Parameter	**Availability**	**Value**
Production rate	Set point & actual	8,000 – 20,000 tablets/h
Turret speed	Actual	Dependent on production rate
Feed frame speed	Set point & actual	30 rpm
Main compression force	Set point & actual	Controlled
Pre-compression force	Actual	Controlled
Main compression height	Set point & actual	Manipulated
Pre-compression height	Set point & actual	4.05 mm
Fill depth	Set point & actual	Manipulated

The modeling and simulations presented in this chapter were conducted in the Matlab and Simulink environment. The Parameter Estimation Toolbox, which is built into Matlab was used for regression of the dynamic models.

4.2. Systematic Modelling Framework for Pharmaceutical Process Control System Design

The modeling of the tablet compaction process followed a systematic framework presented in Figure 8. This framework is generalized can be used as a guideline for the development of control relevant models in the future.

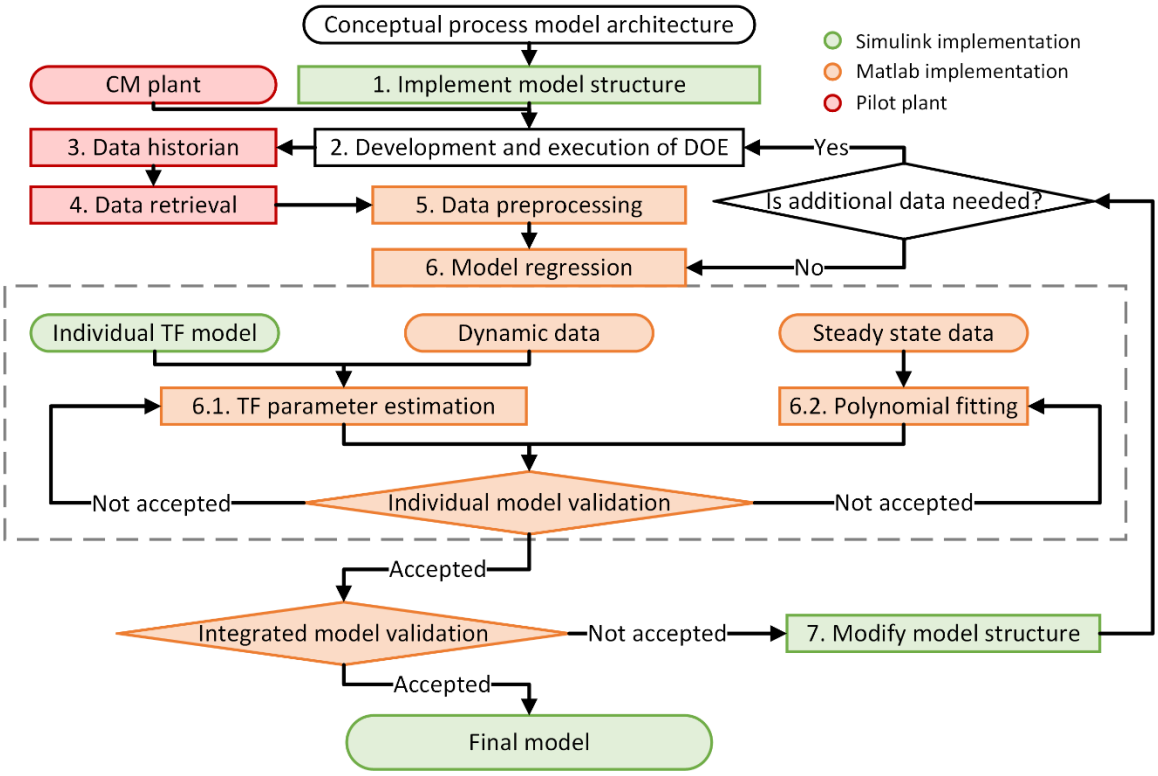

Figure 8. Systematic modeling framework. DOE: Design of experiments [54].

Initially, the overall structure of the model is conceptualized, and the relevant inputs and outputs, as well as, intermediate process variables are identified. Once the model has been conceptualized, its structure is implemented in the simulation platform of choice (Simulink). The structure of the model is dependent on the interaction between different process variables and the availability of data for each of these variables. Multiple modeling approaches can be used in this step, including differential equations, state-space equations, transfer functions, and a combination of dynamic and static models.

An experimental plan is then designed and executed to ensure that dynamic information rich data is collected. A key aspect to be considered in this step is the possible presence of non-linearities in the process. These non-linearities can be identified and

characterized through the analysis of step responses at varied operating conditions. Different step responses for the same step change at different ranges are a strong indicator of non-linearities. The data generated from the experiments is collected through the control platform's continuous historian and stored in an SQL database. Once in the SQL database, the data can be retrieved through a spreadsheet and preprocessed using Matlab. During preprocessing, the raw data is organized according to each individual experiment and the absolute timestamps are converted to relative time from the start of the experiment.

Models relating each variable pair are regressed individually to closely match experimental data, and the fitting procedure varies according to the nature of the model being implemented. Transfer functions representing the dynamic behavior of the system are fitted using Matlab's Parameter Estimation Toolbox. During this procedure, the transfer function parameters are optimized through the Nelder Mead simplex algorithm to minimize the sum of the squared error between the experimental data and the transfer function output [33]. The steady state models implemented in this work consisted of polynomial equations and were regressed using Matlab's polynomial fitting functionality (*polyfit*).

Each model is then individually validated, and if the performance of the model is not satisfactory, the fitting procedure is repeated. Individual validations are followed by the performance evaluation of the full integrated model. If the integrated model does not meet the desired performance standards, its structure is modified, and the fitting is repeated. New experiments can be performed if additional data is required for the fitting of the modified structure. The coefficient of determination (R^2) was the performance metric used to evaluate both the integrated and individual models. Models with a R^2 value bigger than 0.9 were considered satisfactory.

4.3. Model Structure

4.3.1. Transfer Functions

Transfer functions are algebraic expression that describe the dynamic relationship between an input and an output variable [52]. These expressions offer a compact form of representing a model and were selected as the main modeling strategy for this work due to their ease of implementation, interpretation, and solution using Simulink. The model developed in this study consists of a series of low order transfer functions arranged to represent a multiple input, multiple output (MIMO) tablet compaction process. The dynamic behavior of each input-output variable pair was represented by either a first order or second order transfer function depending on its characteristic response and the value of the regression coefficient (R^2) for the different order transfer functions. A first order transfer function was always preferred if its performance was satisfactory. The general form of the transfer function implemented in this work is presented in Equation 8. First order transfer functions can be obtained from this Equation 8 by setting the value of τ_1 to zero.

$$\frac{Y(s)}{U(s)} = \frac{K}{\tau_1 s^2 + \tau_2 s + 1} \tag{8}$$

where $U(s)$ and $Y(s)$ are the input and output signals, respectively, K is process gain, and τ_i are the time constants. The values of the transfer function parameters are fitted to minimize the difference between the simulated and the experimental data. The fitting procedure is described in detail in Section 4.5.

4.3.2. Variable Transport Delays

An accurate representation of transport delays is necessary when building a control relevant model since they can heavily influence controller tuning parameters, adversely affecting control loop stability [52]. Variable delays are observed in tablet compaction due to the characteristic nature of this process. These delays consist of two fractions as seen in Equation 9. The first fraction is related to the sensing method and has a constant value, while the second fraction is inherent of the process itself and is dependent on process variables such as turret speed and number of dies in the tablet press. This fraction varies according to Equation 10.

$$\theta = \theta_s + \theta_p(\omega) \tag{9}$$

$$\theta_p(\omega) = \frac{60\ \Delta n_p}{\omega\ n_p} \tag{10}$$

where θ_s is the sensor time delay, $\theta_p(\omega)$ is the process time delay, θ is the overall time delay, ω is turret speed, Δn_p is the number of dies between actuation and sensing, and n_p is the total number of dies in the tablet press.

4.4. Nonlinear Force Behavior

Main and pre-compression forces are the main variables that need to be controlled during compaction as they directly relate to tablet breaking force and can be made to affect tablet weight. Information about the nonlinear correlation between tablet tensile strength and compaction force has been previously described in the literature [59]. A relation

between compaction pressure and volume has been described by Kawakita [60]. In this work empirical correlations between compression forces and the ratios of the fill depth and compression heights have been developed. The nonlinearity has been introduced in the dynamic model of the tablet press and is of extreme importance for process control. If the nonlinearities of a system are not properly accounted for during control strategy development, the resulting controller will only be stable only in a very narrow operational range.

Experiments have been conducted to analyze how the compression forces are affected by the compression ratios, defined as the ratio between fill depth and compression height. The steady state values of the forces were plotted against their respective compression ratios (Figure 9).

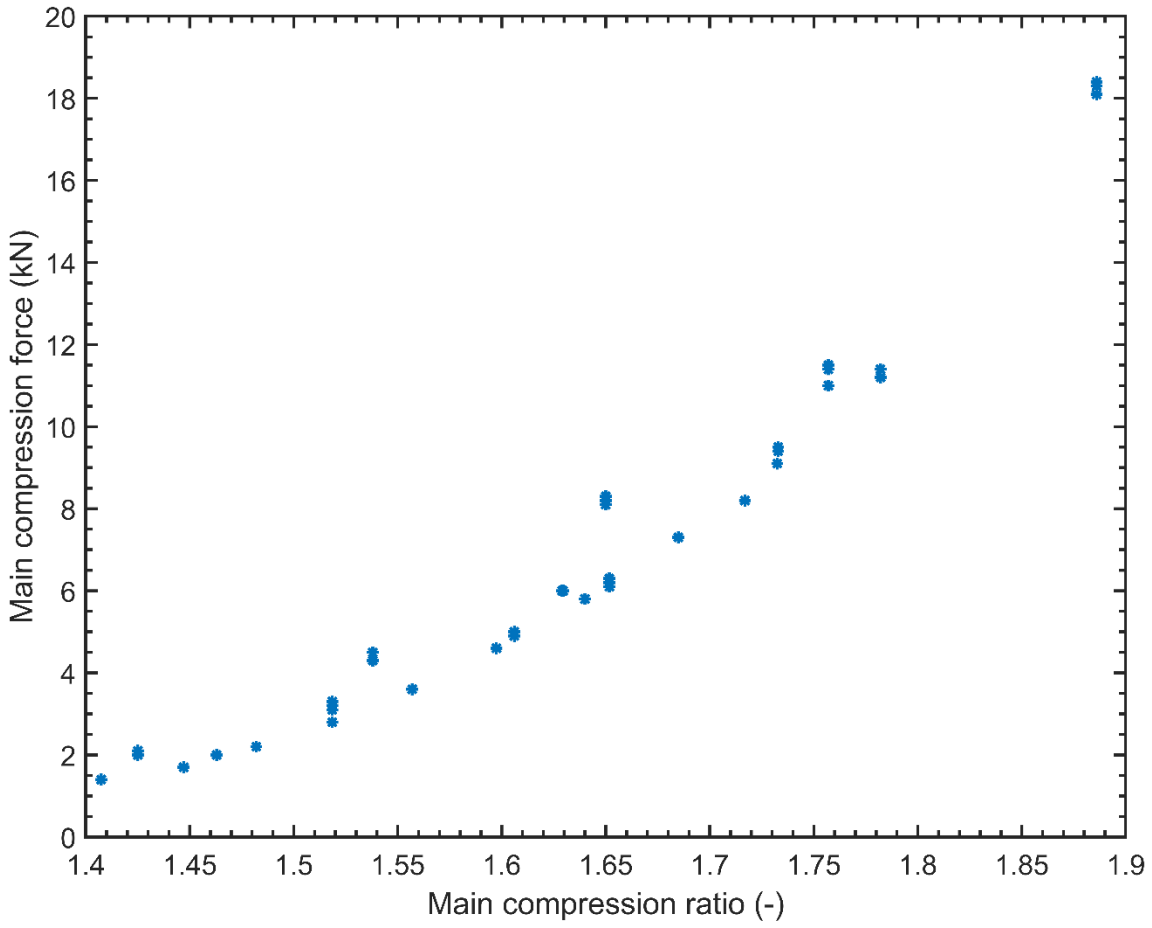

Figure 9. Nonlinear main compression force behavior [54].

As expected, a nonlinear trend was observed for both pre and main compression forces. Two different empirical equations, exponential and a second order polynomial, were fitted to the data and the latter yielded a better fit. The form of the fitted equation is show below (Equation 11).

$$F = a_1 r^2 + a_2 r + a_3 \tag{11}$$

where r is the ratio of fill depth and compression height, F is the compaction force, and a_i are the polynomial coefficients of the model. The numerical values of these constants are provided in Section 7.4.2.

This approach allows the model to represent the dependence of one output variable on two input variables through a single equation. It is important to notice that only steady state data was used to fit these empirical relations. These relations only provide non-dynamic information of the systems. In order to capture the dynamic behavior of the system, these polynomials must be and preceded by a transfer function with unitary gain.

4.5. Model Regression

4.5.1. Linear Models

Prior to fitting, all the model inputs, outputs, and intermediate variables were identified through analysis of historical process data. Following this identification, transfer functions were created to relate these variables. The parameters for each individual transfer function were fitted using a combination of Matlab, Simulink, and the Parameter Estimation Toolbox. Initially, experimental data for each input-output pair was loaded into the Matlab workspace. A Simulink model containing a parameterized transfer function (Equation 8) followed by a transport delay was then loaded and the Parameter Estimation Toolbox is opened. The fitting procedure takes place using this toolbox, which minimizes a user selected cost function by varying the length of the transport delay and the parameters of the transfer function trough built in optimization algorithms. For this work, the Trust-Region-Reflexive algorithm with a sum of the squared errors cost function was selected for dynamic model fitting.

It is important to note that when using transfer functions to represent the dynamics of nonlinear processes, the transfer function parameters are only valid around the operational range at which they were fitted. Pre- and main compression force transfer functions were fitted in ranges of 1.4-3.2 kN and 5-12 kN respectively.

4.5.2. Nonlinear Models

A two-step fitting procedure has been used to model the relation between the compression ratios and the compression forces, as well as the relation between tablet breaking force and main compression ratio. Initially, the polynomials were fitted based on steady state data. Following this, a Simulink model containing a polynomial equation followed by a parametrized transfer function with unitary gain and a transport delay was loaded. The dynamic parameters of this model were then fitted according to the procedure described in the section above.

4.6. Model Implementation

A flexible process model was developed using Simulink, allowing virtual experiments to be conducted in a simple and quick manner, while reducing material usage and costs. Key input and output parameters are available for manipulation and monitoring in the model, creating a similar environment as the on seen in the tablet press. The model structure was developed in such way to allow the user to access each individual step of the tableting operations, resulting in a model that is divided in five modules. The first four modules capture the behavior of the mechanical actuators, pre-compression stage, main compression stage and tablet CQAs. The fifth module represents the tablet diversion system. The Simulink flowsheet is organized using subsystem masks to facilitate the

understanding of the implementation. An overview of the implementation is presented in Figure 10. Four main modules and snapshots of their implementation can be seen in the image.

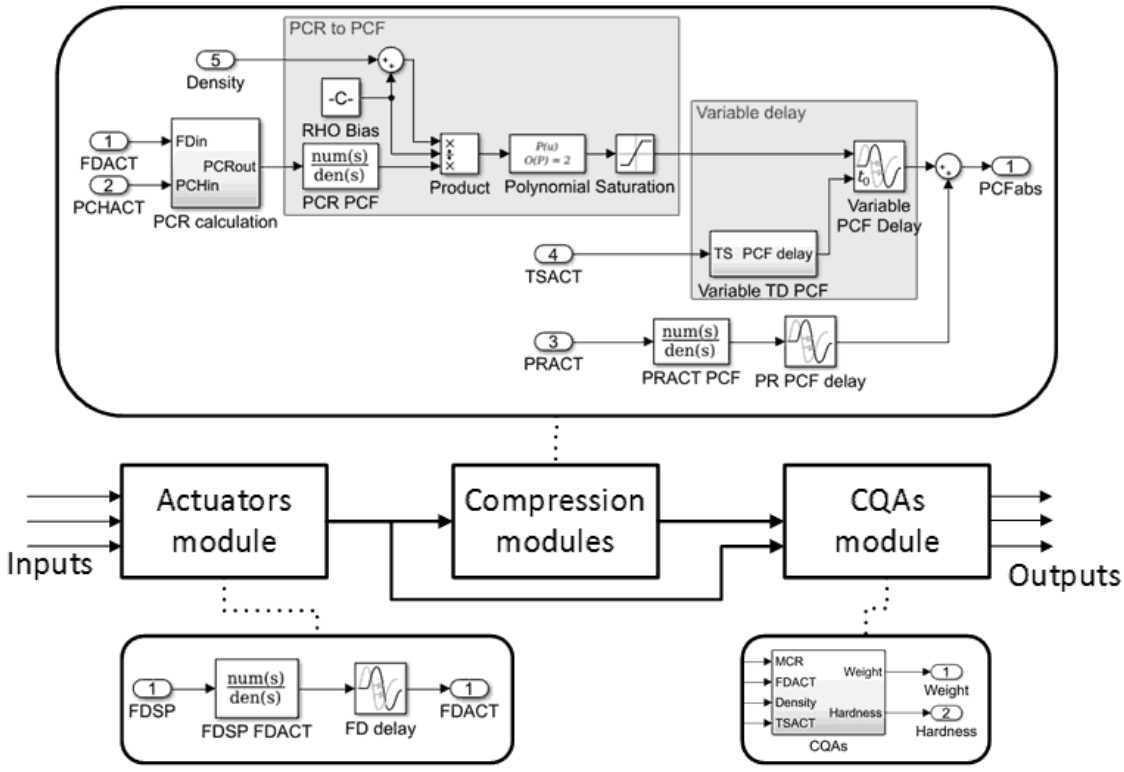

Figure 10. Model implementation overview [54].

4.6.1. Actuators Module

The actuators module is composed of a series of transfer function relating the set point and actual values for the actuators of the tablet press. Fill depth, pre-compression height and main compression height actuators were modeled according to first order dynamics, while a second order transfer function was used to represent the production rate actuator. Turret speed is also calculated in this module based on the actual production rate

(PR) value using Equation 12. The fitted parameters for the actuator models are given in Table 4.

$$\omega = \frac{1000PR}{60N_p} \tag{12}$$

where turret speed (ω) is given in rotations per minute, production rate is given in thousands of tablets per hour and N_p is the total number of punches in the press.

Table 4. Model parameters — Actuators

Model Inputs	Model Outputs	Model Details					R^2
		Order	τ_1 (s)	τ_2 (s)	θ (s)	Gain	
Fill depth set point	Fill depth	1	1.0694	-	5.4986	1	0.9966
Main compression height set point	Main compression height	1	0.1658	-	5.3616	1	0.9973
Pre-compression height set point	Pre-compression height	1	0.1658	-	5.3616	1	0.9973
Production rate set point	Production rate	2	0.9	0.9968	8	1	0.9824

4.6.2. Compression Modules

To accurately represent the behavior of the compression forces their interaction with fill depth, compression heights, production rate and blend density were modeled. It was recognized that compression forces are affected by a combination of the amount of powder filled into the die and the height to which the powder is compressed. This combination was captured by relating the compression forces to the ratios between fill depth and compression heights. The interactions between the production rate and the compression forces were modeled using a second order transfer function followed by a

constant transport delay. The response of the production rate model was added to the response of the nonlinear compression model. An important remark is the fact that the polynomial equation that was used in the nonlinear compression was fitted against absolute values of compression ratio. Since the input variables of this model are deviation variables, it is important to convert them to absolute values before computing the polynomial calculation. A methodology to capture variations in density was also added to this model. Changes in powder density result in variations on the amount of powder being fed into the die. This behavior can be captured by linear changes in fill depth as a function of density. The modified fill depth calculation is presented in Equation 13.

$$FD^* = \frac{\rho}{\rho_{ref}} FD \tag{13}$$

where FD^* is the modified fill depth value, FD is the actual fill depth, ρ is the powder bulk density in the feed frame and ρ_{ref} is the reference value of bulk density at which the polynomial coefficients of Equation 13 were fitted.

Compression force models were developed to capture the effects of fill depth, compression heights, production rate and blend density on the compression forces. Table 5 summarizes the details and parameters of the transfer function models for critical process parameters. Table 6 presents the polynomial coefficients from Equation 11 fitted to the experimental compression force data.

Table 5. Model parameters — Critical process parameters

Model Inputs	Model Outputs	Model Details					
		Order	τ_1(s)	τ_2(s)	Θmax(s)	Gain	R^2
Pre-compression ratio	Pre-compression force	1	2.5058	-	12.5	1	0.9680
Main compression ratio	Main compression force	1	3.4244	-	15	1	0.9659

Table 6. Model parameters — Polynomial coefficients

Polynomial Constants	Pre-compression Force (–)	Main Compression Force (–)
a_1	80.92	55.97
a_2	−219.40	−150.34
a_3	149.83	101.98

4.6.3. Critical Quality Attributes Module

The critical quality attributes module calculates tablet weight and breaking force based on fill depth, density, compression forces and turret speed. Tablet weight was modeled using a first order transfer function with unitary gain followed by the weight calculation described in Equation 14 and a variable transport delay. It is important to notice that the transfer function used to model the tablet weight behavior also incorporates the dynamics of the tablet weight measurement technique.

$$W = A_p \rho F D \tag{14}$$

where W is the tablet weight, A_p is the area of the punch, ρ is the powder bulk density in the feed frame and FD is the fill depth.

Tablet breaking force is calculated using a polynomial relationship between the breaking force and main compression ratio followed by a variable transport delay. Effects of density variations on tablet breaking force were modeled using the modified fill depth approach presented in Section 4.6.2. Since no dynamic data was available for tablet breaking force, the models were based on the main compression ratio dynamics. A fixed transport delay was used to model and represent the hypothetical behavior of a tablet breaking force sensor.

The fitted coefficients used in the tablet breaking force model were $a_1 = 258.8846$, $a_2 = -695.3997$ and $a_3 = 468.2229$. The resulting transfer function model used to represent tablet weight has a gain dependent of the powder density and punch geometry, with a first order time constant of 6.5 s and a transport delay of 12 s.

4.6.4. Tablet Diversion Module

A module representing the tablet diversion system was also developed. This module quantifies the total number of tablets produced during the simulation as well as the number of tablets inside and outside specifications. The total production is computed through the integration of the production rate over time. The good production is obtained by multiplying the production rate signal by a series of logic signals coming from relay block and then integrating this overall signal over time. The relay blocks output a value of 1 (true) if the tablets are within specification and a value of 0 (false) if tablets are outside

specification. Each relay block analyzes one specific critical quality attribute (weight, hardness and API potency). The bad production is calculated by simply subtracting the good production from the total production.

Chapter 5 : Advanced Model Predictive Control Strategy for Tablet Compression

Acknowledgements

This chapter is based on following manuscript previously published by the authors which is highly acknowledged [54]". The use of the manuscript as the core element of this chapter has been authorized by the co-authors. The author has contributed to in the elaboration of the manuscript, development of the model described in the publication, and execution of the experiments.

F. Nunes de Barros, A. Bhaskar, and R. Singh*, "A Validated Model for Design and Evaluation of Control Architectures for a Continuous Tablet Compaction Process," *Processes*, vol. 5, no. 4, p. 76, 2017.

This work is supported by the Rutgers Research Council through grant 202342 RC-17-Singh R, the US Food and Drug Administration (FDA) through grant 11695471, Glaxo

Smith Kline (GSK) through grant AWD00002346 to Singh, and National Science Foundation Engineering Research Center on Structured Organic Particulate Systems.

*Corresponding author (Email: ravendra.singh@rutgers.edu)

5.1. Materials and Methods

Controller tuning, and closed loop experiments performed in this chapter were based on the same formulation described in Chapter 3. Matlab and Simulink were used as the simulation platform for the control system evaluation through virtual experiments. Two built-in Matlab toolboxes, Control System Toolbox and MPC Toolbox, were used throughout this chapter for design of control strategies.

5.2. Controller Tuning and Implementation

Both controller tuning methods presented in this section make use of a linearized process model. The linearization point at which the controllers were tuned are given in Table 1.

Table 7. Linearization points for controller tuning

Variable	MCF (kN)	PCF (kN)	Tablet weight (mg)	Tablet breaking force (kN)
Linearization point	10	5	400	40

MCF: Main compression force; PCF: Pre-compression force

5.2.1. Tuning and Implementation of PI Controller

The PI controller implemented in this work was tuned according to the modified SIMC method presented by Skogestad [61]. This method consists of a rule based tuning approach that considers both controller performance and robustness. One of the advantages

of the SIMC method is that only one parameter (τ_c) needs to be adjusted. Lower τ_c values lead to a tighter controller with better performance. On the other hand, controllers tuned with higher values of τ_c are smoother and more robust. The value of $\tau_c = 21.03 \cong \theta$ was used to tune the only PI controller implemented in this Chapter, yielding the following tuning parameters: $K_c = 0.0204$ and $\tau_I = 0.0019$. The selected value of τ_c followed the guidelines recommended by Skogestad as the tightest value that maintains a smooth control.

The implementation was achieved in Simulink using the PID block. When a linear control algorithm such as PI is used to control nonlinear processes, it is necessary to ensure that the process is within the controller operational range before close loop operation is started. For this reason, a Switch block was placed before the controller block allowing the transition from open loop operation to closed loop operation to take place once the operational range is reached. The signal coming from the Switch block is connected to the PID block tracking signal (TR). This signal is used by the controller to cancel out any action taken by the controller during open loop operation. Back-calculation was selected as the anti-windup method, avoiding saturation of the integral action when the output of the controller is constrained.

5.2.2. Tuning and Implementation of MPC

Model predictive control uses a linearized process model to make predictions of the future states of a multiple input-multiple output system (MIMO). An important aspect when developing an MPC is the generation of a linear model that can accurately represent the process behavior at an operational point.

Pre-compression and main compression forces are two of the controlled variables evaluated in this section which are nonlinear in nature. This nonlinearity is described in Section 4.4 and can be characterized by a transfer function with a gain that is dependent on the compression ratio being applied to the system at a given instant. Upon differentiation of Equation 11 it is possible to obtain the gain of this transfer function at any operational point (Equation 15).

$$k(r) = \frac{d}{dr}(a_1 r^2 + a_2 r + a_3) \qquad at\ r = R \tag{15}$$

where R is the value of the compression ratio where the system is linearized, and k is the gain of the system.

The transfer function containing this linearized gain and the previously regressed time constants is then used to replace the nonlinear Simulink model. The order of the Pade approximation for all transport delays is set to 30. The inbuilt MPC controller design toolbox is then used to generate a controller containing finite impulse response (FIR) model of the system. The value of control horizon, prediction horizon, penalty on move, and penalty on error of the controller can be adjusted during this step. In order for the controller to be able to handle unmeasured disturbances, an integrated white noise model can be added to the system. Table 8 presents the tuning parameters for all the MPC controllers used in this Chapter.

Table 8. MPC tuning parameters

Controller	Ts (s)	P (Samples)	M (Samples)	Output Weight		Input Rate Weight	
				CV 1 (-)	CV 2 (-)	MV 1 (-)	MV 2 (-)
MCF	1	40	2	1	-	0.1	-
Strategy 1	1	25	2	0.135	0.135	0.739	0.739
Strategy 2—Master	4	20	2	1	1	0.1	0.1
Strategy 2—Slave	1	25	2	0.135	0.135	0.739	0.739
Strategy 3—Master	4	20	2	1	1	0.1	0.1
Strategy 3—Slave	4	20	2	1	-	0.1	-

Ts: Sampling time, P: Prediction horizon, M: Control horizon, CV: Controlled variable, MV: Manipulated variable

Key configurations were necessary to ensure the proper operation of the MPC block in Simulink. Similar to what was done for the PID controller, a switch was added to allow the transition from open to closed loop operation, with the only difference that the signal from the switch was sent to the controller block through the *MV target* port. It was also necessary to set the order of the Pade approximation of the transport delays to 30.

5.3. Design and Evaluation of Control Systems

Three different control strategies were developed and evaluated with the goal of ensuring that the critical quality attributes of the tablet compaction process were maintained at their desired values. These strategies were evaluated under two different scenarios, which consisted of a set point tracking experiment and a disturbance rejection experiment, where variations in powder density were used as an unmeasured disturbance. The variations in density applied to the system had the form of a white noise disturbance, followed by a ramp disturbance and a step change (Figure 11).

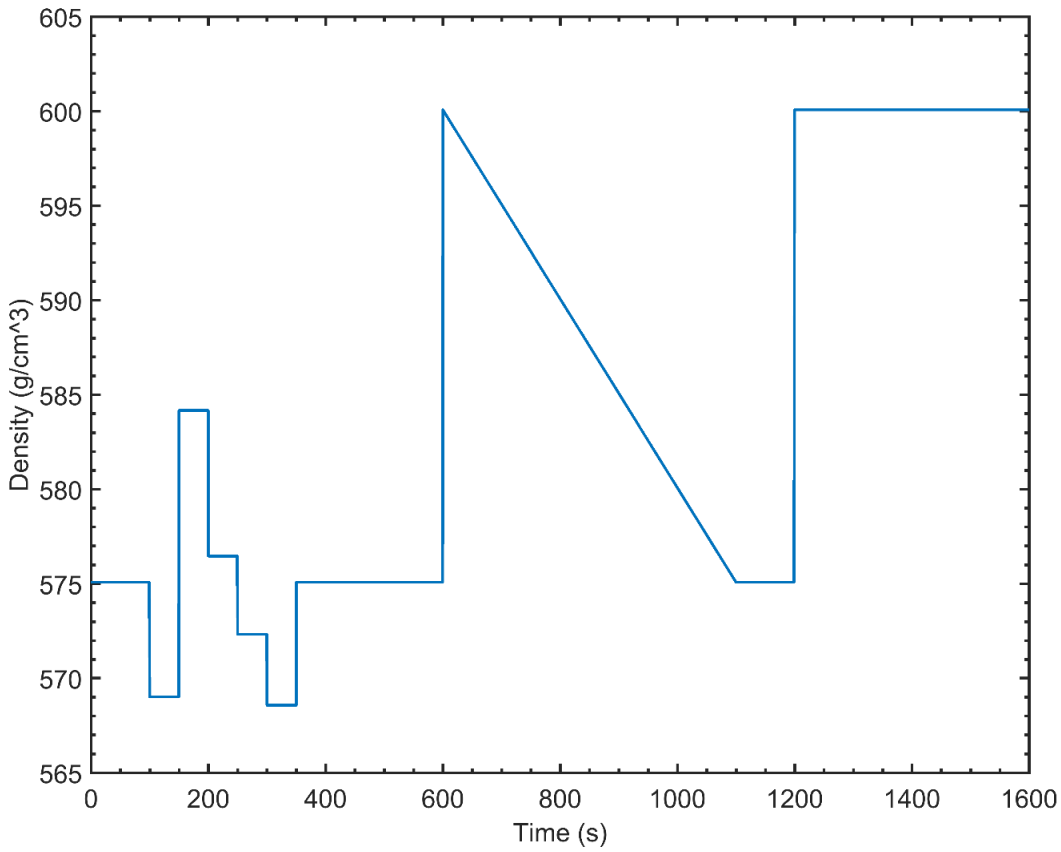

Figure 11. Density variations for disturbance rejection.

5.3.1. Strategy 1 – Simultaneous Control of Pre- and Main Compression Forces

A control strategy for simultaneously controlling pre- and main compression forces through fill depth and main compression height using a MIMO MPC has been evaluated. From a review of the mechanisms behind the compression process, it has been postulated that tablet weight and breaking force can be indirectly controlled through the pre- and main compression forces, respectively, using this strategy. This strategy was also implemented in the pilot plant. The experimental implementation was used to validate the applicability of the developed model.

Currently, it is not feasible to measure tablet weight and hardness in real time with enough precision to allow strategies 2 and 3 to be implemented in the pilot plant. For this reason, these strategies were only evaluated in a simulation environment.

5.3.2. Strategy 2 – Cascade Control of Weight and Tablet Breaking Force

If sensors for both tablet weight and breaking force are available, it is possible to control these variables using a cascade arrangement, where the slave controller uses the strategy described in Section 5.3.1. The master controller provides the pre- and main compression force set points to the slave controller in order to track the tablet weight and breaking force. The performance of this strategy is heavily dependent on the sampling rate of the sensors.

5.3.3. Strategy 3 – Direct Control of Weight and Tablet Breaking Force

The possibility of controlling tablet weight directly through fill depth and tablet breaking force in a cascade arrangement might be desired if a fast sensor for tablet weight is available. Such sensor has been previously developed and implemented as a proof of concept in a previous work [17]. This strategy consists of a SISO MPC for main compression for which actuates on the ratio between fill depth and main compression height. This is used to calculate main compression height based on fill depth values, thus minimizing the variations in main compression force cause by changes in fill depth. A secondary MPC is used to control tablet weight and breaking force through manipulations in fill depth and main compression force setpoint.

Chapter 6 : Framework for Implementation of Residence Time Distribution Based Diversion System

Acknowledgements

This work is supported by the US Food and Drug Administration (FDA), through grant 5U01FD005535 and National Science Foundation Engineering Research Center on Structured Organic Particulate Systems.

6.1. RTD Based Diversion System

Tablets have been traditionally classified as good (within specifications) or bad (out of specifications) based on offline measurements of representative samples. Several assays based on tablet samples are necessary to ensure product quality and must be satisfied before releasing the tablets into the market. However, there are no methods and tools available that can be used for real time assurance of tablet quality. Recently, the use of spectroscopic tools for the real-time monitoring of blend and tablet composition has increased in popularity [62]. Although NIR measurements have proven suitable for online monitoring of blend composition, monitoring of tablet composition is still not reliable or fast enough for real-time diversion applications. Blend composition measurements prior to the compaction operation can yield accurate results and are a common practice in continuous manufacturing, but a framework describing how to proceed in case the blend composition is out of specification has not yet been established.

The logical solution to this problem would be to detect if the incoming blend is out of specification and simply reject tablets after a pre-determined time delay. This solution

would ensure that all tablets containing the out of specification blend are appropriately rejected, but it could also result in the rejection of tablets that are within specification. To overcome this issue, a methodology for tablet rejection based on the real-time prediction of API concentration in tablets using RTD approach has been developed [63]. Figure 12 presents the main concept of RTD based control system, where the input and the residence time distribution of the system are used to predict the API concentration in tablets. The tablets are diverted based on this predicted concertation. In this work, the RTD based diversion methodology has been implemented in a direct compaction pilot plant.

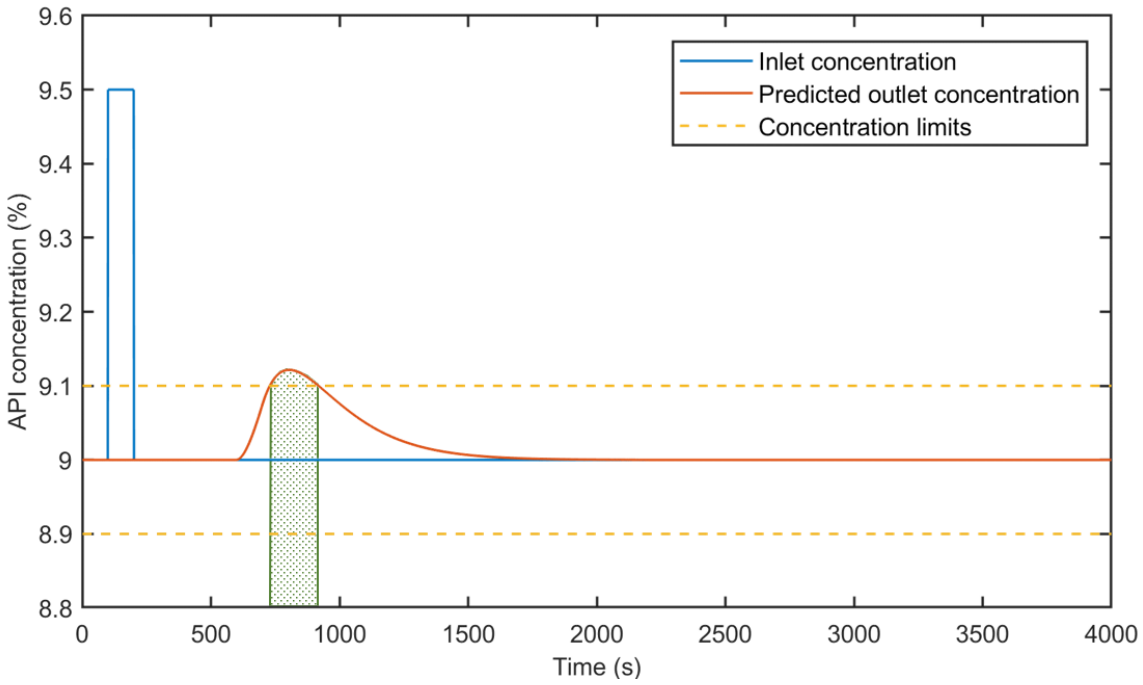

Figure 12. RTD based diversion methodology. The area highlighted in green represents the diverted tablets.

6.2. Systematic Framework for Implementation of RTD based Diversion System

A systematic framework has been developed to guide future implementations of diversion systems based on RTDs. This framework has been generalized to be implemented around any set of unit operations.

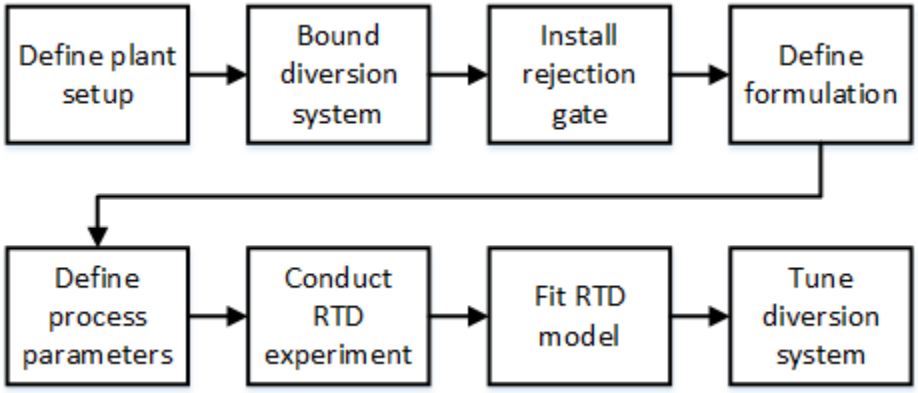

Figure 13. Systematic framework for implementation of RTD diversion system.

It is known that the residence time distribution of a system is characteristic of its unit operations. Hence, the plant setup needs to be defined before any RTD determination efforts occur. Even slight changes in setup of the plant can have a strong influence on the RTD of the system (e.g. using a chute with larger dimensions can completely change the RTD). It is also important to establish the type and location of the PAT sensors. Once the plant configuration is fixed, the boundaries of the rejection system must be defined. The downstream boundary should be chosen based on the closest location, downstream of the unit operation producing undesirable products, where the diversion gate can be installed. The upstream boundary is dependent on the closest PAT sensor upstream of the unit operation.

The installation of the diversion gate and its integration with the control system starts with the definition of the kind of actuation used to operate the gate. Most commercially available systems have either electric or pneumatic actuation. Both systems make use of a solenoid operated through a relay controlled by the control system, with the only difference that the pneumatic gates also require a compressed air line. Once the gate

is installed, it is necessary to understand any transport delays between the actuation in the control system and the actual actuation in the gate. This delay must later be incorporated in the RTD of the system.

As previously mentioned, RTDs are heavily influence by material flow properties and process parameters. An RTD is only valid for the formulation and processing parameters at which the experiments were conducted, and extrapolations are rarely valid. For this reason, the next two key steps in the framework are fixing the powder formulation to be used and fixing any process parameters that can influence the mixing or the mass flowrate of the system.

The most important step in the implementation of the tablet diversion system is the experimental determination of the system's RTD. This step is an area of research in itself and multiple studies have been published on various unit operations [41], [43], [46], [47]. Tracer selection is an important aspect when conducting RTD experiments. The selected tracer must have similar flow properties as the bulk formulation, while still being easily detectable. The RTD determination of a tablet press feed frame has been described in detail in Chapter 3. A few detection techniques can be highlighted including, colorimetric techniques, detection based on concentration, density, and detection of radioactive tracers. Two other important considerations when describing the mixing of a unit operation are the sampling technique and the type of disturbance applied to characterize the system (step or pulse). The rate at which samples are collected must produce a manageable number of samples, while still being frequent enough to ensure that all the information about the mixing is captured, especially at the beginning of the experiment when the slope of the tracer concentration profile is more accentuated. The choice between a step or a pulse

experiment depends on the amount of tracer available. Step changes are easier to realize and detect but require more tracer and can yield inaccurate RTDs if the tracer is inappropriately selected. Pulses are harder to achieve and detect but have the advantage of requiring less tracer and yielding a more accurate RTD.

The last steps in the framework involves fitting an RTD model to the experimental data and tuning the diversion system. Model fitting is done to obtain a clean RTD, without noise, that represents the system. The key aspect to be considered during fitting is the type of model being used. The two main models are tank-in-series and dispersion, and their usage depends on the system being modelled [55]. The procedure for fitting an RTD model has been described in detail in Section 3.5. Once the model is obtained and integrated, the tuning of the diversion system occurs. In this step, the safety margin of the RTD prediction is determined. This margin can be tuned by tightening the nominal limits for diversion by a tuning constant.

6.3. Integration of Diversion Mechanism

The integration of a diversion mechanism was necessary to divert the bad production from the total production. A rejection mechanism consisting of a gate actuated using a solenoid coil was already installed in the tablet press, but its control was not available to the end user (Figure 14). To overcome this issue, the coil was wired directly to the control platform through a 24 VDC discrete output port, which can be operated using the control system.

The signal sent to the discrete output port is generated in a DeltaV control module using a *discrete output* (DO) block. This block references the physical address of the port

in the control system and can assume values of 1 or 0 according to its input. The inputs received from the DO block can be set locally by the user or remotely by another control module. When a signal of value 1 is sent to the diversion mechanism, 24 VDC current flows through the solenoid causing the position of the diversion gate to change, once the signal reverts back to 0, the gate returns to its original position.

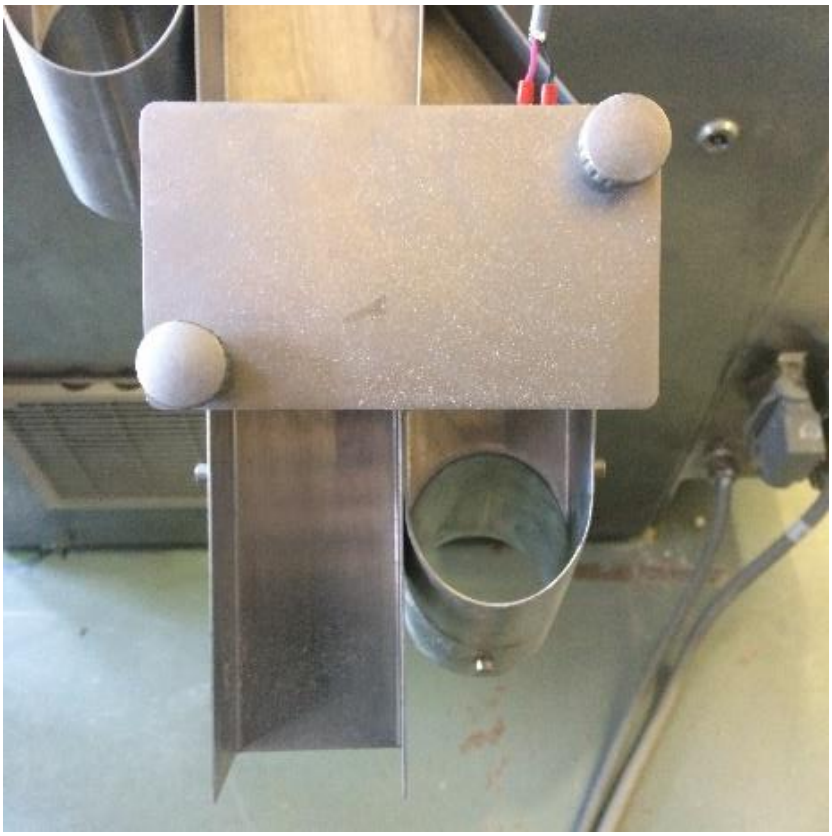

Figure 14. Tablet diversion mechanism.

6.4. Real-time prediction of concentration in DeltaV

Real-time prediction of API concentration in tablets has been implemented based on the convolution of the residence time distribution with the inlet concentration in the tablet press. This concept of concentration predictions using convolution has been

described in detail by Engisch & Muzzio but had not yet been implemented in real-time on an experimental setup [35].

In the referenced paper, the authors used the *conv* function built into Matlab to successfully compute the convolution integral. Although no pre-existing tools for calculation of the convolution integral were available in the control system that was used in the experiments, it was noticed by the authors that a finite impulse response (FIR) filter could be used to emulate the results obtained through the *conv* function. A FIR filter is available through the *MPC Simulate* block in the control platform. In this implementation, the cumulative residence time distribution coefficients ($F(t)$) are manually entered in the *MPC Simulate* block as the FIR coefficients.

The FIR coefficients used by the *MPC Simulate* block are loaded through a text file using DeltaV MPC Predict tool. This text file consists of a standard heading pre-defined by DeltaV. In this heading it is possible to select the sampling rate, in seconds, of the MPC block. The file also contains a series of 120 coefficients which represent the discretized values of the $F(t)$ curve used in this implementation. Figure 15 exemplifies this implementation and demonstrates the interchangeability of the convolution and FIR methodologies when subjected to a simulated input.

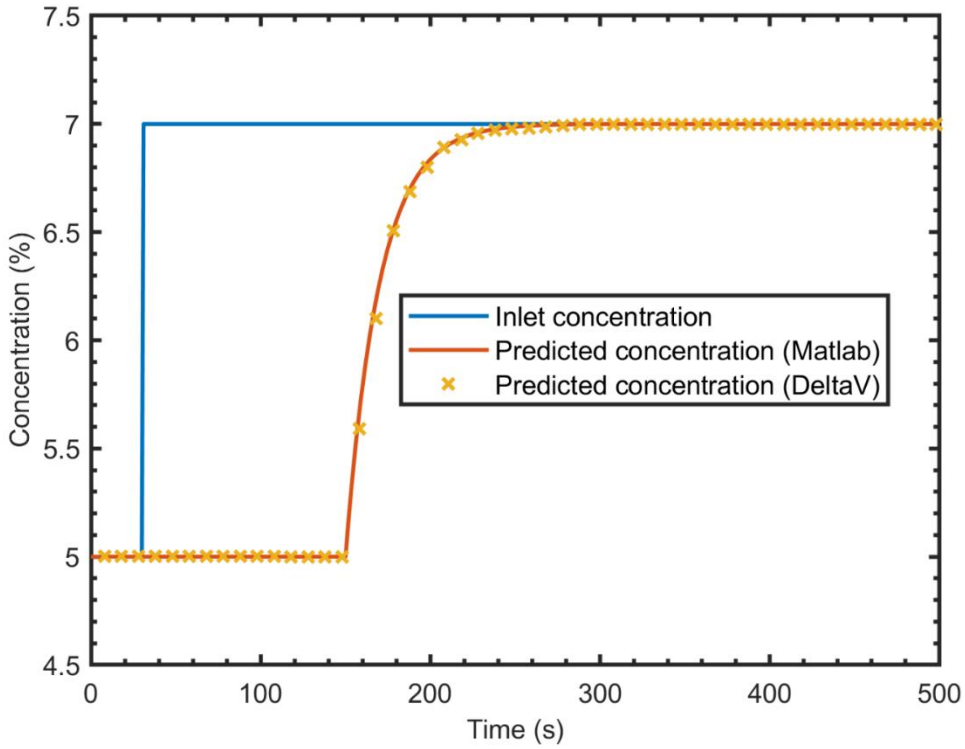

Figure 15. Comparison between convolution in Matlab and DeltaV.

The implementation of the two calculations differs slightly. When the *conv* function is implemented, the inputs are a vector containing concentration data and a vector containing the discretized RTD coefficients obtained from $E(t)$, whereas on the MPC simulate implementation, the inputs are the concentration signal and a vector containing the discretized cumulative RTD coefficients obtained from $F(t)$. Through the analysis of Figure 15, it is possible to conclude the both calculation methods yield the same results.

6.5. Diversion System Implementation

The DeltaV implementation of the diversion system control module is shown in Figure 16. An input parameter block containing a reference to the concentration value obtained through NIR is connected to the *MNPLT1* port on the *MPC Simulate* block. Inside

the MPC block, the input value is convoluted with the finite impulse response MPC model that, in the RTD convolution case, consists of a vector containing the $F(t)$ values that can be obtained through the modeling procedure demonstrated in Chapter 3. This convolution generates a prediction for the API concentration in the tablets.

The predicted concentration from RTD then goes through a *Compare* block, where it is determined if the value is inside the acceptable range. The high and low boundaries of the range are specified through the ports *COMP_VAL1* and *COMP_VAL2*. If it is defined that the API concentration in the tablets is outside specification, the *Compare* block sends a signal to divert the production until the predicted API concentration in the tablets is brought back to specification.

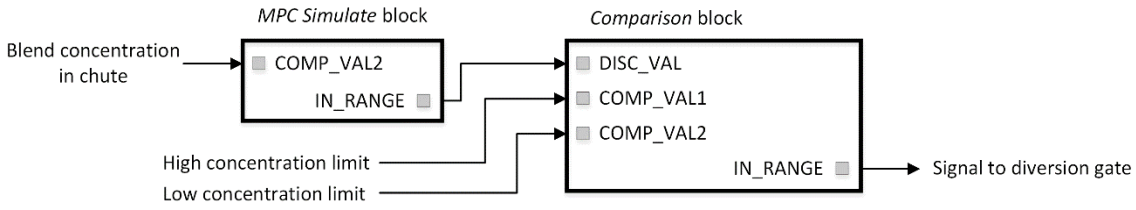

Figure 16. Implementation of diversion system in DeltaV.

A data flow diagram for the diversion system is presented in Figure 17. The diagram is centered on the control module described above, which is connected to two input and two output data streams. In order to achieve an accurate concentration prediction, the cumulative residence time distribution model coming from Matlab is discretized into 120 points and the sampling rate of this discretization is defined. This information is inputted into a text file which is then read by the prediction control module. A second data stream incoming into the control module from a spectroscopic tool consists of the API

concentration in the blend. Once the outlet concentration prediction is achieved and the rejection signal is generated in the control model, the resulting data is saved in a process historian sent to the tablet diversion mechanism.

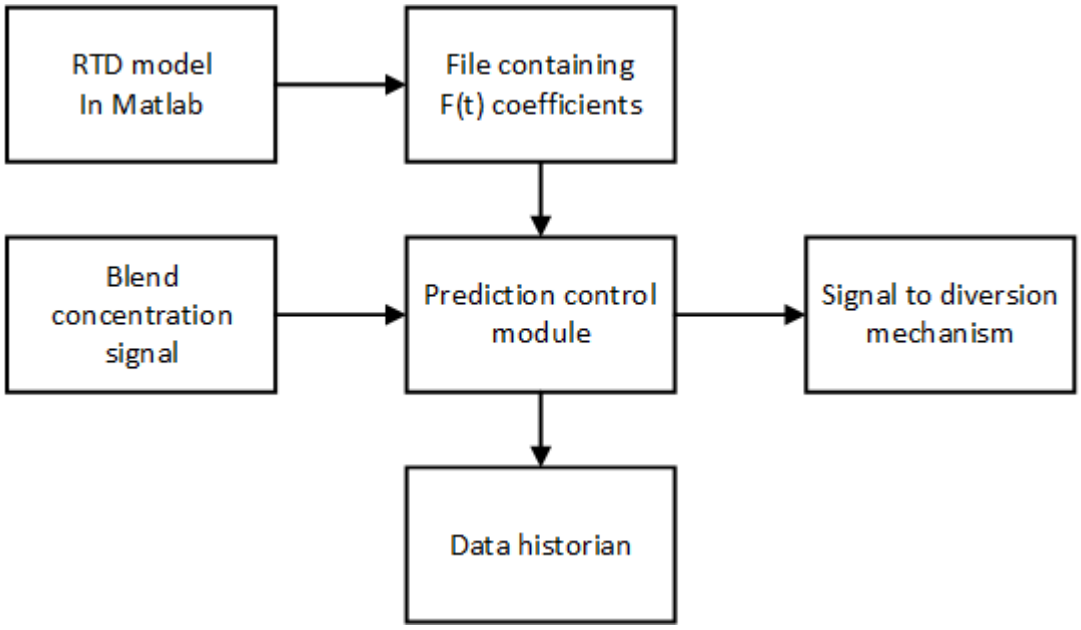

Figure 17. Diversion system data flow diagram.

Chapter 7 : Results and Discussions

Acknowledgements

Some of the results presented in this chapter has been previously published by the authors which is highly acknowledged [54]". The use of the manuscript as the core element of this chapter has been authorized by the co-authors.

F. Nunes de Barros, A. Bhaskar, and R. Singh*, "A Validated Model for Design and Evaluation of Control Architectures for a Continuous Tablet Compaction Process," *Processes*, vol. 5, no. 4, p. 76, 2017.

This work is supported by the Rutgers Research Council through grant 202342 RC-17-Singh R, the US Food and Drug Administration (FDA) through grant 11695471, Glaxo Smith Kline (GSK) through grant AWD00002346 to Singh, and National Science Foundation Engineering Research Center on Structured Organic Particulate Systems.

*Corresponding author (Email: ravendra.singh@rutgers.edu)

7.1. Experimental RTD Determination

Two tracer experiments were conducted to fit and validate the RTD model for a specific set of operating conditions. The experiments consisted of a step down in nominal API concentration from 12 % to 9 % followed by a two minutes long pulse in nominal API concentration at 12 %. The initial sample collection times for the step and pulse experiments were 320 seconds and 430 seconds from tracer injection respectively.

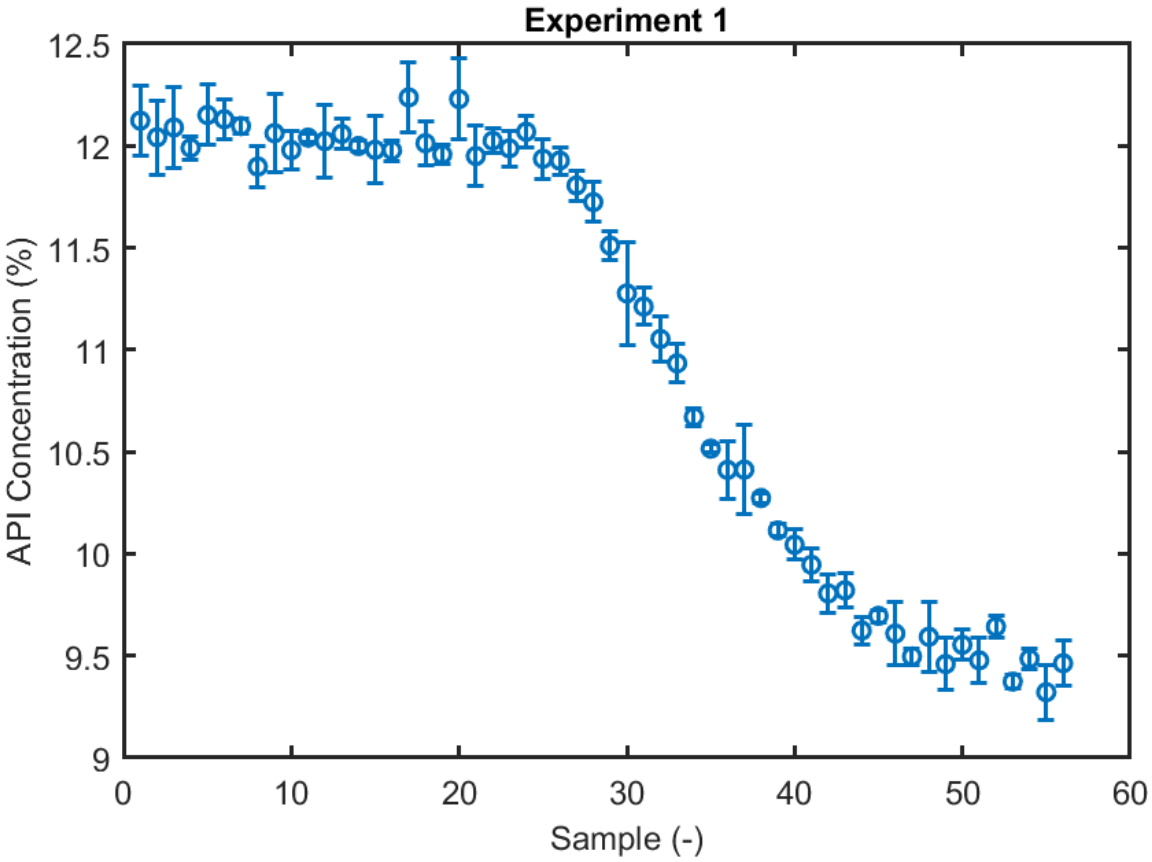

Figure 18. Tracer experiment: step change in API concentration.

The average concentrations of the samples collected during the step change experiment are presented in Figure 18, and the error bars represent the standard deviation between three tablets of each sample. From this image it can be observed that the mixing

in the feed frame presents a similar behavior to what is observed in a system composed of a higher order differential equation. It is also evident that the initial and final API concentrations do not match the 12 % and 9 % nominal concentrations at which the blends were prepared. Inaccuracies during blend preparation and an offset in the NIR calibration model have been identified as the two possible causes for this mismatch and need to be further investigated. Although the actual concentration value is different than the nominal values, it should still be possible to conduct the residence time distribution analysis based on this experiment, with the only difference being that the initial and final concentrations will be additional parameters that need to be fitted. The results of the pulse response of the feed frame are shown in Figure 19. Similar to what is observed in Figure 18, an offset is present between the nominal and actual concentrations. When the two experiments are compared, it can be noticed that there is a difference in the number of samples before the system reacts to the tracer injection. This difference is expected since there is a discrepancy between the times at which the initial sample was collected at each experiment.

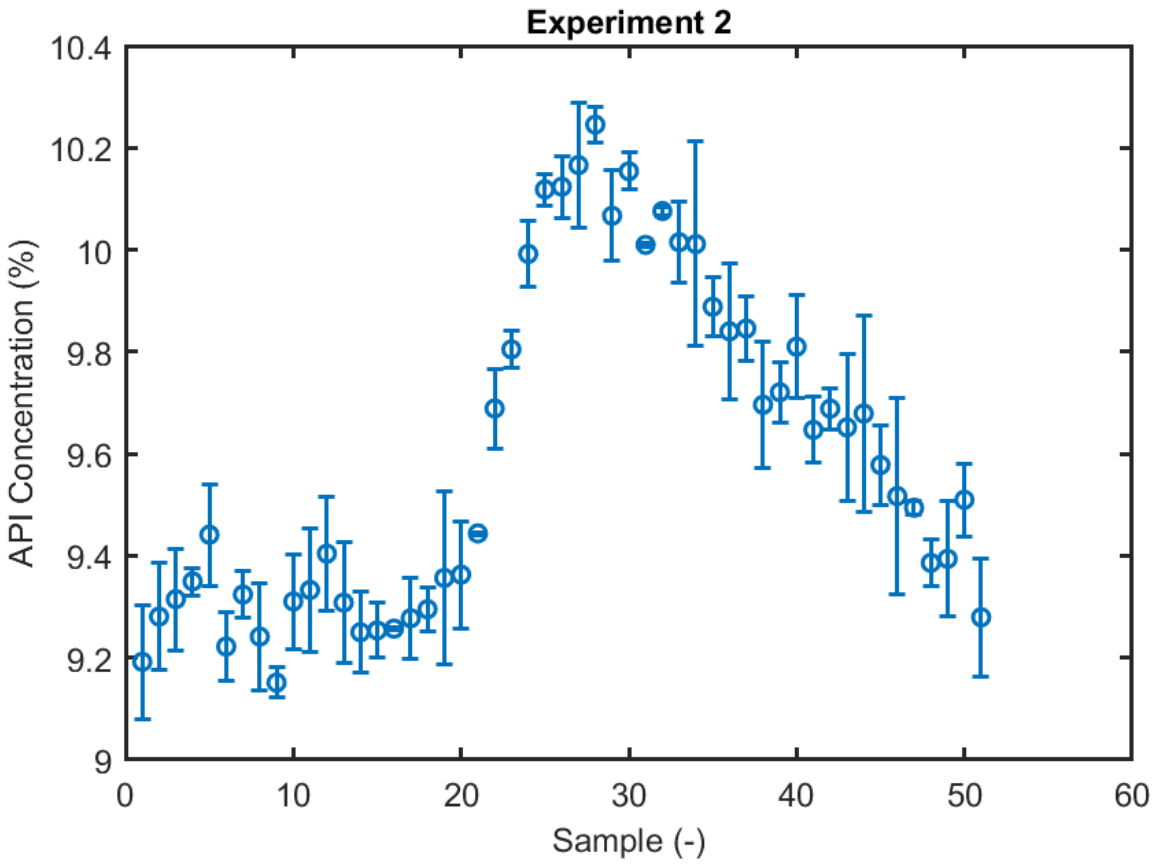

Figure 19. Tracer experiment: pulse in API concentration.

7.2. RTD Model Development

Tank-in-series and dispersion models were developed for the system based on the step experiment presented in Figure 18. The experimental data was converted to a cumulative residence time distribution curve using Equation 3 and fitting initial and final API concentrations, yielding concentration values of 9.35 % and 12.08% respectively. The resulting CRTD plot is shown in Figure 20.

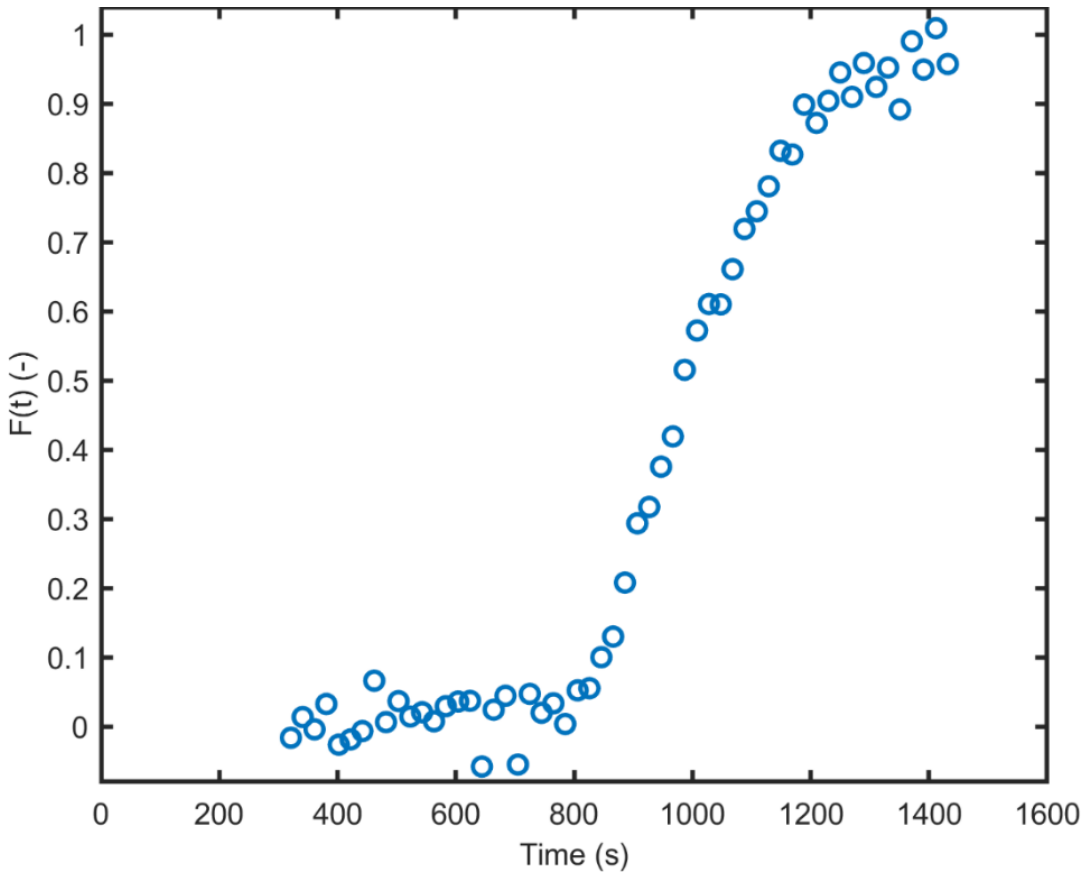

Figure 20. Experimental cumulative residence time distribution.

Through the graphical analysis of Figure 20, it can be observed that the system starts reacting approximately 800 seconds after the tracer injection and this reaction tapers off at approximately 1400 seconds. Once the experimental $F(t)$ curve is generated, the residence time distribution models can be fitted using the toolbox described in Section 3.5. The results of the model fitting procedure are presented in Figure 21, while the fitted parameters are presented in Table 9.

Table 9. Residence time distribution model parameters.

Model	Mean residence time (s)	Dead time (s)	Peclet number (-)	Number of tanks (-)	SSE (-)	R2 (-)
Dispersion	314	644	10.24	-	0.6045	0.9973
Tank-in-series	278.7	740.8	-	3	0.6105	0.9973

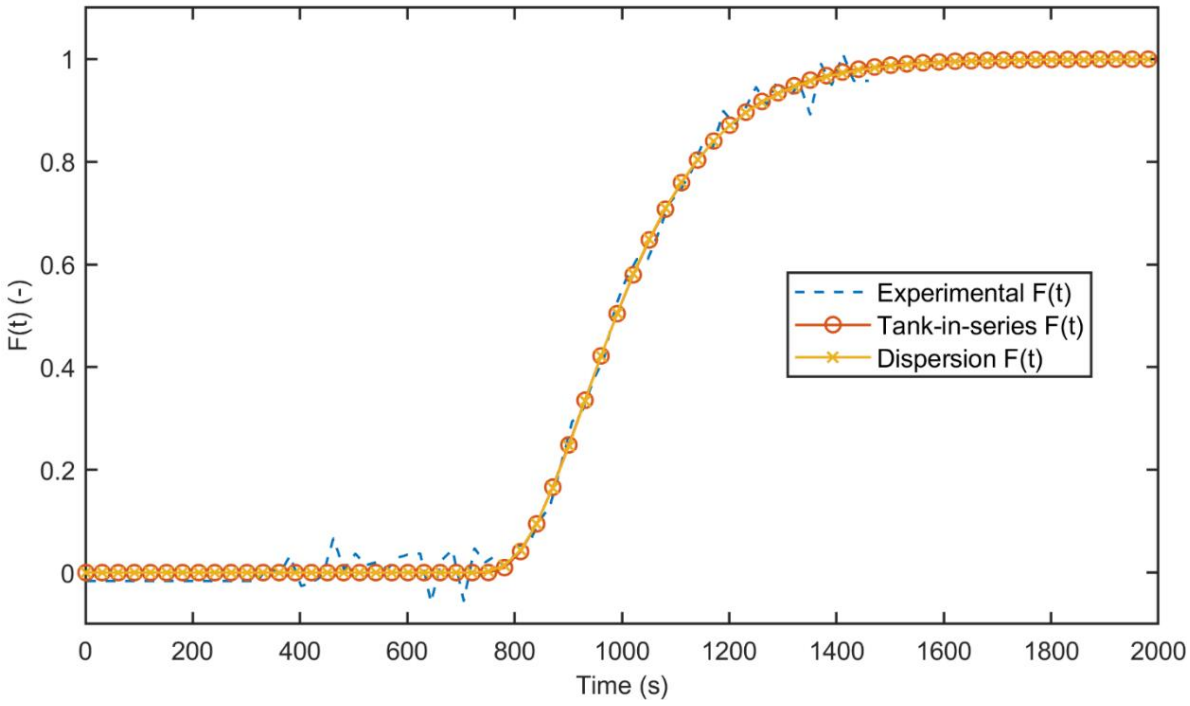

Figure 21. Residence time distribution models.

From Figure 21 it can be observed that both models yielded similar results, presenting a close fit to the experimental data. The values of the regression coefficients presented in Table 9 also support this observation. One interesting result from the model fitting procedure is that although both models resulted in almost identical residence time distributions, the fitted dead times presented a considerable difference. This result shows that the fitted dispersion model has a slower concentration buildup when compared to the tank-in-series model.

7.3. RTD Model Validation

The fitted residence time distribution models were validated using the data generated during the pulse injection experiment. To conduct this validation, the measured input concentration of tracer was convoluted with the residence time distribution curve calculated through the models. The convolution generated a prediction of the system output concentration, which was then compared to the system response to pulse injection observed during the experimental procedure. The comparison is presented in Figure 22. A small offset from the expected values was observed in both NIR models. This offset can be easily removed by adjusting the NIR model and, for this reason, the offset was fixed during post processing of the data to facilitate the comparison.

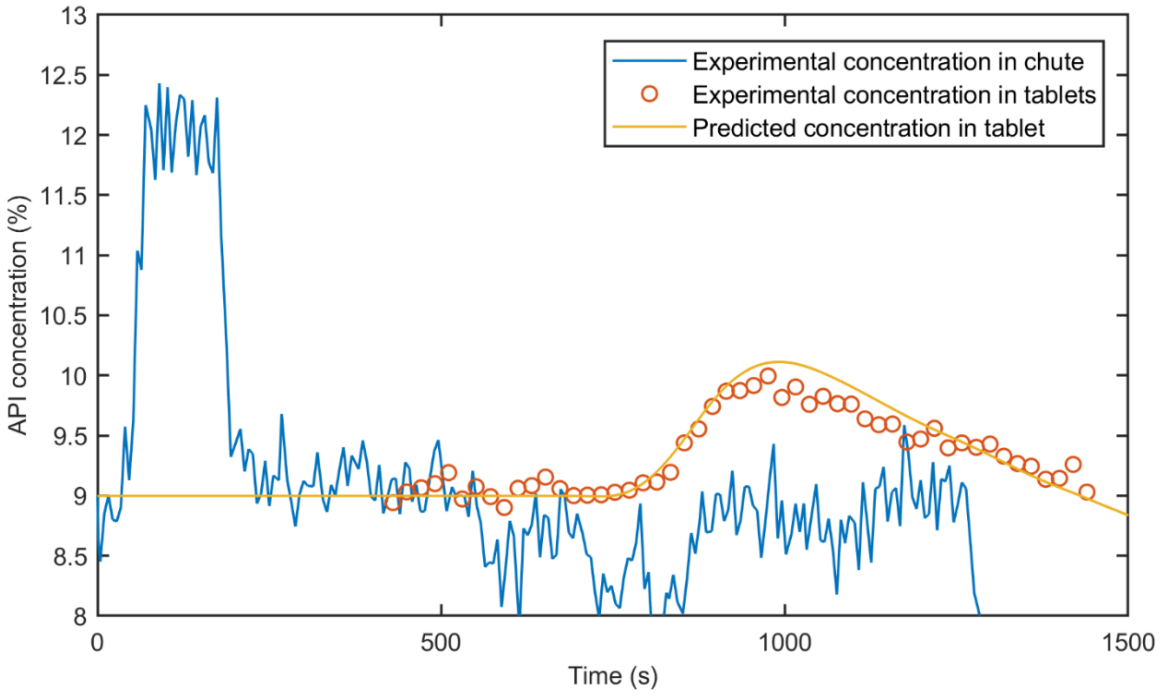

Figure 22. RTD model validation using adjusted experimental data.

From Figure 22 it can be observed that the general trend of the response to the pulse injection is captured by the prediction. Another important observation is the fact that even though the input concentration data has a fair amount of noise, the resulting concentration prediction is noise free, since the noise gets filtered by the mixing present in the feed frame. When the offset is removed, the experimental and predicted concentration values present a close relation. These results validate the proposed residence time distribution modeling strategy and framework presented in this manuscript, while also emphasizing the importance of accurate NIR calibration models.

7.4. Tablet Compaction Model Validation

The dynamics of the interactions between multiple process parameters was captured using mathematical models as described in Chapter 3. This section is organized

to demonstrate the dynamics of set point and actual actuator values, critical process parameters and their respective actuators, and critical quality attributes and critical process parameters.

7.4.1. Actuator Dynamics

Figure 25 presents the dynamics of the three main actuators in the tablet compaction process. Set point, simulated, and actual values have been plotted to show the model performance. From Figure 23 it can be concluded that the fill depth actuator model presents dynamics characteristic of a first order system. A good model fit was achieved for the fill depth model, with a coefficient of determination of 0.9966.

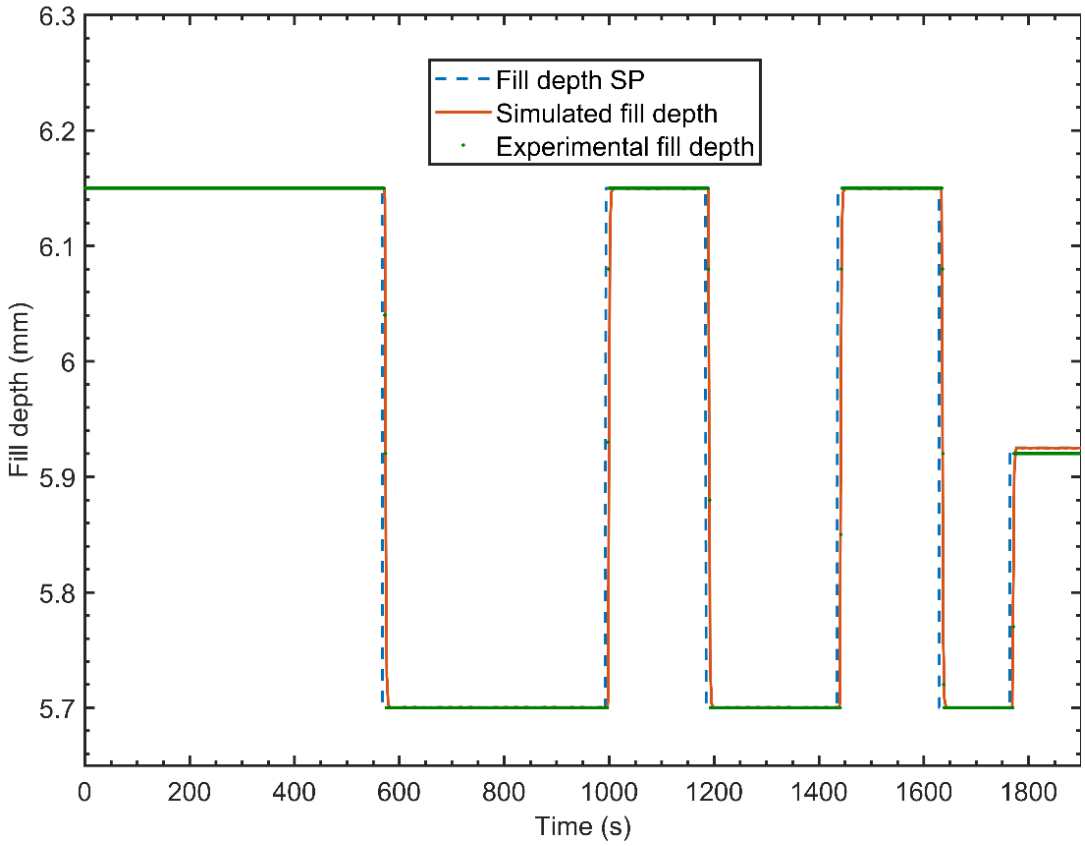

Figure 23. Fill depth model validation. SP: set point.

In Figure 24,a small steady state offset is observed in the main compression height model. This offset can be explained by the fact that the simulated results have a higher number of significant digits when compared to the experimental values. A coefficient of determination (R^2) of 0.9973 was obtained for this fit. The main compression height model parameters have also been used to calculate the pre-compression height dynamics. This assumption is made based on the fact that the main and pre-compression height actuators have the same mechanical working principle and configuration.

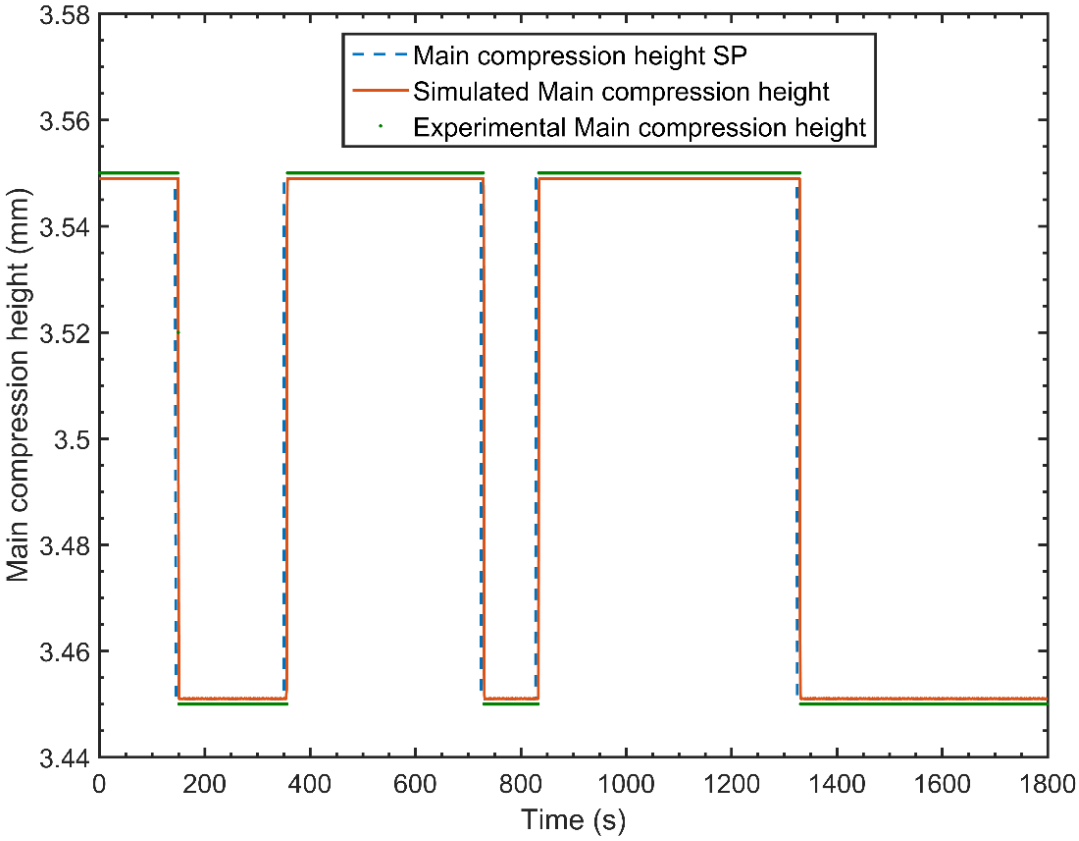

Figure 24. Main compression height model validation. SP: set point.

Figure 25 presents the validation of the production rate actuator. This model is characterized by a second order dynamic response, where a slight overshoot is observed. The model accurately captures the actuator behavior, with a high R^2 value (0.9824). This value is lower than the values obtained for the fill depth and main compression height actuators because of small oscillations present in the experimental data.

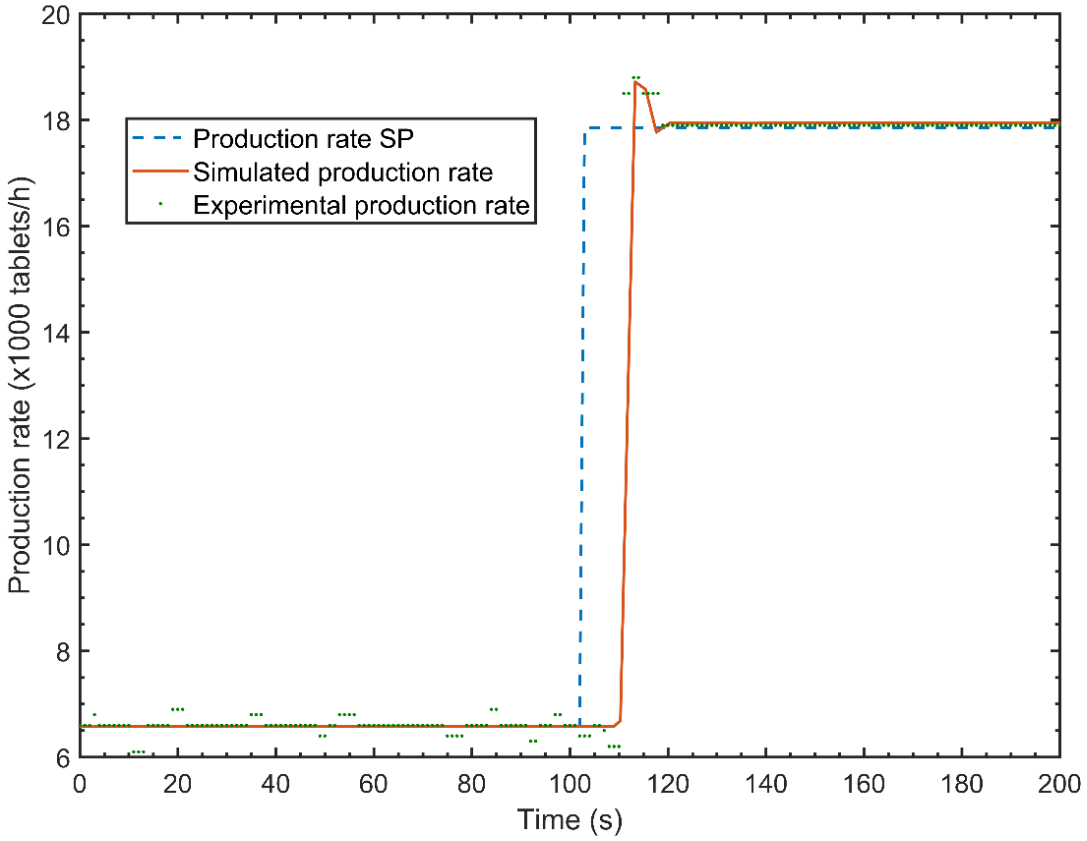

Figure 25. Production rate model validation. SP: set point.

From the R^2 values obtained for the models as well as from the presented plots, it can be concluded that the models closely match the experimental data.

7.4.2. Critical Process Parameter Interaction

Pre-compression force validation is plotted in Figure 26, which is divided in two levels. Variations in main compression ratio resulting from changes in fill depth are presented in the top plot, while the bottom plot represents the response in pre-compression force in both simulated and experimental scenarios. The fill depth variations ranged from 5.8 mm to 6.6 mm and it can be observed that the simulated system closely matched the experimental setup.

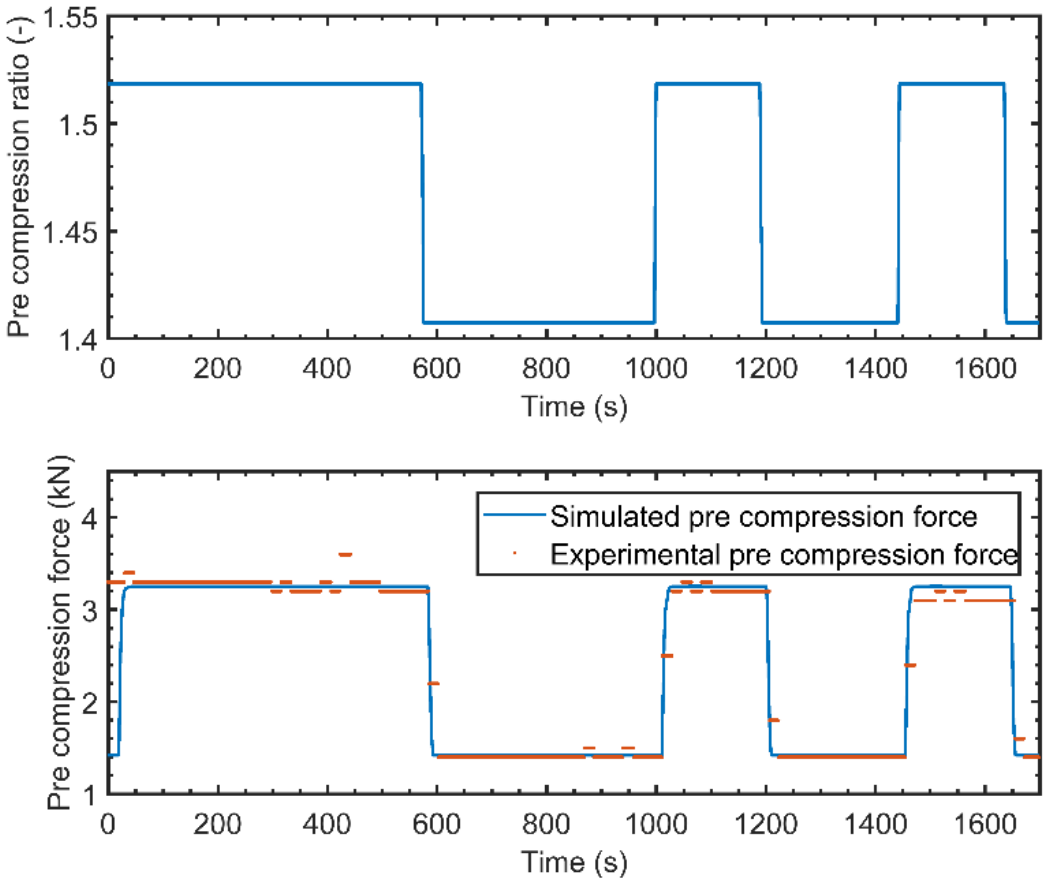

Figure 26. Pre-compression force model validation.

Figure 27 presents the main compression force response with respect to changes in main compression ratio, which were caused by actuations in the fill depth and main compression height. This model was developed in such a way to incorporate interactions between main compression height and fill depth. As expected in for the compaction process, the image shows that main compression force increases when the main compression ratio increases.

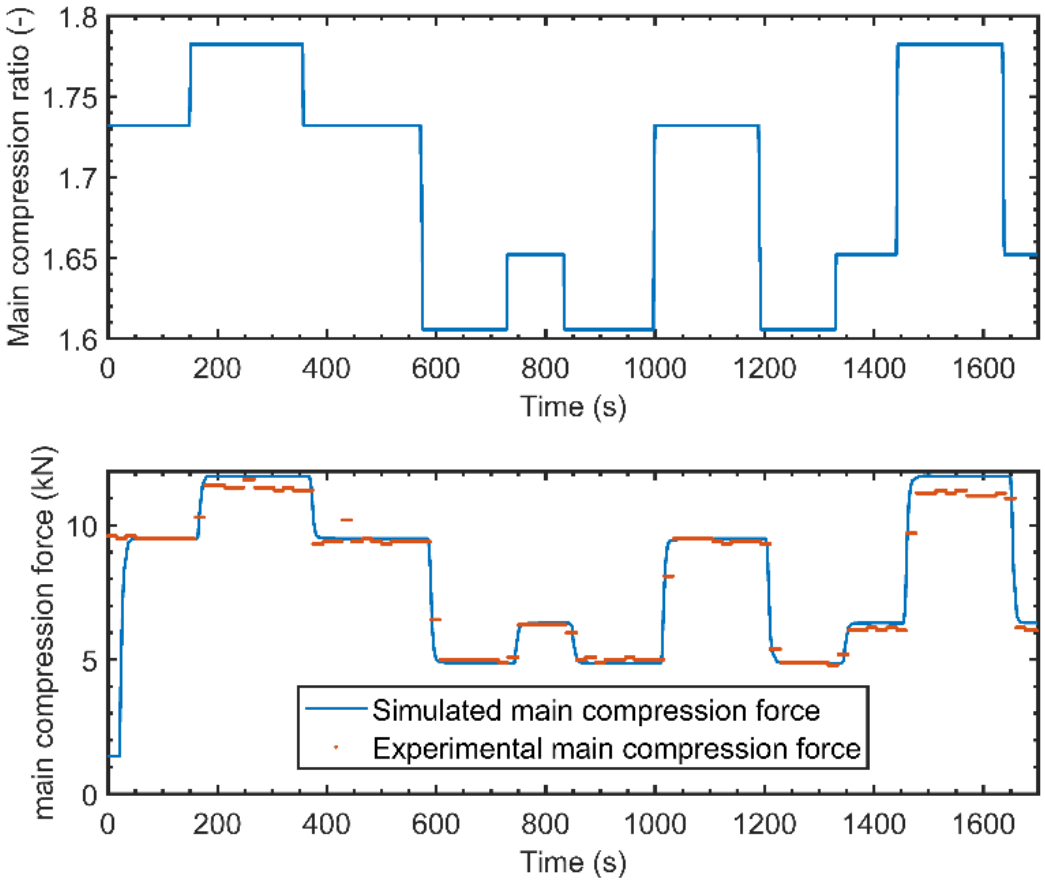

Figure 27. Main compression force model validation.

7.4.3. Critical Quality Attributes

The validation of the model relating tablet breaking force to main compression ratio is presented in Figure 28a. This model was developed based on steady state data and for this reason, the model was not validated against dynamic data. A non-linear trend between tablet breaking force and main compression ratio can be observed in this figure. Although this model is considered accurate for control system design, the inclusion of dynamic data to this representation should be a focus of future research.

The model response presented in Figure 28b was developed to predict the tablet weight and validated against experimental data. From the image it can be observed that a decrease in fill depth results in a reduction in tablet weight over time. Through regression, it was determined that this dynamic behavior can be captured by a first order transfer function.

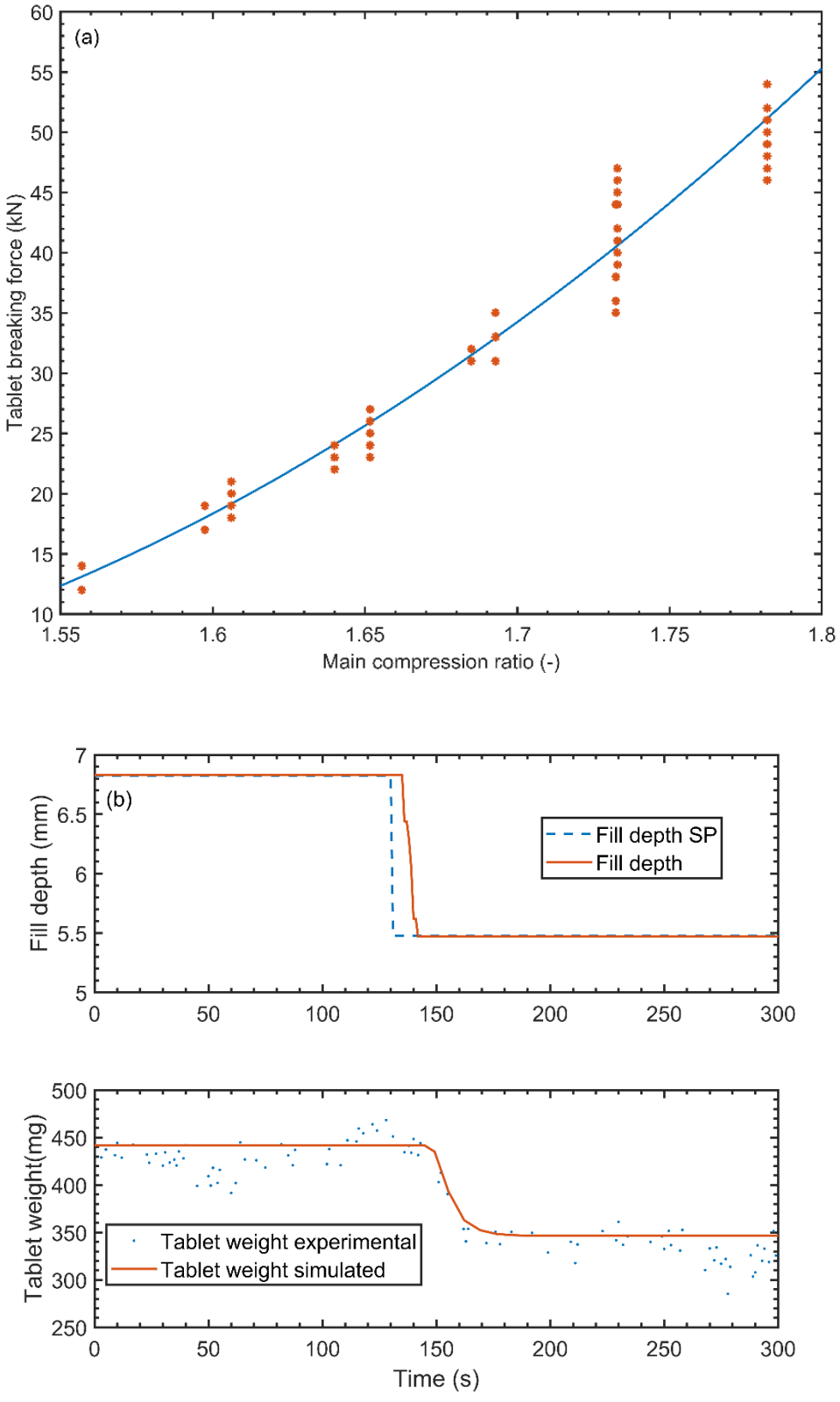

Figure 28. (a) Tablet breaking force model validation (b) Tablet weight model validation

7.5. Control System Design, Evaluation and Validation for Tablet Compaction Operation

This section exemplifies the applications of the validated model, developed in Chapter 3, for the design of control systems. The selected simulation environment provides flexibility in terms of the controls strategies that can be evaluated, reduces the time spent in experiments, consequently reducing the amount of material and expenses required to develop and implement a new control system. In the first part of this section, different control algorithms are compared in order to determine the best alternative to be used in the compaction process. Then, the selected control algorithm is used in the evaluation of various control strategies. Individual characteristics of the strategies are then discussed and guidelines for selecting the optimal control strategy for a given system are presented.

7.5.1. Control Algorithm Performance Analysis

Two steps changes in main compression force setpoint were applied to the system and the dynamic response was observed. The first step change was within the operational range at which the controllers were tuned, with an increase in MCF setpoint from 8 kN to 12 kN. The second step was from 12 kN to 4 kN and was outside the operational range of the controllers. This was done in order to evaluate the influence of the nonlinearities on the performance of the controllers.

Figure 29 show the dynamic behavior of the different control algorithm in response to changes in MCF setpoint.

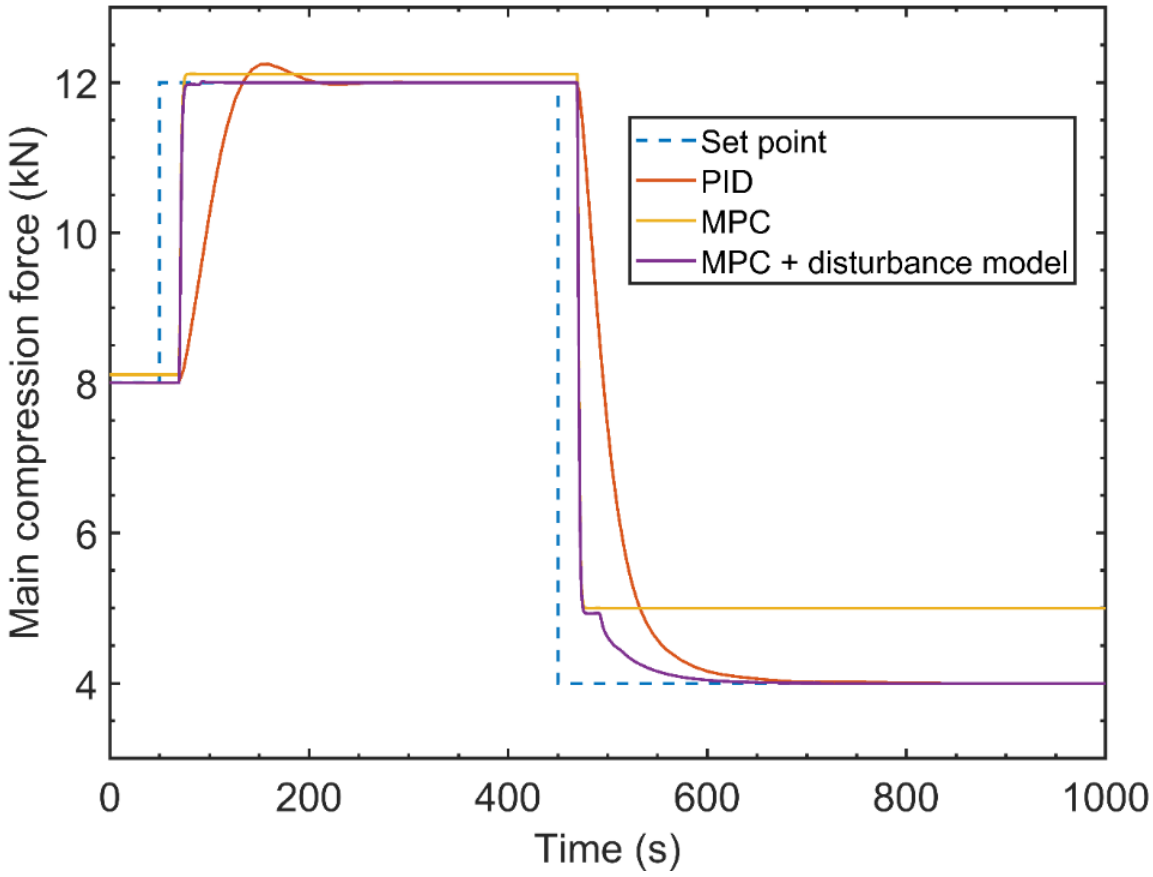

Figure 29. Control algorithm comparison.

From Figure 29, it can be observed that the percent overshoot and the time to steady state are different for the two step changes. This behavior is expected and characteristic when a linear controller is implemented on a nonlinear system. All the controller exhibited a better performance when operated within the range at which they were tuned. A significant performance increase was observed when an integrated white noise unmeasured disturbance model was added to the MPC. The unmeasured disturbance model can handle mismatches between the linear MPC model and the nonlinear behavior of the plant, eliminating the steady state offset seen in the standard MPC. These mismatches become more significant as the setpoint moves away from the operational range of the controller.

A comparison between the PI controller and the MPC with unmeasured disturbance leads to the conclusion that the latter presents a better performance, with a smaller response time and less overshoot.

The simulations were replicated in the pilot plant using the PI and MPC algorithms available in the control platform (DeltaV). For this comparison, only the step change from 8 kN to 12 kN was considered. Figure 30 shows the results of this comparison. The superiority of the MPC over the PI algorithm was again verified. A small difference between the experimental and simulated results. This difference is expected, as the controllers used in the experimental setup followed the auto-tuning routine available in the control platform, which differed from the tuning method used in Simulink.

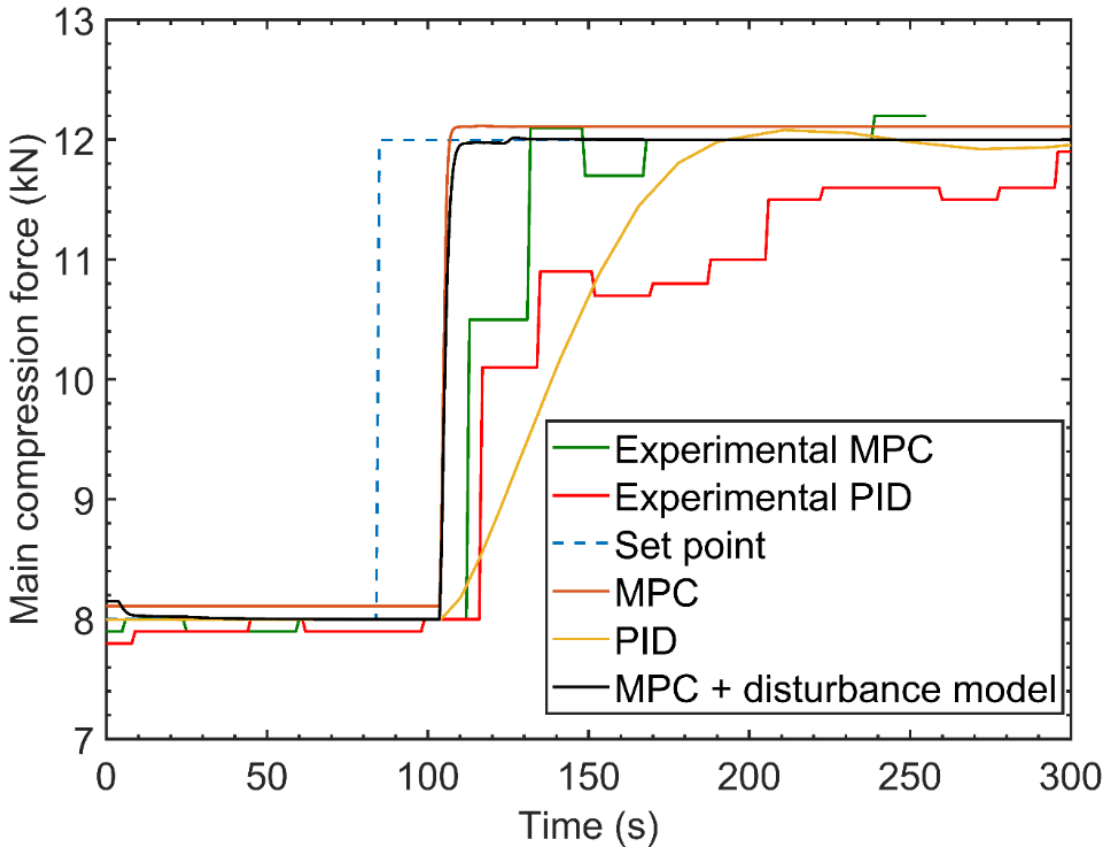

Figure 30. Simulated and actual close loop responses.

Performance metrics for both simulated and experimental control algorithms are presented in Table 10. The MPC control algorithm will be used in the subsequent simulations and experiments conducted in this Chapter, since it presented a superior performance when compared to the PI algorithm.

Table 10. Closed loop performance metrics

Strategy	IAE (kN.s)	ITAE (kN.s)	ISE (kN.s)	Rise time (s)	Settling time (s)	Overshoot (%)	Steady state error (%)
Experimental PID	289.95	18506	693.45	121	211	0	0
Simulated PID	204	6596.2	626.48	64	120	6.1112	0

Experimental MPC	180.5	5688.6	564.33	46	153	0	-7.5
Simulated MPC	111.655	5216.2	317.788	23	24	0	2.7782
MPC with disturbance model	86.83	954.49	333.68	23	25	0.448	0

7.6. Control Strategy Evaluation

7.6.1. Strategy 1 – Simultaneous Control of Pre- and Main Compression Forces

The set point changes applied to the simulated system with pre- and main compression force control and the respective response in these variables are presented in Figure 31a. The actuation signal generated by the controller is presented in Figure 31b. From the figures it can be observed that both compression forces are able to track their respective set points through the controller actions. As expected, changes in main compression force set point do not affect the pre-compression force, since the actuation occurs after the pre-compression station. In the case of an open loop scenario, manipulations in fill depth (PCF actuator) would lead to large variations in both compression forces. When changes in pre-compression force setpoint occur, a direct actuation in fill depth is generated. This actuation is then compensated with actions in main compression height in order to mitigate the effects on main compression force. This behavior is an indication that the controller model is able to successfully capture the interactions between manipulated and controlled variables.

Figure 31c shows the effects that the changes in the set points of the compression forces have in tablet weight and breaking force. Direct interactions between tablet weight and pre-compression force as well as between tablet breaking force and main compression

force can be observed, indicating that the tablet CQAs can be indirectly controlled to the compression forces' setpoints.

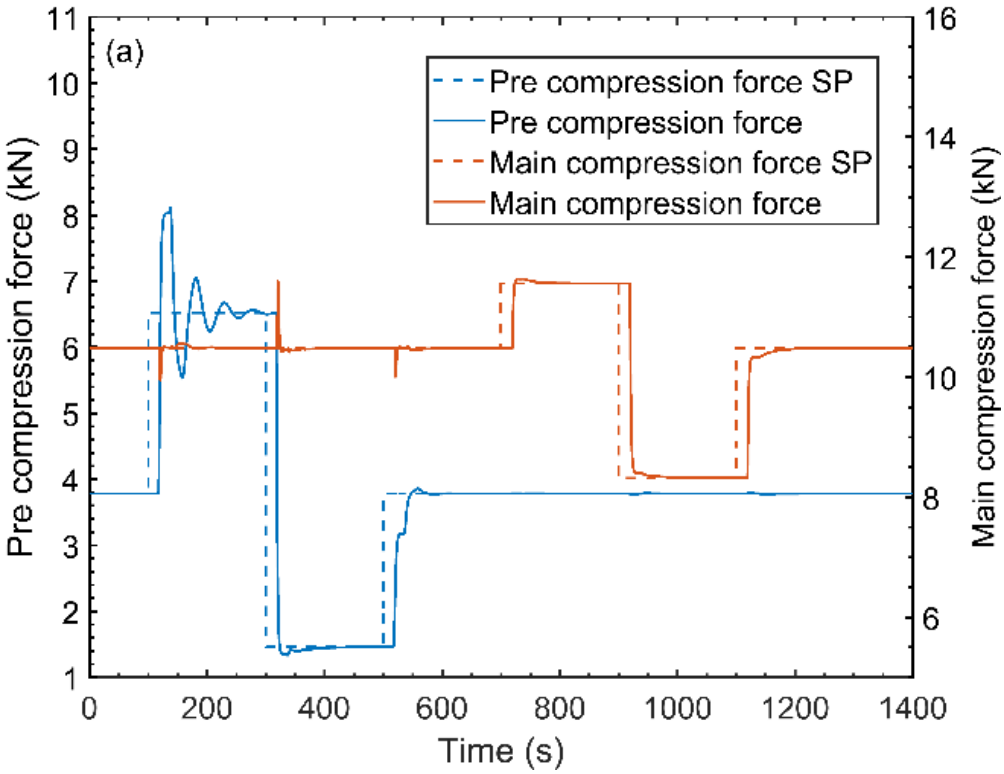
(a)
Pre compression force SP
Pre compression force
Main compression force SP
Main compression force
Pre compression force (kN)
Main compression force (kN)
Time (s)
11
10
9
8
7
6
5
4
3
2
1
16
14
12
10
8
6
0
200
400
600
800
1000
1200
1400

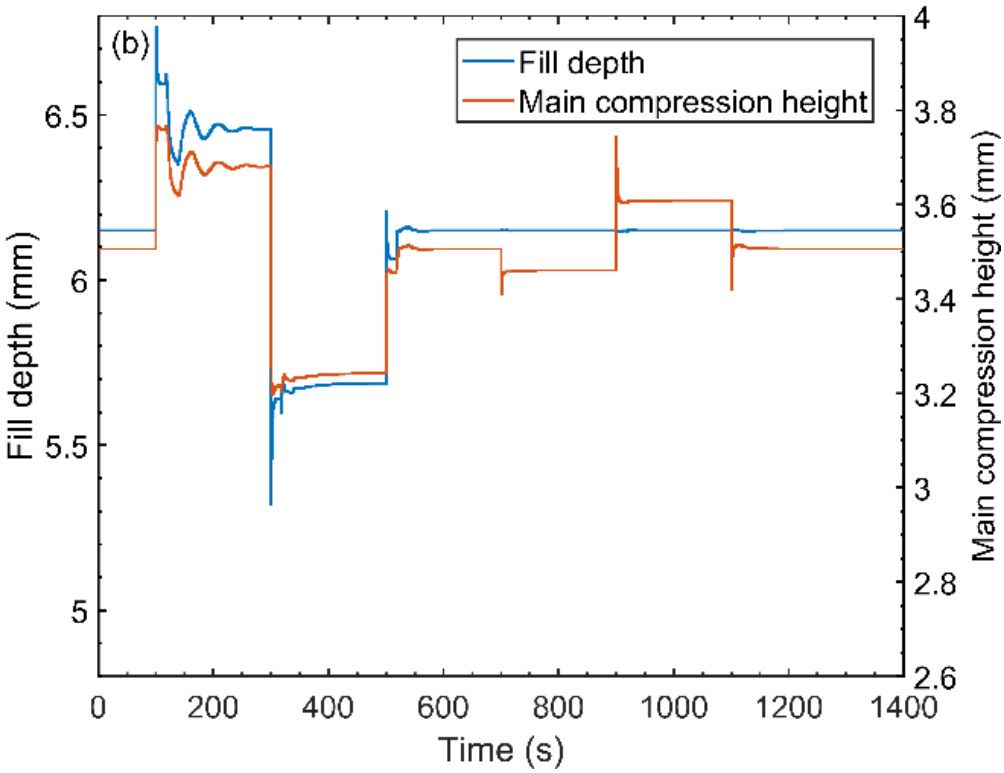
(b)
Fill depth
Main compression height
Fill depth (mm)
Main compression height (mm)
Time (s)
6.5
6
5.5
5
4
3.8
3.6
3.4
3.2
3
2.8
2.6
0
200
400
600
800
1000
1200
1400

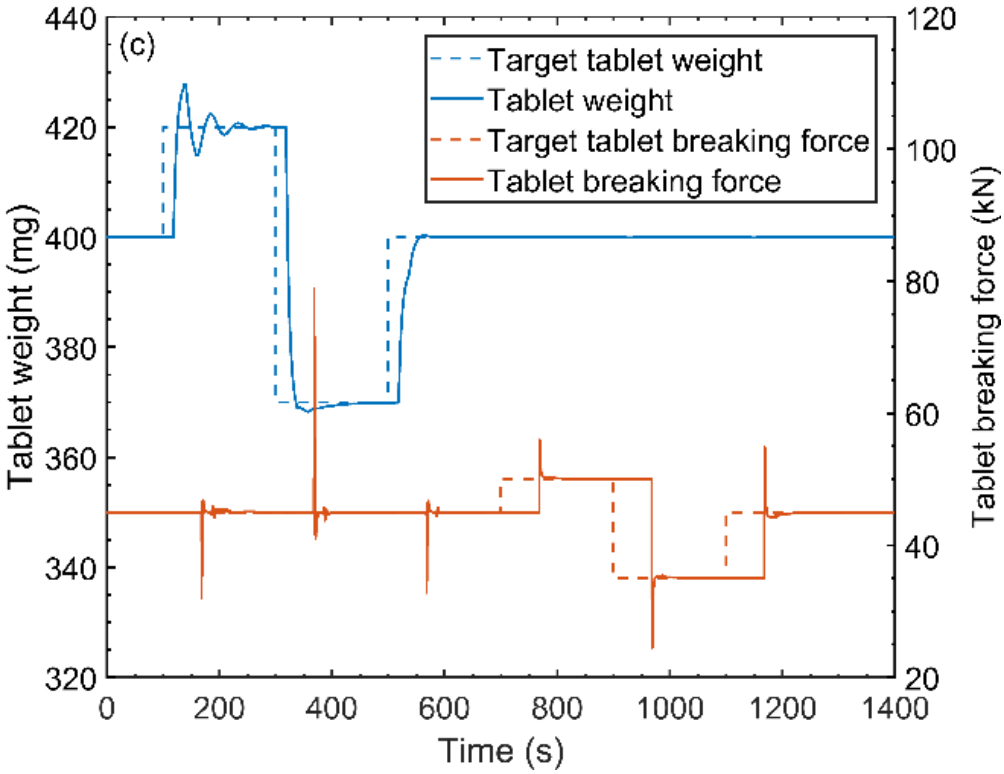

Figure 31. Control strategy 1 – Set point tracking scenario. (a) Critical process parameters (b) Actuators (c) Critical quality attributes.

Figure 32 shows the system response to the disturbance rejection scenario presented in Section 5.3. When a white noise disturbance is applied to density, the controller takes action to bring the controlled variables to their respective set points as seen in Figure 32a,b. It can be observed that the effect of the density variations is not completely mitigated by the controller because of the high frequency at which the white noise occurs. A large deviation from set point followed by a steady state offset is observed when the system undergoes a ramp disturbance in density. This steady state offset has been previously observed by other authors when ramp disturbances are applied to MPCs with integrated white noise models [28]. Applying a step change in density results in a large oscillation in the controller, which is dampened after approximately 100 s. It is important to note that

disturbances of high magnitude have been applied to the system for demonstration purposes. The disturbances observed in practical scenarios have a lesser magnitude and consequently, controller performance will be better.

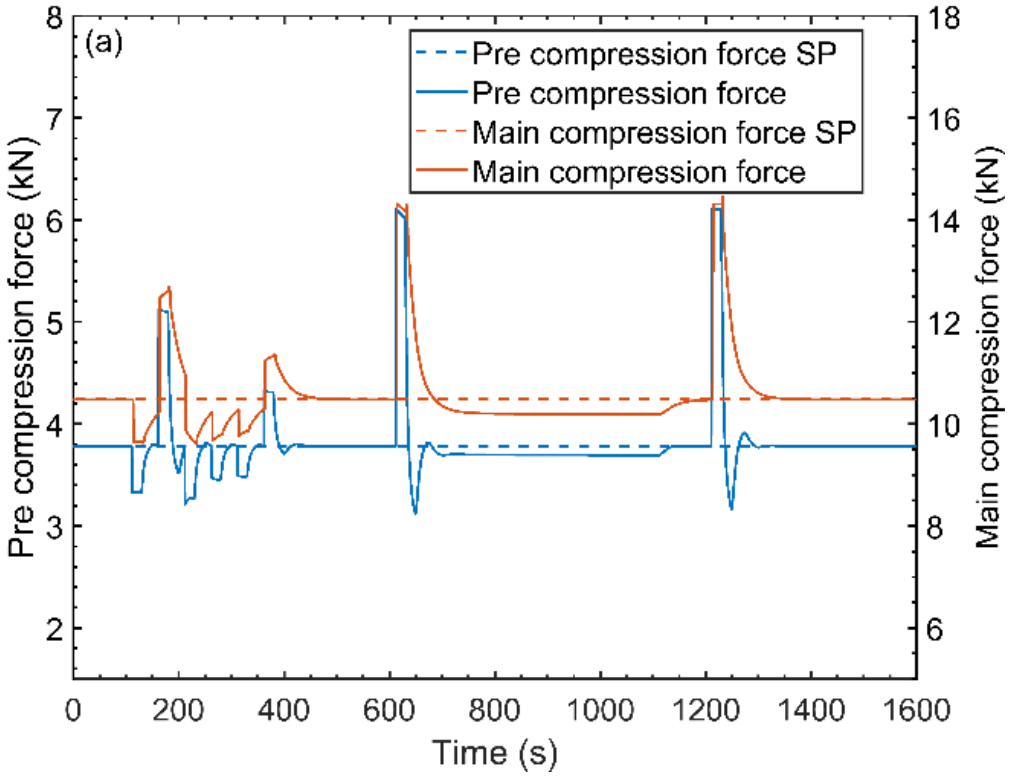
(a)
Pre compression force SP
Pre compression force
Main compression force SP
Main compression force
Pre compression force (kN)
Main compression force (kN)
Time (s)
8
7
6
5
4
3
2
18
16
14
12
10
8
6
0
200
400
600
800
1000
1200
1400
1600

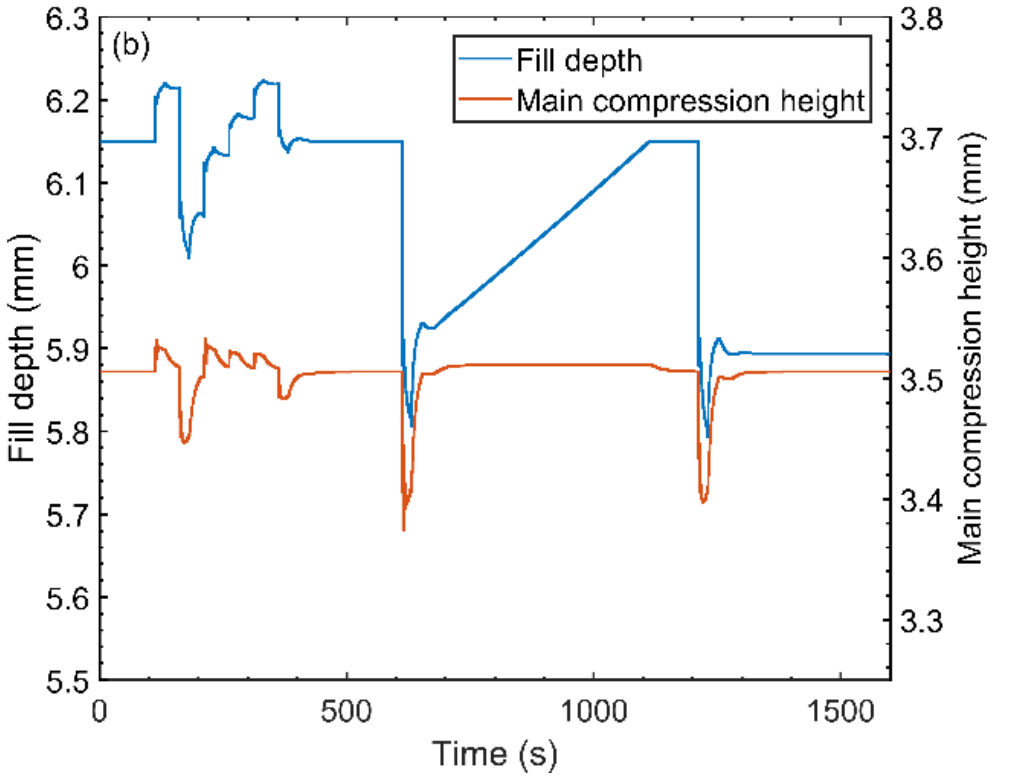
(b)
Fill depth
Main compression height
Fill depth (mm)
Main compression height (mm)
Time (s)
6.3
6.2
6.1
6
5.9
5.8
5.7
5.6
5.5
3.8
3.7
3.6
3.5
3.4
3.3
0
500
1000
1500

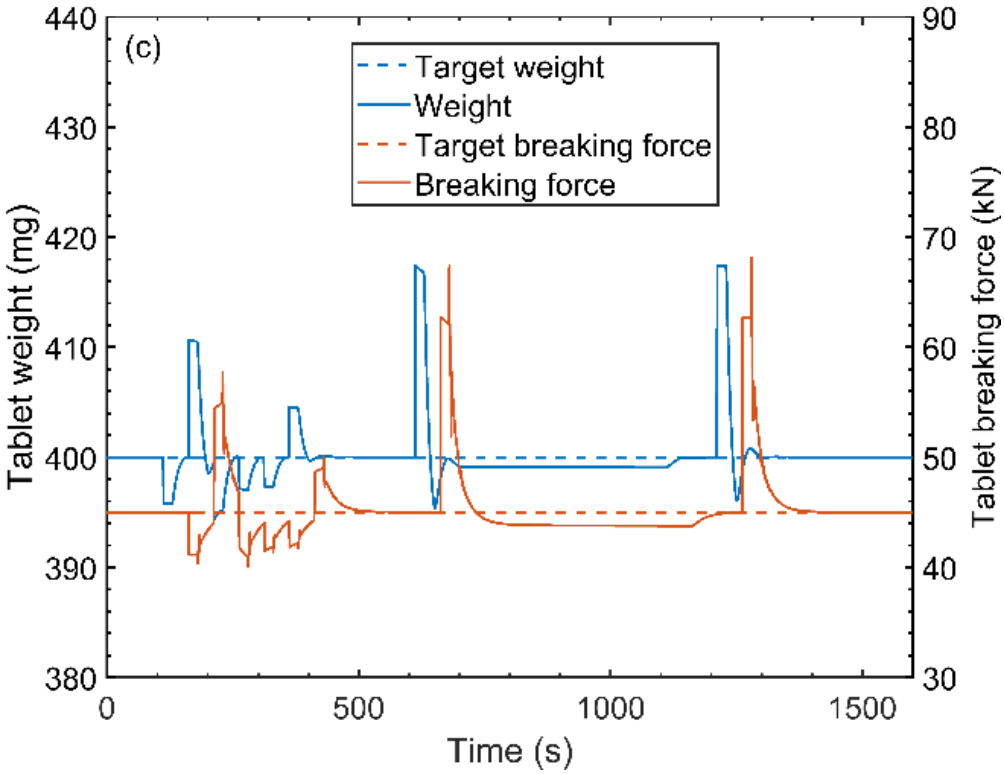

Figure 32. Control strategy 1 – Disturbance rejection scenario. (a) Critical process parameters (b) Actuators (c) Critical quality attributes.

The main advantage of the presented control strategy is that it does not require online sensor for tablet weight and breaking force, since these critical quality attributes are indirectly controlled through the compression forces. This strategy has a relatively fast response time in comparison to strategies involving cascade arrangement. The downside of this strategy is the fact that it requires a relationship between the compression forces and the tablet CQAs to be established during plant setup. Because tablet weight and pre-compression force are dependent of each other in this system, it is necessary to fine tune pre-compression height to ensure that both variables are in the desired range. It is also important to note that the controller needs to be retuned if any changes in pre-compression forces are made. A few disturbances can change the relationship between tablet CQAs and

the compression forces, such as fluctuations in tablet composition. If these variations occur, the system is able to stabilize the compression forces, but the tablet CQAs will deviate from their desired values. The best way to prevent these fluctuations is by ensuring control of blend composition, as proposed by Singh et al. [23].

To verify the applicability of the developed model, this control strategy has also been implemented in an experimental setup and the result were compared to the simulation output. The effect that changes in the set points of compression forces have on tablet weight and breaking force have not been evaluated during the experiments, since no experimental dynamic data could be obtained for those variables. The comparison between the simulation and experimental results is presented in Figure 33 where a close match between simulation and experiments is observed, demonstrating the capabilities of the model for control system design.

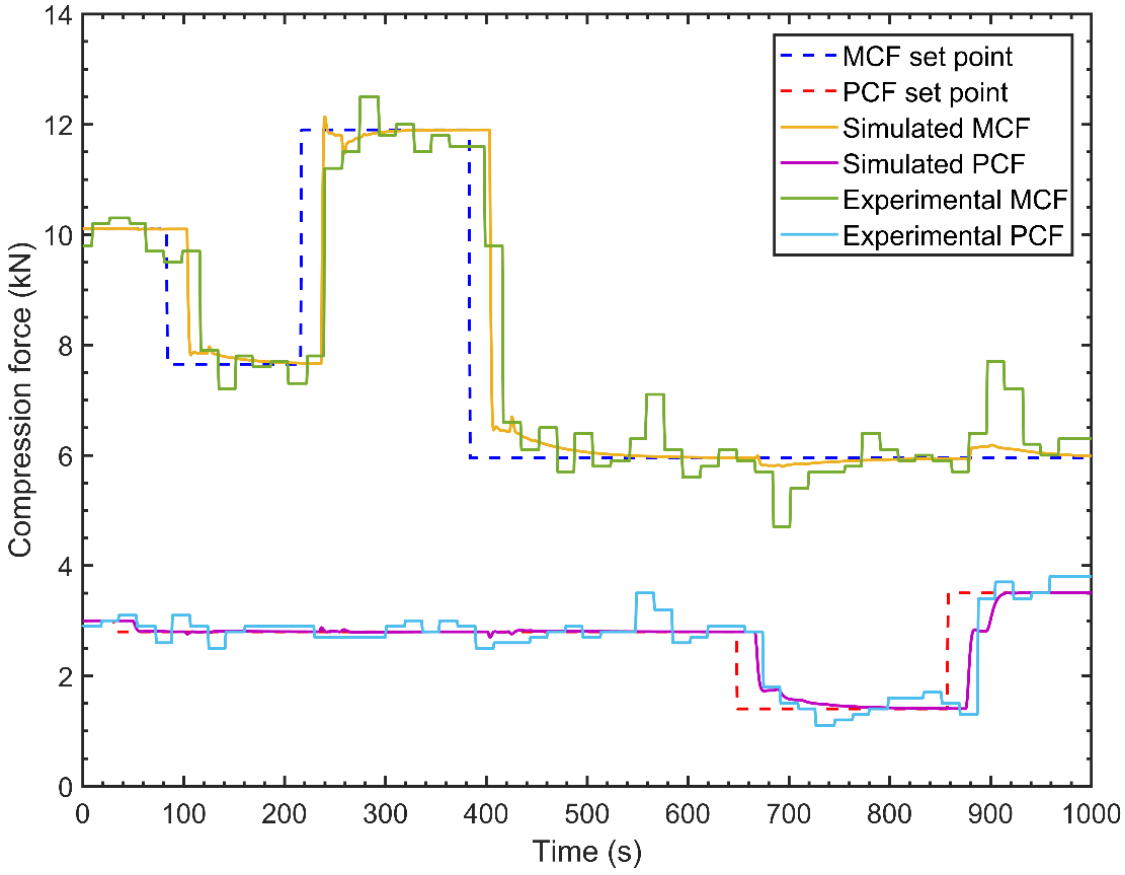

Figure 33. Control strategy 1 - Experimental validation.

7.6.2. Strategy 2 – Cascade Control of Weight and Breaking Force

The response of the simulate system with the double cascade control arrangement to the set point tracking scenario is presented in Figure 34. Both tablet weight and breaking force are able to successfully track their set points by actuating on the set points of the compression forces. Overshoots in tablet weight are observed when set point changes are made in this variable. These oscillations are also observed in the pre-compression force and are most likely caused by the fact that the MPC internal model is not able to capture the non linear behavior of the compression forces, which becomes more pronounced as the compression forces move away from the operating point at which the controllers were

tuned. Spikes in tablet breaking force are seen in Figure 34a when changes are made in the set points of the tablet CQAs. These spikes can be avoided by limiting the maximum rate of change of the manipulated variable of the compression force controller (slave).

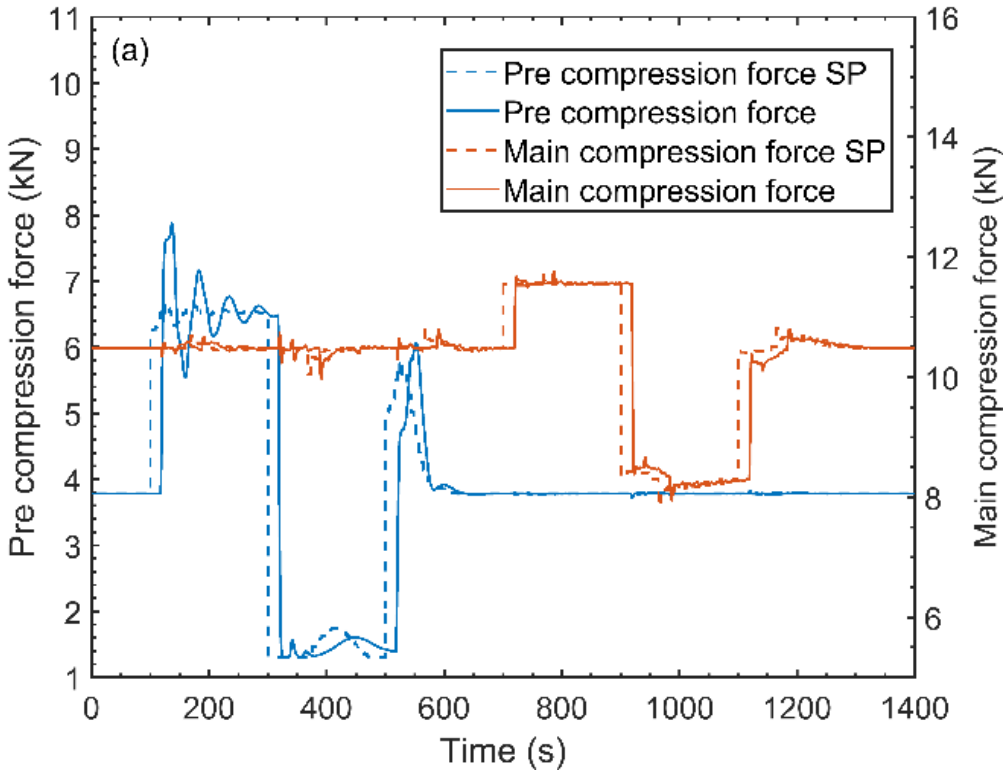
(a)
Pre compression force SP
Pre compression force
Main compression force SP
Main compression force
Pre compression force (kN)
Main compression force (kN)
Time (s)
11
10
9
8
7
6
5
4
3
2
1
16
14
12
10
8
6
0
200
400
600
800
1000
1200
1400

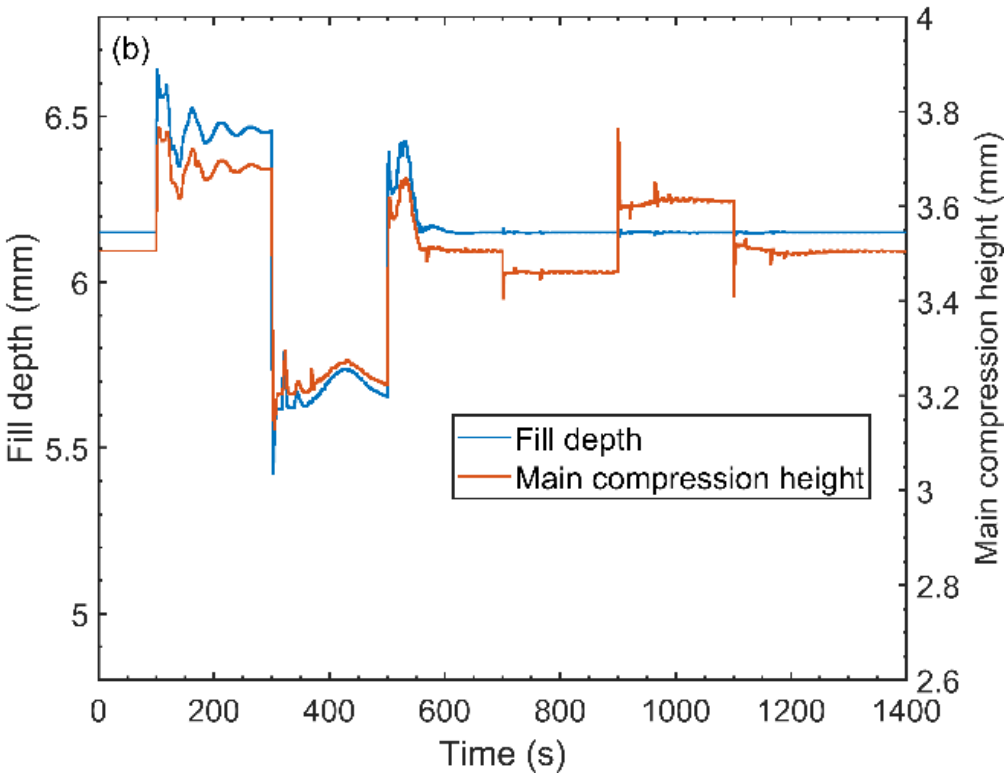
(b)
Fill depth
Main compression height
Fill depth (mm)
Main compression height (mm)
Time (s)
6.5
6
5.5
5
4
3.8
3.6
3.4
3.2
3
2.8
2.6
0
200
400
600
800
1000
1200
1400

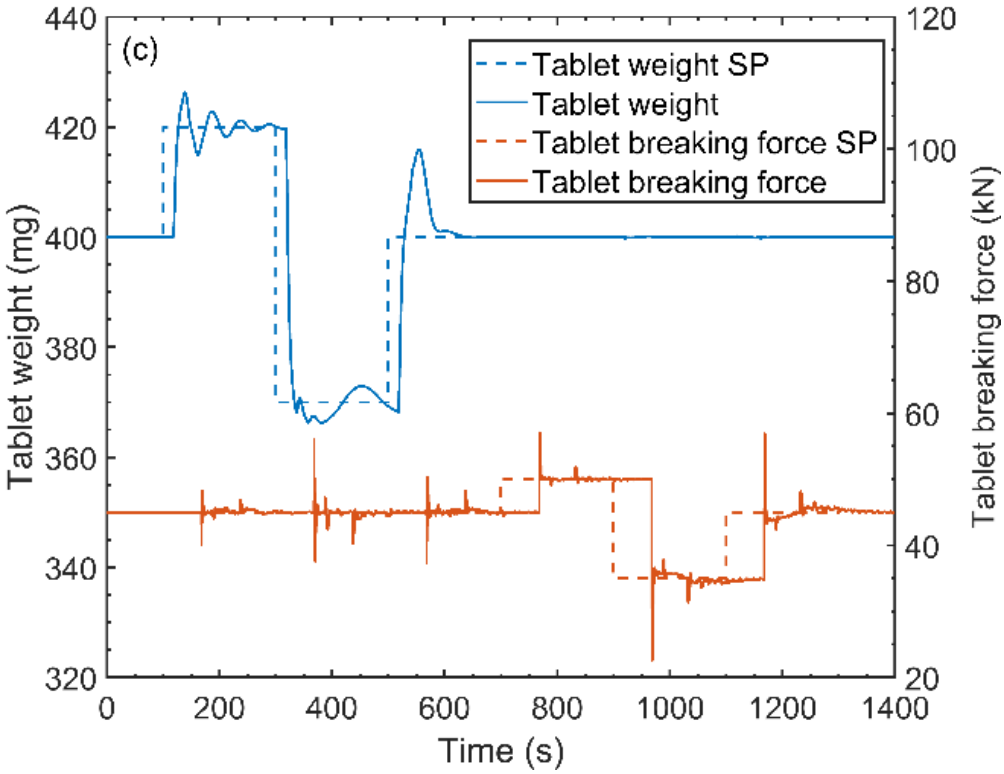

Figure 34. Control strategy 2 – Set point tracking scenario. (a) Critical process parameters (b) Actuators (c) Critical quality attributes. SP: Set point.

Figure 35 presents the system's response under the disturbance rejection scenario. The resulting response is similar to what is observed for control strategy 1 in Figure 32, with the main difference being in the fact that no steady state offset is observed between the CQAs and their set points. This occurs because in this system the inner control loop partially absorbs the effect of the ramp perturbation, resulting a step like disturbance in the compression forces. The step disturbance then gets completely eliminated by the master control loop, resulting in a response where no offset is observed between the CQAs and their set points.

The advantage of control strategy 2 lies in the fact that tablet weight and breaking force are monitored in real time and controlled through a cascade arrangement. This allows the usage of tablet weight and breaking force sensor with relatively slow sampling rates. Directly sensing the tablet CQAs eliminates the need of correlations between the compression forces and the CQAs, which can often times be inaccurate, as mentioned in Section 7.6.1. This control strategy is able to more adequately handle certain disturbance that cannot be handle by control strategy 1. The main disadvantage of this cascade arrangement is that a second layer of non-linearities is added to the system by relating tablet weight to pre-compression force. These accumulated non-linearities result in a narrower stability margin for the controllers. This control strategy, due to its cascade arrangement, has slightly longer response times than strategy 1. Although not as critical as in strategy 1, it is still necessary to tune the compression force controller with the adequate pre-compression for range in mind.

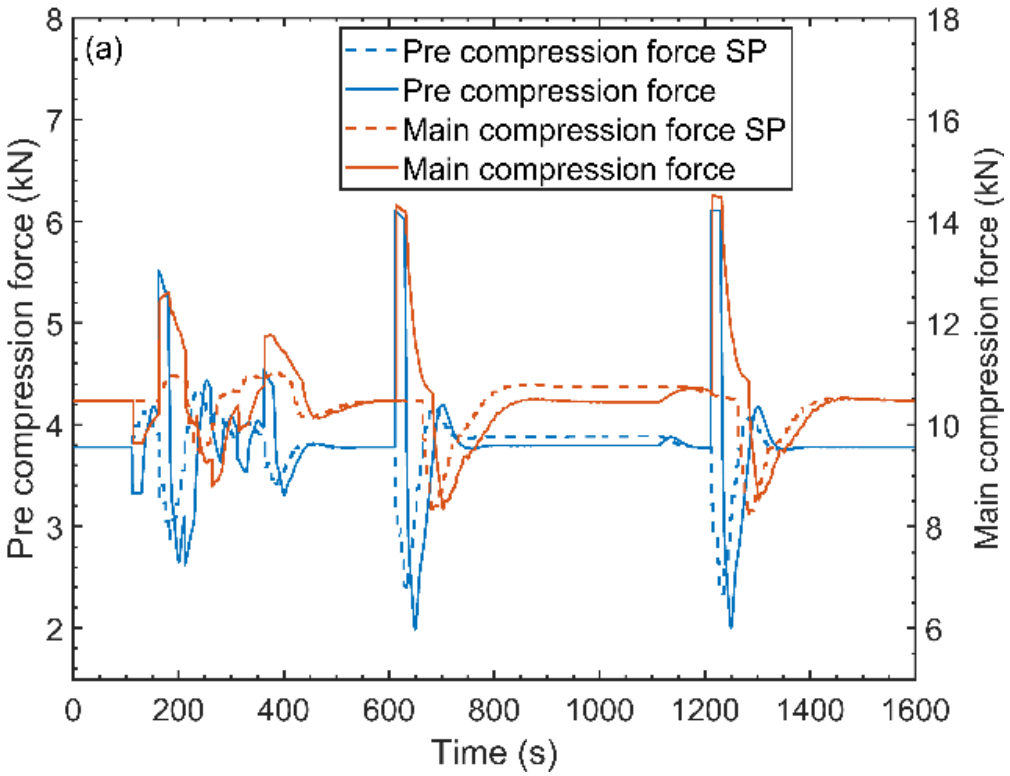
(a)
Pre compression force SP
Pre compression force
Main compression force SP
Main compression force
Pre compression force (kN)
Main compression force (kN)
Time (s)
8
7
6
5
4
3
2
18
16
14
12
10
8
6
0
200
400
600
800
1000
1200
1400
1600

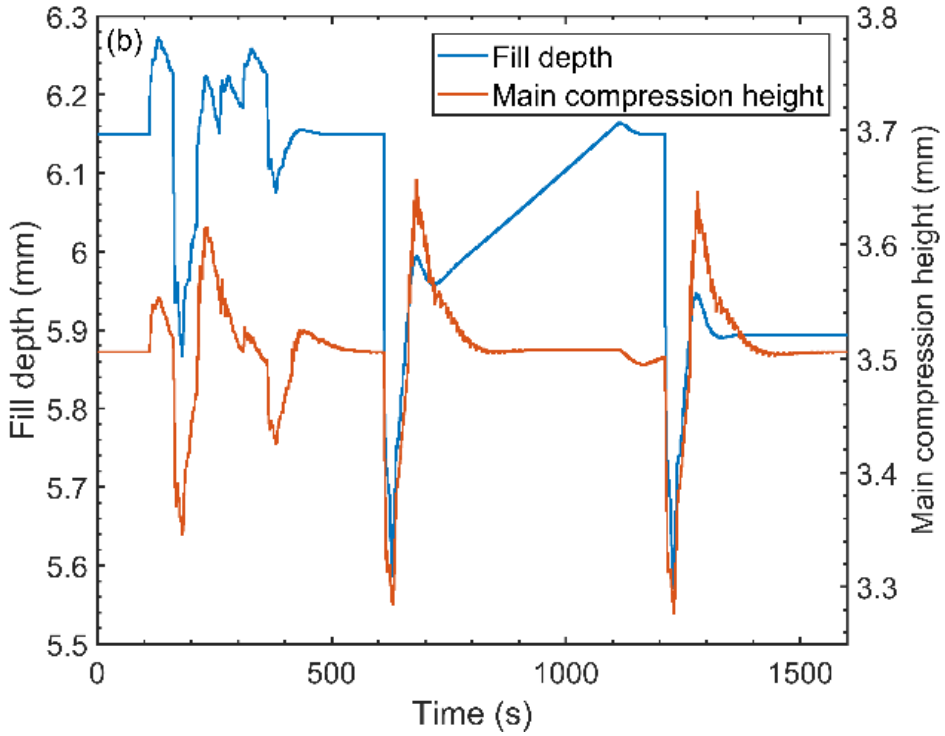
(b)
Fill depth
Main compression height
Fill depth (mm)
Main compression height (mm)
Time (s)
6.3
6.2
6.1
6
5.9
5.8
5.7
5.6
5.5
3.8
3.7
3.6
3.5
3.4
3.3
0
500
1000
1500

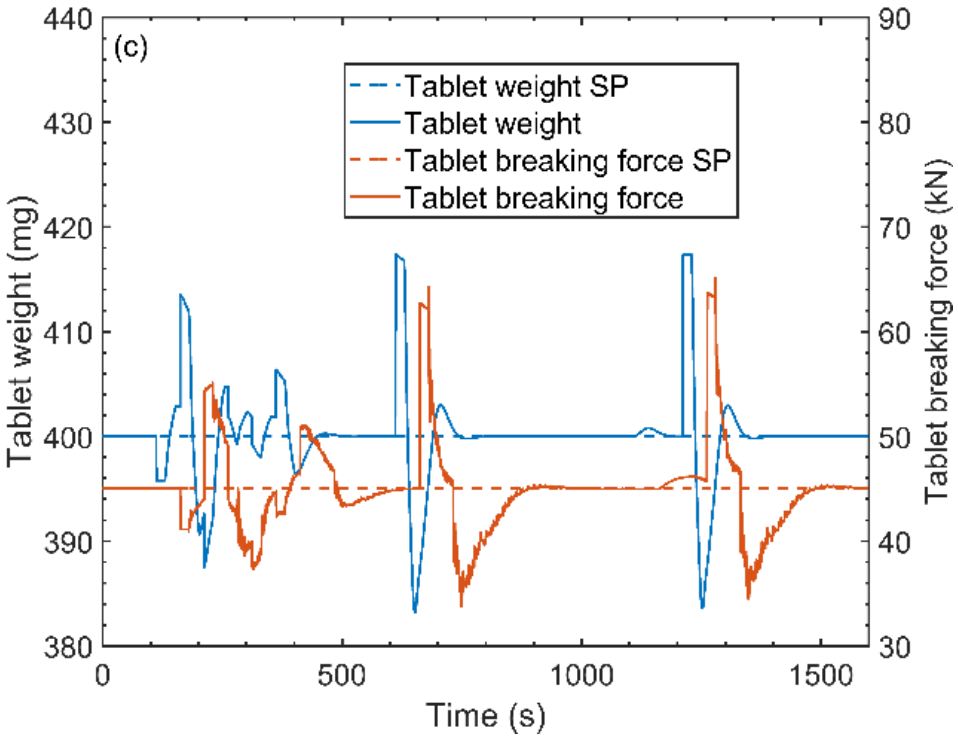

Figure 35. Control strategy 2 – Disturbance rejection scenario. (a) Critical process parameters (b) Actuators (c) Critical quality attributes.

7.6.3. Strategy 3 – Direct Control of Tablet Weight and Cascade Tablet Breaking Force Control

Figure 36 shows the simulated response of a system with direct control of tablet weight and cascade control of tablet hardness. Similar responses are seen in all the three step changes applied in tablet weight, which is a characteristic of a linear system. Interactions between tablet weight and breaking force can be noticed in Figure 36a in the form of peaks in tablet breaking force. Changes in tablet weight set points cause fast actuations in fill depth, which lead to variations in main compression force. These variations are mitigated by the main compression force controller through manipulations in main compression height. A difference in the dynamics of the controllers causes the

sharp peaks in main compression force observe in Figure 36a. The tablet breaking force controller is able to track its set point when no changes in tablet weight are made.

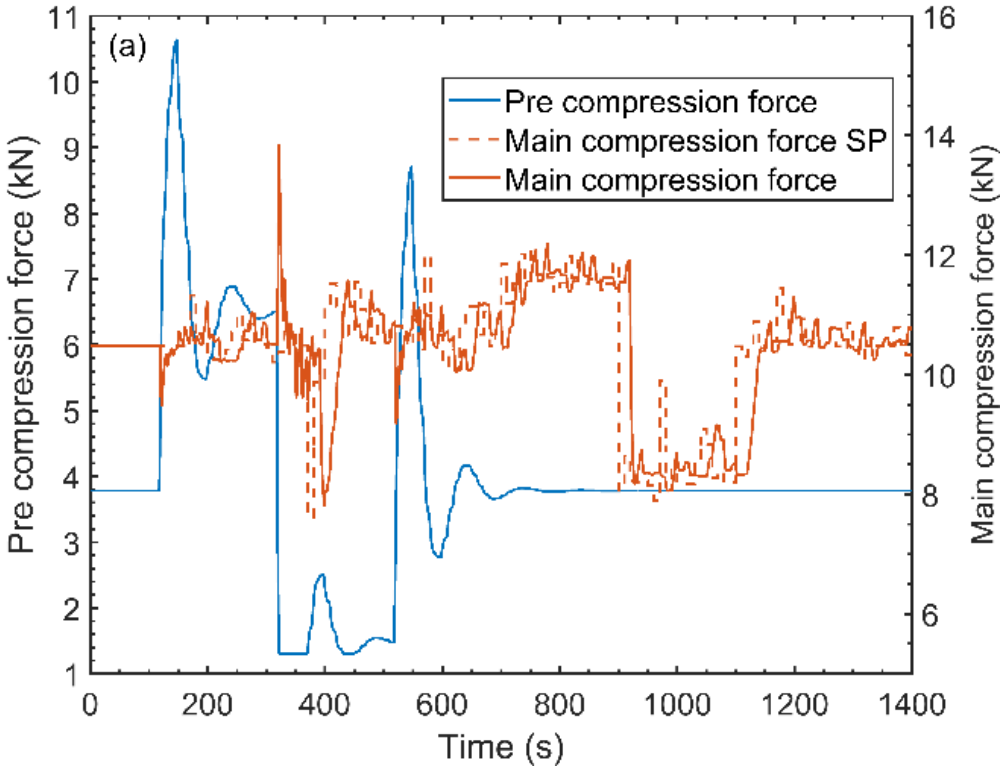
(a)
Pre compression force
Main compression force SP
Main compression force
Pre compression force (kN)
Main compression force (kN)
Time (s)
11
10
9
8
7
6
5
4
3
2
1
16
14
12
10
8
6
0
200
400
600
800
1000
1200
1400

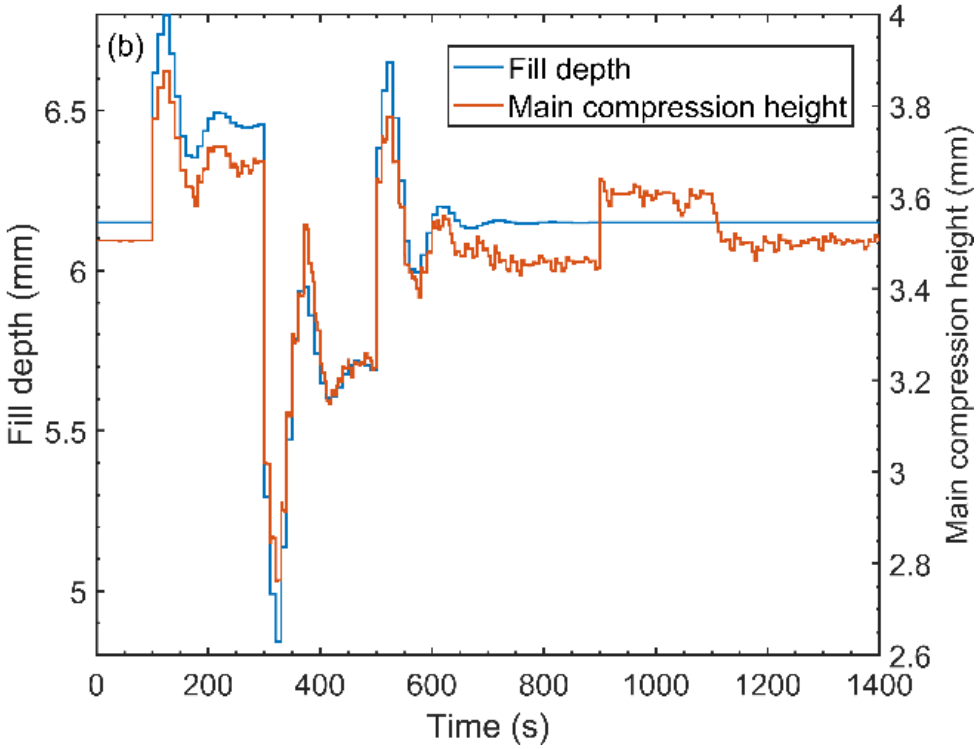
(b)
Fill depth
Main compression height
Fill depth (mm)
Main compression height (mm)
Time (s)
6.5
6
5.5
5
4
3.8
3.6
3.4
3.2
3
2.8
2.6
0
200
400
600
800
1000
1200
1400

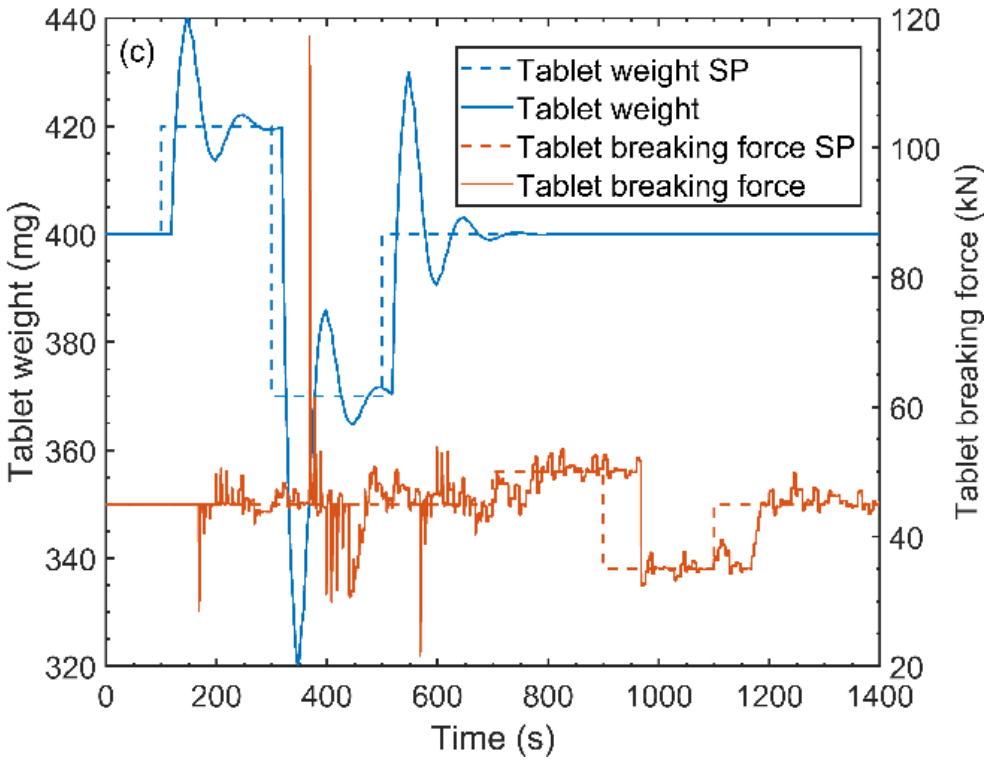

Figure 36. Control Strategy 3 – Set point tracking scenario. (a) Critical process parameters (b) Actuators (c) Critical quality attributes

The response of the system consisting of control strategy 3 to the disturbance rejection scenario is presented in Figure 37. The analysis of this response is similar to what is described for strategy 1. The main advantage of control strategy 3 is the fact that the inner compression force controller isolates the non-linear behavior of the main compression force from the master controller, which actuates on variables that linearly affect tablet weight and breaking force. In this strategy, it is possible to control pre-compression force independently without affecting any of the tablet CQAs, making it easier to avoid tablet defects related to inadequate dwell times. Theoretically, if the controller models are properly regressed, control strategy 3 should present the best performance

among the evaluated strategies. This strategy can be further improved by using fill depth as a measure disturbance signal in the main compression force controller.

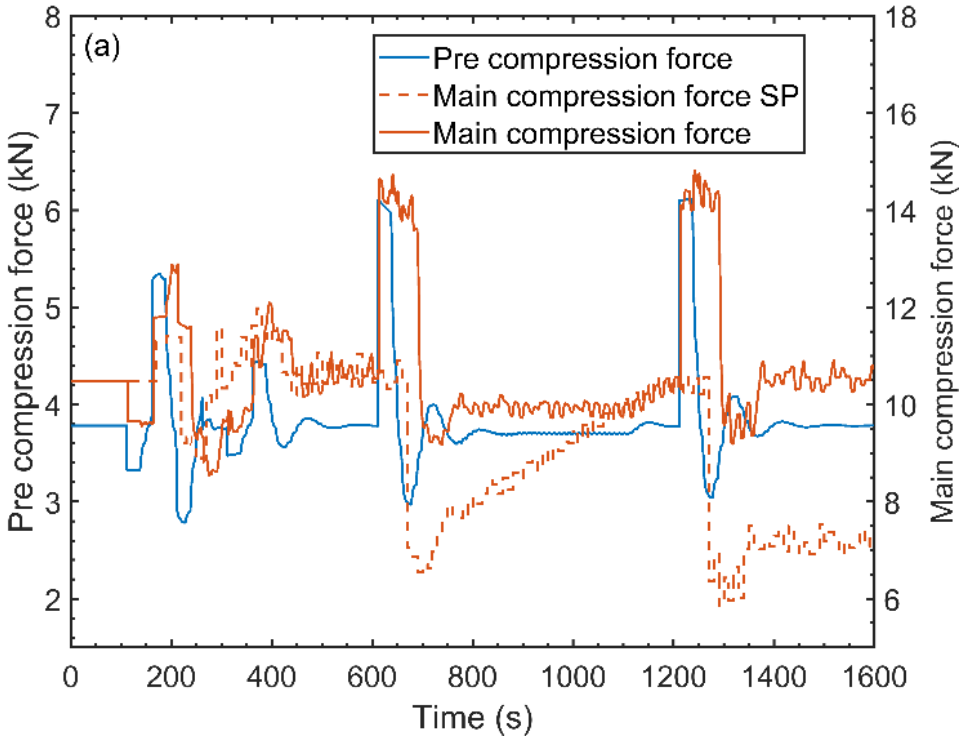
(a)
Pre compression force
Main compression force SP
Main compression force
Pre compression force (kN)
Main compression force (kN)
Time (s)
8
7
6
5
4
3
2
18
16
14
12
10
8
6
0
200
400
600
800
1000
1200
1400
1600

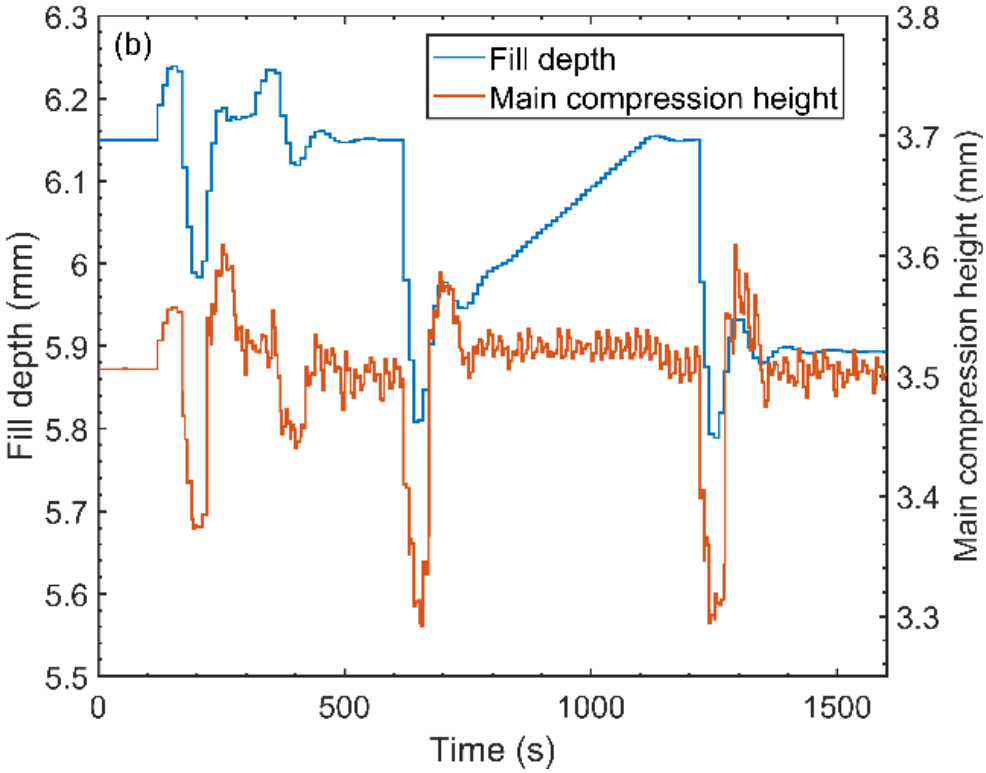
(b)
Fill depth
Main compression height
Fill depth (mm)
Main compression height (mm)
Time (s)
6.3
6.2
6.1
6
5.9
5.8
5.7
5.6
5.5
3.8
3.7
3.6
3.5
3.4
3.3
0
500
1000
1500

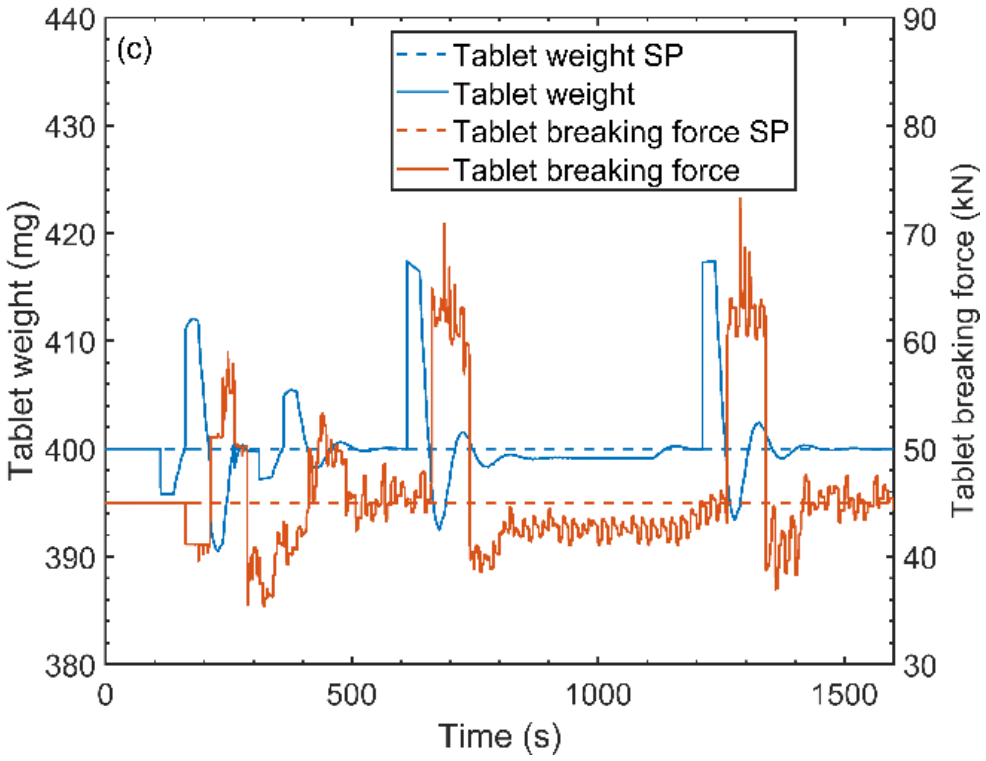

Figure 37. Control strategy 3 – Disturbance rejection scenario. (a) Critical process parameters (b) Actuators (c) Critical quality attributes.

7.7. Demonstration of RTD Based Diversion System

Three simulated scenarios have been created to demonstrate the implementation of the RTD based diversion system in a commercially available control platform (Figure 38). The NIR signal has been simulated using an input parameter block and the $F(t)$ coefficients used in this demonstration correspond to the response of a first order system.

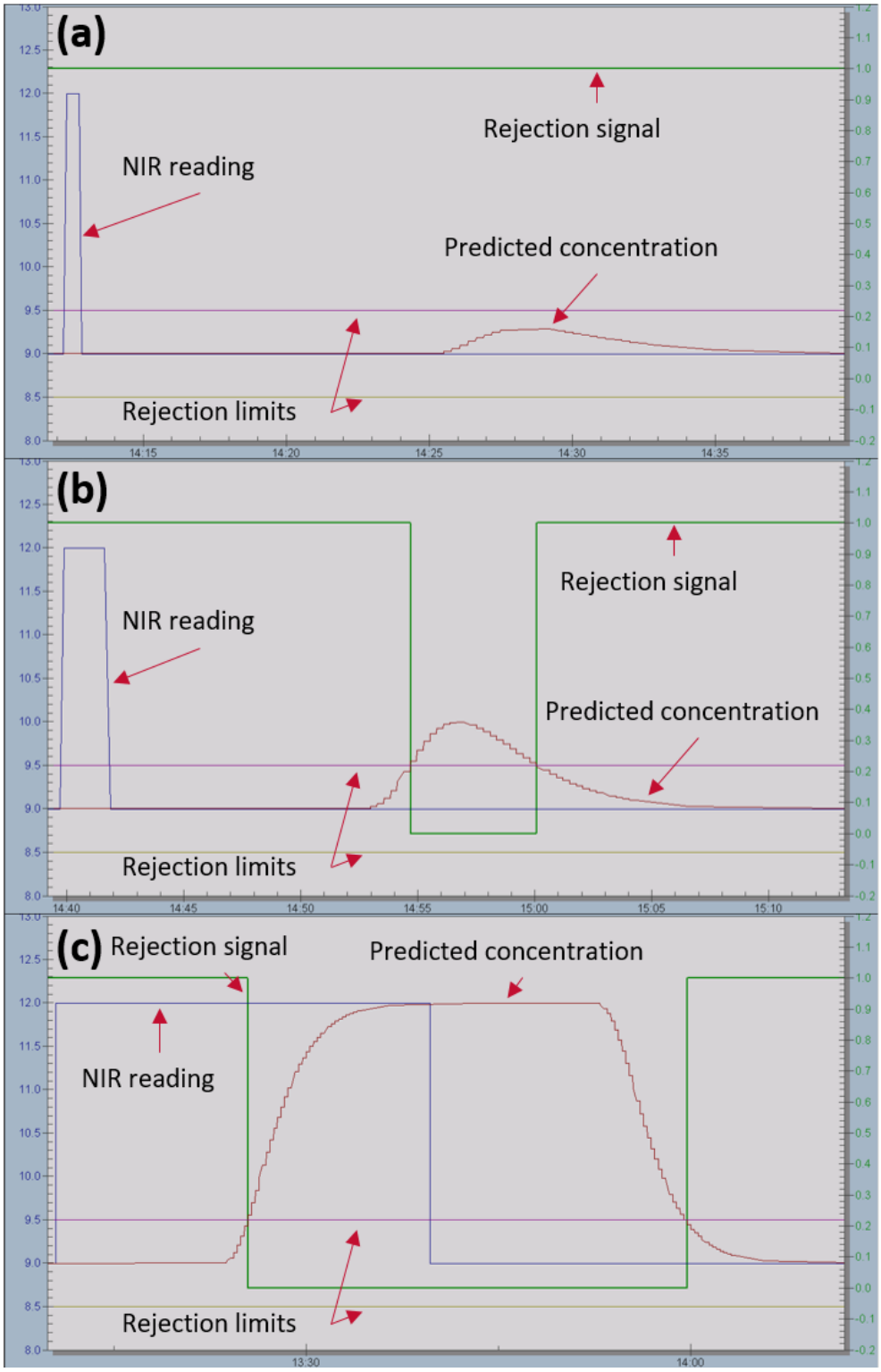

Figure 38. Demonstration of diversion system in DeltaV. X-axis: Time (hh:mm); Y-axis left: Concentration (%); Y-axis right: Rejection signal (-)

In the first scenario (Figure 38a), a pulse with 10 seconds duration and 1% magnitude was applied to the system. The pulse spreads across the tablet press according to the RTD resulting in predicted concentrations that do not trigger the rejection mechanism. This result is a clear example of a situation where an RTD based diversion yields a better performance than the traditional time delay based diversion system. The second scenario (Figure 38b) consists again of a pulse with 10 seconds duration but with 12% magnitude. The larger magnitude results in a disturbance that violates the concentration limits and triggers the diversion system for approximately 17 seconds.

When a step disturbance with a magnitude of 3% is applied to the system (Figure 38c), the diversion system is triggered after 2 seconds and only returns to its normal state 6 seconds after the input concentration value is brought back to 9%. This scenario replicates a situation where a traditional delay based diversion system would achieve the same performance as an RTD based system.

Chapter 8 : Conclusions and Future Perspectives

8.1. Conclusions

In this work, multiple tools for the development and implementation of diversion and control strategies on continuous pharmaceutical manufacturing processes have been presented. A framework describing the development of validated dynamic process models has been introduced and a tablet compaction model was successfully created according to the framework. The dynamic model was able to accurately capture the nonlinear behavior and interactions that are present in a tablet press. The main advantage of the implemented model over previous modelling efforts for this unit operation lies in the fact that the selected modeling strategy allows for fast execution of the simulation while still maintaining accuracy.

The applicability of this compaction model in the process system engineering field is wide and one of its examples has been demonstrated in this work through the evaluation of control algorithms and advanced control strategies. It was concluded that, for the studied control loops, the MPC algorithms presents a better performance when compared to the traditional PID algorithm. Three different control strategies have been evaluated using simulated set point tracking and disturbance rejection scenarios. Possible cases where each strategy can be used, as well as the advantages and disadvantages of each strategy were discussed. One of the simulated strategies was selected and implemented in the pilot plant available at Rutgers University. The resulting data from this experiment closely matched the simulations, validating the applicability of the developed model.

Although process control has proven itself as an invaluable tool for maintaining product quality in continuous pharmaceutical manufacturing, it is still necessary to have diversion systems for situations when the control system is not able to mitigate disturbances in the process. For this reason, a framework for the implementation of a product diversion system based on residence time distributions has been created.

The residence time distribution of the chute, feed frame and tablet press assembly has been determined experimentally and modeled through two different approaches. Both approaches, tank-in-series and dispersion, yielded similar results by accurately capturing the mixing behavior of the studied system. A novel automated tablet sampling strategy was devised to conduct the RTD determination experiments, facilitating the attribution of timestamps to the collected samples. The fitted RTD profile was validated by convoluting it with the input API concentration of the system for the pulse tracer experiment and the resulting curve presented a similar shape as the concentration measured from the collected tablets. An RTD modeling toolbox has also been developed as part of this work and will be an important tool in future modeling efforts.

The implementation of the RTD based diversion system was demonstrated using a simulated input in the control platform (DeltaV). Although not natively supported by DeltaV, convolution between an input and the RTD profile was achieved by modifying the MPC simulate tool available in DeltaV. This convolution method was compared to the convolution function available in Matlab, yielding similar responses and hence validating the methodology used in DeltaV.

8.2. Future Perspectives

The first part of this work introduced a generalized framework for creating validated dynamic models of continuous pharmaceutical operations and modeled the tablet press available at Rutgers University. In order to fully represent the tablet press, it is still necessary to incorporate the developed RTD and a nonlinear relation between production rate and the compression forces. The developed model was completely empirical and only valid for a specific formulation. Including the influence of material properties should be a topic for future research, making the model more generalized and increasing its possible application.

Three control strategies were developed for the tablet compaction operation and one of these strategies was tested using a standalone tablet press. Although this strategy was able to perform well in this scenario, it is important to evaluate how the control system will behave when the complete direct compaction line is run. Further investigation on the stability of this strategy also need to be conducted. Additionally, the performance of these strategies should be evaluated for blends with less than ideal flow properties.

The RTD models determined in this thesis must still be expanded to be representative not only at different processing conditions, but also for different materials. Understanding how the mixing profile of the feed frame changes with materials, varying turret speeds, paddle speeds, and fill depth is the next step in this workstream and is an extremely complex area of research. Once this is understood, it will be necessary to work towards the derivation of a convolution methodology that is able to handle time varying vectors.

There is a growing interest coming from pharmaceutical industries and regulatory bodies on the topic of real time product diversion system based on residence time distributions. The experimental demonstration of the developed diversion system is a study that still needs to be conducted to fully validate this methodology.

There are still many directions to be explored on the presented research topics. This work should serve as stepping stone for the expansion of the knowledge space on the applications of process control and dynamic modeling in the pharmaceutical industry.

Appendix A: Nomenclature

Symbols	Description
API	Active pharmaceutical ingredient
CPP	Critical process parameter
CQA	Critical quality attribute
CSTR	Continuously stirred tank reactor
DC	Direct current
DO	Discrete output
FD	Fill depth
FIR	Finite impulse response
FT-NIR	Fourier transform -near infrared
HART	Highway addressable remote transducer
MCF	Main compression force
MCH	Main compression height
MgSt	Magnesium stearate
MIMO	Multi input multi output
MNPLT	Manipulated
MPC	Model predictive control
MV	Manipulated variable
NIR	Near infrared
OPC	OLE for process control
PAT	Process analytical technology

PCF	Pre-compression force
PCH	Pre-compression height
PFR	Plug flow reactor
PID	Proportional integra derivative
QbD	Quality by design
QbT	Quality by testing
RMSEP	Root mean square error of prediction
RSEP	Relative standard error of prediction
RTD	Residence time distribution
SISO	Single input single output
SSE	Sum of the squared error
TIS	Tanks-in-series
TR	Tracking

References

[1] PhRMA, “PhRMA Profile 2016,” 2016.

[2] J. A. Dimasi, H. G. Grabowski, and R. W. Hansen, “Innovation in the pharmaceutical industry: New estimates of R&D costs,” *J. Health Econ.*, vol. 47, pp. 20–33, 2016.

[3] R. Singh, A. Sahay, K. M. Karry, F. Muzzio, M. Ierapetritou, and R. Ramachandran, “Implementation of an advanced hybrid MPC–PID control system using PAT tools into a direct compaction continuous pharmaceutical tablet manufacturing pilot plant,” 2014.

[4] F. J. Muzzio *et al.*, “Model-Predictive Design, Control, and Optimization. Applying model-predictive methods and a continuous process-control framework to a continuous tablet-manufacturing process.,” *Parmaceutical Technology*, 2013. [Online]. Available: http://www.pharmtech.com/model-predictive-design-control-and-optimization. [Accessed: 07-Jun-2017].

[5] J. Rehrl, J. Kruisz, S. Sacher, J. Khinast, and M. Horn, “Optimized continuous pharmaceutical manufacturing via model-predictive control,” *Int. J. Pharm.*, vol. 510, no. 1, pp. 100–115, Aug. 2016.

[6] R. Singh, A. Sahay, F. Muzzio, M. Ierapetritou, and R. Ramachandran, “A systematic framework for onsite design and implementation of a control system in

a continuous tablet manufacturing process," *Comput. Chem. Eng.*, vol. 66, pp. 186–200, 2014.

[7] U.S. Department of Health and Human Services Food and Drug Administration, "Guidance for Industry: ICH Q8(R2) Pharmaceutical Development," *Workshop: Quality by Design in pharmaceutical*, vol. 8, no. November. p. 28, 2009.

[8] International conference on harmonisation of technical requirements for registration of pharmaceuticals for human use, "Pharmaceutical Development Q8(R2)," in *ICH Harmonised Tripartite Guideline*, 2009, no. Version 4, pp. 1–28.

[9] Q. Su, M. Moreno, A. Giridhar, G. V. Reklaitis, and Z. K. Nagy, "A Systematic Framework for Process Control Design and Risk Analysis in Continuous Pharmaceutical Solid-Dosage Manufacturing," *J. Pharm. Innov.*, pp. 1–20, Oct. 2017.

[10] A. Almaya *et al.*, "Control Strategies for Drug Product Continuous Direct Compression—State of Control, Product Collection Strategies, and Startup/Shutdown Operations for the Production of Clinical Trial Materials and Commercial Products," *J. Pharm. Sci.*, vol. 106, no. 4, pp. 930–943, 2017.

[11] E. P. Gatzke and F. J. Doyle, "Model predictive control of a granulation system using soft output constraints and prioritized control objectives," *Powder Technol.*, vol. 121, no. 2–3, pp. 149–158, 2001.

[12] M. Pottmann, B. A. Ogunnaike, A. A. Adetayo, and B. J. Ennis, "Model-based control of a granulation system," *Powder Technol.*, vol. 108, no. 2–3, pp. 192–201,

2000.

[13] C. F. W. Sanders, M. J. Hounslow, and F. J. Doyle, “Identification of models for control of wet granulation,” *Powder Technol.*, vol. 188, no. 3, pp. 255–263, 2009.

[14] R. Singh, “Model-based control system design and evaluation for continuous tablet manufacturing processes (via direct compaction, via roller compaction, via wet granulation),” 2018, pp. 317–351.

[15] R. Singh, M. Ierapetritou, and R. Ramachandran, “An engineering study on the enhanced control and operation of continuous manufacturing of pharmaceutical tablets via roller compaction,” *Int. J. Pharm.*, vol. 438, no. 1–2, pp. 307–326, 2012.

[16] X. J. Zhao, C. Gatumel, J. L. Dirion, H. Berthiaux, and M. Cabassud, “Implementation of a control loop for a continuous powder mixing process,” in *AIChE 2013 Annual Meeting*, 2013.

[17] A. Bhaskar, F. N. Barros, and R. Singh, “Development and implementation of an advanced model predictive control system into continuous pharmaceutical tablet compaction process,” *Int. J. Pharm.*, 2017.

[18] R. Singh, F. Muzzio, M. Ierapetritou, and R. Ramachandran, “A Combined Feed-Forward/Feed-Back Control System for a QbD-Based Continuous Tablet Manufacturing Process,” *Processes*, vol. 3, no. 2, pp. 339–356, May 2015.

[19] R. Singh, F. Muzzio, M. Ierapetritou, and R. Ramachandran, “Plant-Wide Control of a Continuous Tablet Manufacturing for Quality-By-Design Based

Pharmaceutical Manufacturing," in *Computer Aided Chemical Engineering*, vol. 37, 2015, pp. 2183–2188.

[20] R. Singh, M. Ierapetritou, and R. Ramachandran, "System-wide hybrid MPC–PID control of a continuous pharmaceutical tablet manufacturing process via direct compaction," *Eur. J. Pharm. Biopharm.*, vol. 85, pp. 1164–1182, 2013.

[21] A. Mesbah, J. A. Paulson, R. Lakerveld, and R. D. Braatz, "Model Predictive Control of an Integrated Continuous Pharmaceutical Manufacturing Pilot Plant," *Org. Process Res. Dev.*, vol. 21, no. 6, pp. 844–854, 2017.

[22] R. Singh, A. D. Román-Ospino, R. J. Romañach, M. Ierapetritou, and R. Ramachandran, "Real time monitoring of powder blend bulk density for coupled feed-forward/feed-back control of a continuous direct compaction tablet manufacturing process," *Int. J. Pharm.*, vol. 495, no. 1, pp. 612–625, Nov. 2015.

[23] R. Singh, A. Sahay, K. M. Karry, F. Muzzio, M. Ierapetritou, and R. Ramachandran, "Implementation of an advanced hybrid MPC-PID control system using PAT tools into a direct compaction continuous pharmaceutical tablet manufacturing pilot plant," *Int. J. Pharm.*, vol. 473, no. 1–2, pp. 38–54, Oct. 2014.

[24] J. Huang and D. L. Pla, "GMP Implementation of Advanced Process Control in Tablet Manufacturing," *American Pharmaceutical Review*, 2017. [Online]. Available: http://www.americanpharmaceuticalreview.com/Featured-Articles/335415-GMP-Implementation-of-Advanced-Process-Control-in-Tablet-Manufacturing/. [Accessed: 31-Oct-2017].

[25] S. Di Cairano, *An Industry perspective on MPC in large volumes applications: Potential benefits and open challenges*, vol. 4, no. PART 1. IFAC, 2012.

[26] S. J. Qin, T. a T. a. Badgwell, S. J. Qin, and T. a T. a. Badgwell, "A survey of industrial model predictive control technology," *Control Eng. Pract.*, vol. 11, pp. 733–764, 2003.

[27] D. Q. Mayne, "Model predictive control: Recent developments and future promise," *Automatica*, vol. 50, no. 12, pp. 2967–2986, 2014.

[28] M. A. Zagrobelny, "MPC Performance Monitoring and Disturbance Model Identification," University of Winsconsin-Madison, 2014.

[29] D. Q. Mayne, S. V. Raković, R. Findeisen, and F. Allgöwer, "Robust output feedback model predictive control of constrained linear systems," *Automatica*, vol. 42, no. 7, pp. 1217–1222, 2006.

[30] D. Q. Mayne, J. B. Rawlings, C. V. Rao, and P. O. M. Scokaert, "Constrained model predictive control: Stability and optimality," *Automatica*, vol. 36, no. 6, pp. 789–814, 2000.

[31] S. Streif, M. Kögel, T. Bäthge, and R. Findeisen, "Robust Nonlinear Model Predictive Control with Constraint Satisfaction: A Relaxation-based Approach," *FAC World Congr.*, vol. 47, pp. 11073–11079, 2014.

[32] M. Maiworm, T. Bäthge, and R. Findeisen, "Scenario-based Model Predictive Control: Recursive feasibility and stability," *IFAC-PapersOnLine*, vol. 28, no. 8, pp. 50–56, 2015.

[33] Mathworks, “fminsearch algorithm,” *Matlab documentation*, 2017. .

[34] F. Allgöwer, R. Findeisen, and C. Ebenbauer, “Nonlinear model predictive control,” in *CONTROL SYSTEMS, ROBOTICS AND AUTOMATION*, vol. XI, .

[35] W. Engisch and F. Muzzio, “Using Residence Time Distributions (RTDs) to Address the Traceability of Raw Materials in Continuous Pharmaceutical Manufacturing,” *J. Pharm. Innov.*, vol. 11, no. 1, pp. 64–81, 2016.

[36] Y. Gao, F. J. Muzzio, and M. G. Ierapetritou, “A review of the Residence Time Distribution (RTD) applications in solid unit operations,” *Powder Technol.*, vol. 228, pp. 416–423, 2012.

[37] B. Van Snick *et al.*, “Development of a continuous direct compression platform for low-dose drug products,” *Int. J. Pharm.*, vol. 529, no. 1–2, pp. 329–346, 2017.

[38] P. M. Portillo, A. U. Vanarase, A. Ingram, J. K. Seville, M. G. Ierapetritou, and F. J. Muzzio, “Investigation of the effect of impeller rotation rate, powder flow rate, and cohesion on powder flow behavior in a continuous blender using PEPT,” *Chem. Eng. Sci.*, vol. 65, no. 21, pp. 5658–5668, 2010.

[39] J. G. Osorio and F. J. Muzzio, “Effects of processing parameters and blade patterns on continuous pharmaceutical powder mixing,” *Chem. Eng. Process. Process Intensif.*, vol. 109, pp. 59–67, 2016.

[40] A. U. Vanarase and F. J. Muzzio, “Effect of operating conditions and design parameters in a continuous powder mixer,” *Powder Technol.*, vol. 208, no. 1, pp. 26–36, 2011.

[41] A. Kumar *et al.*, “Conceptual framework for model-based analysis of residence time distribution in twin-screw granulation,” *Eur. J. Pharm. Sci.*, vol. 71, pp. 25–34, 2015.

[42] D. Barrasso, S. Walia, and R. Ramachandran, “Multi-component population balance modeling of continuous granulation processes: A parametric study and comparison with experimental trends,” *Powder Technol.*, vol. 241, pp. 85–97, 2013.

[43] H. Mangal and P. Kleinebudde, “Experimental determination of residence time distribution in continuous dry granulation,” *Int. J. Pharm.*, vol. 524, no. 1–2, pp. 91–100, 2017.

[44] J. Kruisz, J. Rehrl, S. Sacher, I. Aigner, M. Horn, and J. G. Khinast, “RTD modeling of a continuous dry granulation process for process control and materials diversion,” *Int. J. Pharm.*, vol. 528, no. 1–2, 2017.

[45] R. Mendez, C. Velazquez, and F. J. Muzzio, “Effect of feed frame design and operating parameters on powder attrition, particle breakage, and powder properties,” *Powder Technol.*, vol. 229, pp. 253–260, 2012.

[46] D. Mateo-Ortiz and R. Méndez, “Relationship between residence time distribution and forces applied by paddles on powder attrition during the die filling process,” *Powder Technol.*, vol. 278, pp. 111–117, 2015.

[47] R. Mendez, F. Muzzio, and C. Velazquez, “Study of the effects of feed frames on powder blend properties during the filling of tablet press dies,” *Powder Technol.*,

vol. 200, no. 3, pp. 105–116, 2010.

[48] X. Xie and V. M. Puri, “Uniformity of powder die filling using a feed shoe: A review,” *Part. Sci. Technol.*, vol. 24, no. 4, pp. 411–426, 2006.

[49] R. V. A. Visioli, *PID Control in the Third Millennium: Lessons Learned and New Approaches*. 2012.

[50] R. Ramachandran, J. Arjunan, A. Chaudhury, and M. G. Ierapetritou, “Model-Based Control-Loop Performance of a Continuous Direct Compaction Process,” *J. Pharm. Innov.*, vol. 6, no. 4, pp. 249–263, Dec. 2011.

[51] M. Sen, R. Singh, and R. Ramachandran, “A Hybrid MPC-PID Control System Design for the Continuous Purification and Processing of Active Pharmaceutical Ingredients,” *Processes*, vol. 2, no. 2, pp. 392–418, May 2014.

[52] D. Seborg, T. Edgar, and D. Mellichamp, *Process Dynamics and Control*, 2nd ed. Wiley, 2004.

[53] C. E. García, D. M. Prett, and M. Morari, “Model predictive control: Theory and practice-A survey,” *Automatica*, vol. 25, no. 3, pp. 335–348, 1989.

[54] F. Nunes de Barros, A. Bhaskar, and R. Singh, “A Validated Model for Design and Evaluation of Control Architectures for a Continuous Tablet Compaction Process,” *Processes*, vol. 5, no. 4, p. 76, 2017.

[55] H. S. Fogler, *Elements of Chemical Reaction Engineering*, 5th ed. Prentice Hall, 2016.

[56] J. Wesholowski, H. Podhaisky, and M. Thommes, “Comparison of residence time models for pharmaceutical twin-screw-extrusion processes,” *Powder Technol.*, no. 2017, 2018.

[57] G. Taylor, “Dispersion of Soluble Matter in Solvent Flowing Slowly through a Tube,” *Proc. R. Soc. A Math. Phys. Eng. Sci.*, vol. 219, no. 1137, pp. 186–203, 1953.

[58] Mathworks, “fminsearch algorithm,” *Matlab documentation*, 2017. [Online]. Available: https://www.mathworks.com/help/optim/ug/fminsearch-algorithm.html. [Accessed: 01-Jan-2017].

[59] S. Patel, A. M. Kaushal, and A. K. Bansal, “Compression Physics in the Formulation Development of Tablets,” *Crit. Rev. Ther. Drug Carr. Syst.*, vol. 23, no. 1, pp. 1–66, 2006.

[60] K. Kawakita and K. H. Lüdde, “Some considerations on powder compression equations,” *Powder Technol.*, vol. 4, no. 2, pp. 61–68, 1971.

[61] S. Skogestad and C. Grimholt, “The SIMC method for smooth PID controller tuning,” *Adv. Ind. Control*, no. 9781447124245, pp. 147–175, 2012.

[62] A. D. Román-Ospino, V. Cárdenas, C. Ortega-Zuñiga, and R. Singh, “PAT for pharmaceutical manufacturing process involving solid dosages forms,” vol. 20, 2018, pp. 293–315.

[63] A. Bhaskar and R. Singh, “Residence time distribution (RTD) based control system for continuous pharmaceutical manufacturing process (under review),” *J.*

Pharm. Innov., 2018.

Index